



LAWRENCE
LIVERMORE
NATIONAL
LABORATORY

Recent Developments in X-ray Imaging Technology

R. G. Lanier

October 3, 2012

Disclaimer

This document was prepared as an account of work sponsored by an agency of the United States government. Neither the United States government nor Lawrence Livermore National Security, LLC, nor any of their employees makes any warranty, expressed or implied, or assumes any legal liability or responsibility for the accuracy, completeness, or usefulness of any information, apparatus, product, or process disclosed, or represents that its use would not infringe privately owned rights. Reference herein to any specific commercial product, process, or service by trade name, trademark, manufacturer, or otherwise does not necessarily constitute or imply its endorsement, recommendation, or favoring by the United States government or Lawrence Livermore National Security, LLC. The views and opinions of authors expressed herein do not necessarily state or reflect those of the United States government or Lawrence Livermore National Security, LLC, and shall not be used for advertising or product endorsement purposes.

This work performed under the auspices of the U.S. Department of Energy by Lawrence Livermore National Laboratory under Contract DE-AC52-07NA27344.

Recent Developments in X-ray Imaging Technology

Robert G. Lanier

¹Lawrence Livermore National Laboratory
Livermore, CA

June 12, 2012

(IM # 658363)
LLNL-TR-587512

This work performed under the auspices of the U.S. Department of Energy by Lawrence Livermore National Laboratory under Contract DE-AC52-07NA27344.



Specific Recommendations:

Executive Summary

A review of recent developments in the technology of x-ray imaging hardware has been completed. Based on this review, we believe that the following items merit more detailed scrutiny in regards to their applications to US Homeland Security interests:

- **Fujifilm's** 17" x 17" flat panel detectors which are part of the company's FDR AcSelerate x-ray imaging systems
- **GE Healthcare's** Gemstone™ scintillators for their use in CT units
- CZT baggage scanning units under development by either **Endicott Interconnect Technologies** or **Redlen Technologies** and which employ a new "XENA™" IC with NEXIS™ protocols.
- Dual Energy Line- Scanning devices from either **Hamamatsu Photonics** (C10800 series) or from the **X-Scan Imaging Corporation** (XD8800 and XDR8800 Series Line-Scan Camera).

The bases for these recommendations, as well as other not highlighted above, are noted below. The footnotes document company contact information. Beyond the text highlighting the recommendations, a number of appendices have been added which document the research conducted for this review.

Introductory Comments

A review of recent developments in the technology of x-ray imaging hardware has been completed. The topics reviewed are presented in detail in the appendices. In most cases, either a short report was written to summarize developments in a particular area (Appendices i - iv) or tables have been assembled which provide a snapshot compilation of hardware items currently available from reputable vendors (Appendices v - vii). Finally, Appendix viii is a selected list of titles that speak to various aspects of x-ray imaging technology.

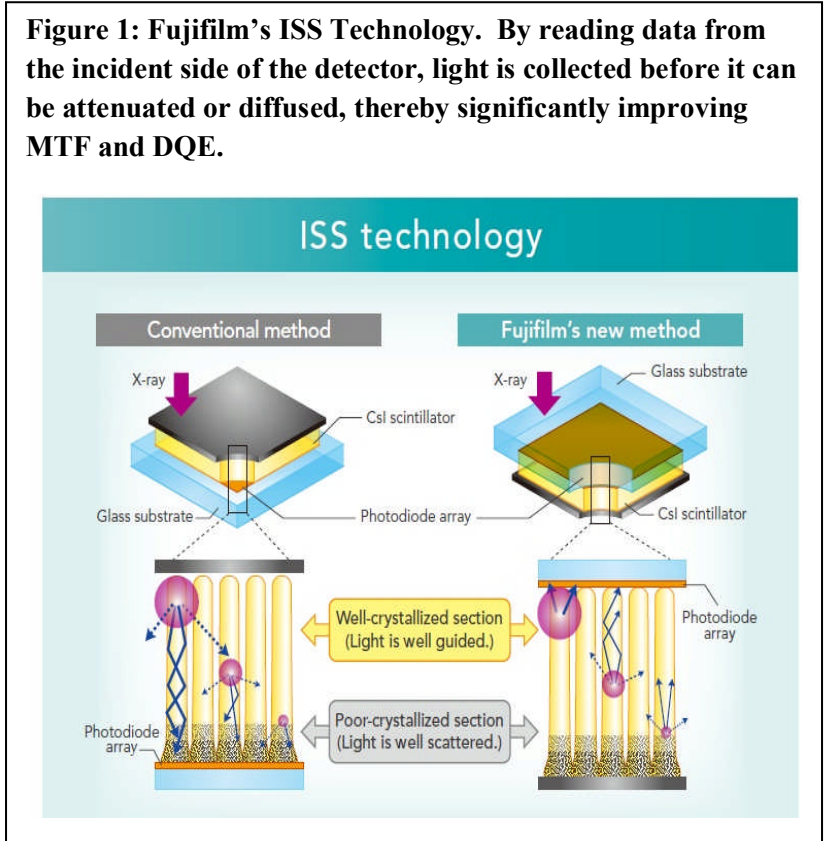
In product information provided by vendors, it is often the case that a vendor will indicate his willingness to partner with R&D centers to develop technologies which may not be available as market items but which could be developed given current state-of-the art knowledge. Reference to these vendors is made in the body of the text or in the footnotes.

Looking into the near future, we offer suggestions of new technology developments which are only now finding their way into the commercial arena or which are shortly expected to make their way there. Most new innovations appear in medical imaging where the emphasis is on maximizing image quality and minimizing patient dose. For industrial applications and for applications directed to US Homeland Security interests, radiation dose is less of a concern unless human subjects are involved.

Acknowledging a short-term perspective and accepting the caveat that medical and industrial imaging applications some time have competing concerns, we note below the following specific areas of developing x-ray imaging hardware:

- Amorphous Selenium (a-Se) flat panel technology with active pixel technology.
- Structured CsI (Cesium Iodide) scintillators
- TFT (thin-film transistor) and CMOS (complementary metal-oxide-semiconductor) technology
- CZT (cadmium-zinc telluride) arrays and their associated electronics.
- Ceramic scintillators

These areas continue to be the subject of a great deal of research and development and none can be considered a “mature technology”. Nevertheless, they are sufficiently developed that vendors have incorporated them into their future business models. This is a clear expression of confidence that the technology improvements will have utility and durability under real-world conditions. Moreover, the fact that industry has made investments in these areas virtually



guarantees that continued improvements are expected in order to protect capital investments.

Finally, throughout the information presented in the appendices we touch on and reference items that would be arguably considered more “next generation technologies”. These include, for example, new scintillators such as HgI₂, PbI₂, PbO₂, GaAs, lutetium-doped crystals, high-pressure gas sensors, large CZT arrays currently built for and used for astronomical research applications, indirect flat-panel imagers with avalanche gain, etc.

Flat panel Imagers

Fujifilm Units

There are at least two commercial flat panel units that appear at the forefront of imaging technology. Both are developed by **Fujifilm**¹ and are the primary imaging devices incorporated into the company’s “**FDR AcSelerate System**”. In summary, the technology associated with the two units is noted below. Both are rated for x-ray energies up to a maximum of 150kVp and each displays an active pixel area of 2880 x 2880 with a pixel pitch of 150µm:

- (1) A CsI 17” x 17” wireless panel (7.9 lbs) that employs what the vendor calls ISS (Irradiated Side Sample, see Figure 1) technology which allows the detector to capture radiation signals on the same side of the irradiated subject and closest to the area where the signals are strongest. The vendor claims enhanced MTF and DQE relative to other flat panel units².
- (2) an amorphous selenium (a-Se) direct-conversion flat panel unit (17” x 17”). The vendor claims reduced radiation dose lifespan and enhanced MTF and DQE relative to other flat panel units.

In publicly available company sales brochures, the **Fujifilm’s FDR AcSelerate** system is advertised with either panel (1) or panel (2) packaged in the same



¹ Medical Technical Support:: (888) FUJI-MED (385-4633); (800) 272-8465; (203) 602-3580

² A Fujifilm representative noted that a Gadox scintillator can be substituted for CsI, with the unit still incorporating the ISS technology.

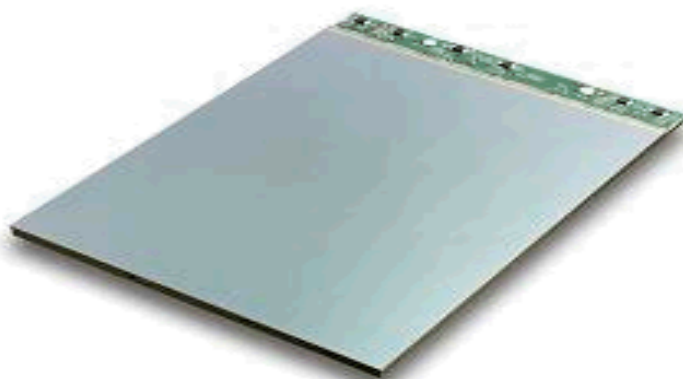
external housing (see Figure 2). This information is available in individual brochures without any cross referencing leading to confusion as to which flat panel is actually used in the **FDR AcSelerate** system. In discussion with a representative from **Fujifilm**, the company has apparently decided that the CsI alternative is technologically superior to the a-Se unit and cheaper to manufacture. Therefore, since the precise imaging technology is generally transparent to most users, the company is quietly making the transition to the CsI unit. The **Fujifilm** representative expressed his willingness to work with US Homeland Security technical experts on either technology for baggage screening applications.

The Dexela Flat Panel Units

The **Dexela**³ flat panel CMOS X-ray detector is a good alternative flat-panel detector. **Dexela** units use a crystalline silicon CMOS sensor which the vendor claims is superior to units created with TFT technology in flexibility, stability, speed and low noise and which results in higher resolution images. A unit available for non-destructive testing is shown in Figure 3.

The panel offers active pixel sensors with a pixel pitch of 74.8 μm and a 3888 x 3072 active pixel area.

Figure 3: Dexela 2923 Flat Panel 12" x 9" Imager for Non-destructive testing.



³ Dexela Limited (UK Office) Wenlock Business Centre 50-52 Wharf Road London N1 7EU; PHONE: +44 (0)20 7148 3107; FAX: +44 (0)20 7148 3107

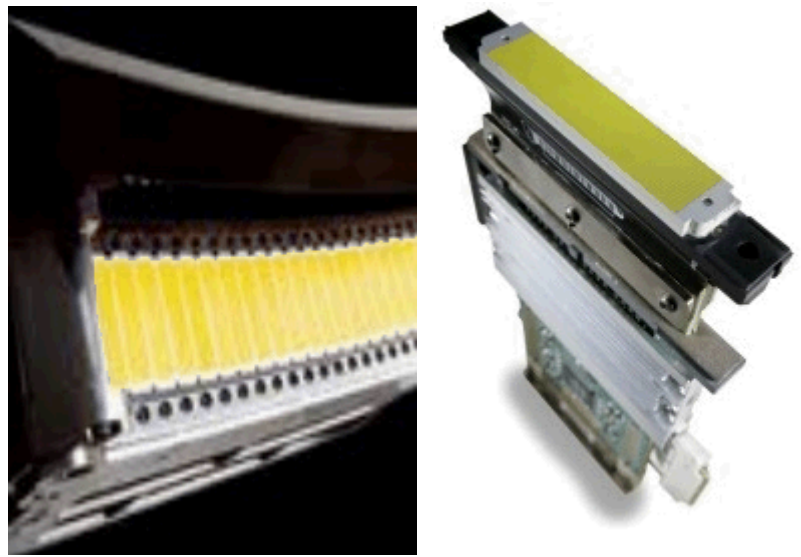
Flat panels from other Vendors

As noted in Appendix vii companies such as **Perkin-Elmer**⁴, **General Electric**⁵, **Teledyne**⁶, **Hamamatsu**⁷, **Varian Medical Systems**⁸, **Allied Vision**⁹, **Konica-Minolta**¹⁰, etc., offer what appear to be reasonably comparable units based on a-Si technology, using **Gadox** or **CsI** scintillators and supported with various electronic designs.

Scintillators for CT (Computed Tomography) Applications

An important issue within the medical community is to obtain quality CT scans at the lowest possible patient dose. This concern has spurred the development of efficient scintillators that provide high light output with minimum after-glow along with radiation stability, chemical stability, and mechanical strength.

Figure 4: GE Gemstone scintillator. Displays show the unit mounted in a CT array and an individual unit with its associated electronics.



Gemstone™ (see Figure 4) is a transparent polycrystalline scintillator for CT from **GE Healthcare**. Competing products are **HiLight™** (also from **GE Healthcare**)

⁴ Customer Care USA Telephone : 800-762-4000 or +1 203-925-4602 FAX : +1 203-944-4904
CustomerCareUS@perkinelmer.com ; Corporate Headquarters 940 Winter Street Waltham Massachusetts 02451 USA

⁵ [GE Healthcare Worldwide - gehealthcare.com](http://gehealthcare.com); 930 East Arques Avenue Sunnyvale, CA 94085; (408) 737-3000

⁶ [Teledyne Microelectronics](http://teledyne.com) • 12964 Panama Street, Los Angeles, CA 90066 310.822.8229 • 800.518.1015 | microelectronics@teledyne.com

⁷ Hamamatsu City Building7F, Tenma 312-32, Naka-ku, Hamamatsu, Japan Zip code:430-0935 Tel (+81)53-456-4960 Fax (+81)53-459-3915

⁸ Varian Medical Systems, Inc., 3100 Hansen Way Palo Alto, CA 94304-1038

⁹ (Head Office, Manufacturing, Customer Care, Technical Support) Allied Vision Technologies GmbH ;Taschenweg 2a; 07646 Stadtroda, Germany Tel.: +49.36428.677-0 Fax.: +49.36428.677-28

¹⁰ Konica-MinoltaKonica Minolta Medical Imaging USA, Inc;
<http://www.konicaminolta.com/medicalusa/about/index.html>

and **GOS**¹¹ (from **Hitachi**¹², **Toshiba**¹³, **Siemens**¹⁴, and **Philips**¹⁵). **GE** claims that **Gemstone™** is the only new CT scintillator developed in the past two decades and further claims that it delivers the best performance characteristics compared to other competing units. It has a primary decay time of ~ 30 ns, or 100 times faster than **GOS** (2 – 3.4 μs). **Gemstone™** has very low afterglow (about 20% of **GOS** at 40 ms), extremely low radiation damage (0.03% vs. 0.65% for **GOS**), and very good chemical durability, mechanical properties, uniformity, and manufacturability. **Gemstone™** has a cubic garnet crystal structure and is based on a rare earth composition system that was invented by **GE**. It is made into a transparent polycrystalline material with processes developed by **GE's** scientists.

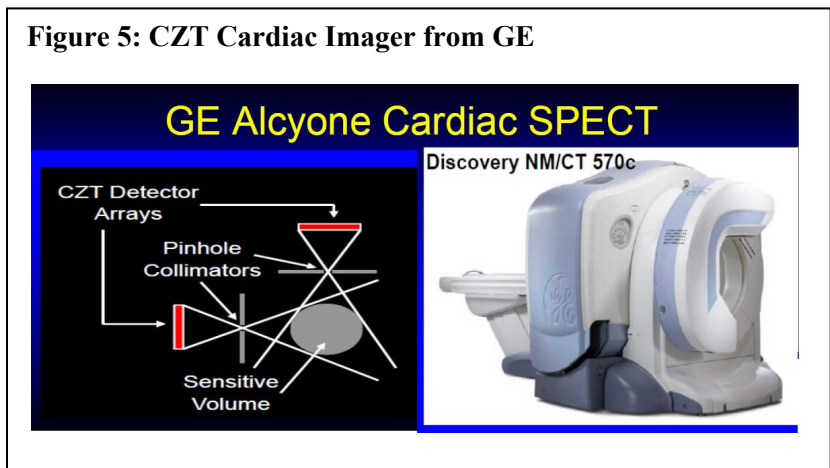
Appendix vii lists some scintillator providers and Appendix iii describes some developments in scintillator research along with collections of new scintillators and their associated properties.

Cadmium-Zinc-Telluride (CZT) Imaging Devices

Over the last two decades, the semiconductor CdZnTe (CZT) has emerged as the material of choice for room temperature detection of hard X-rays and soft γ-rays¹⁶. The techniques for growing the

crystals, the design of the detectors, and the electronics used for reading data from the detectors have been considerably improved over the last few years¹⁷. The commercialization of this technology is currently focused on cardiac imaging with devices such as **D-SPECT (Spectrum Dynamics**¹⁸), **GE Healthcare's Alcyone**

Figure 5: CZT Cardiac Imager from GE



¹¹ The GOS or Gadox scintillators are made of polycrystalline Gadolinium Oxysulfide crystals with dopants of either Praseodymium (Pr), Terbium (Tb) or Europium (Eu) determined by the requirements of the application.

¹² Hitachi HQ; Marunouchi 1-6-1, Chiyoda-ku, Tokyo 100-8220, JAPAN Tel: +81-(0)3-3258-1111 (Switchboard)

¹³ Toshiba America Medical Systems, Inc. 2441 Michelle Drive Tustin, CA 92780 (800) 421-1968

¹⁴ United States Headquarters Siemens Medical Solutions USA, Inc. 51 Valley Stream Parkway Malvern, PA 19355

¹⁵ Philips Healthcare 3000 Minuteman Road Andover, MA 01810-1099

¹⁶ The items described in this section are from approximately 2009 or later.

¹⁷ See for example H. Krawczynski, I. Jung, J. Perkins, A. Burger, M. Groza, Proc. SPIE 5540 (2004) 1. astro-ph/0410077; H. Chen, S.A. Awadalla, F. Harris, et al., IEEE Trans. Nucl. Sci. 55 (2008) 1567 and Q. Li, A. Garson, P. Dowkontt, J. Martin, et al., in: Proc. NSS/MIC conference, 484, 2008. Available from: arXiv:0811.3201.

¹⁸ **Spectrum Dynamics (Israel) Ltd.** 22 Bareket Street North Industrial Park POB 3033 Caesarea 30889, Israel Tel: (+972) 73 7374500 Fax: (+972) 73 7374501

technology family of **SPECT** detectors (see Figure 5), **Cardius X-ACT (Digirad¹⁹)** and **IQ-SPECT (Siemens)**. **CZT** has a marked advantage in the clinical setting because quality images can be obtained with significantly reduced radiation doses.

Research continues emphasizing the use of **CZT** detector arrays for baggage screening. **Endicott Interconnect Technologies²⁰** claims that it has commercialized a prototype automated linear baggage inspection unit (**ABIS**) using a linear array of **CZT** detectors (see Figure 6) with a throughput of 1200 bags/hour.

Additionally, **Redlen Technologies²¹** provides high-resolution **CZT** detectors for medical and commercial applications. From information provided by a company representative, **Redlen** expects to field its first commercial screening unit in 2014. The company further claims to be working with others who are developing baggage scanning systems to use **CZT** technology to address the removal of the European Union (EU) ban on liquid carry ons.

Figure 6: ABIS (Automated Baggage Inspection System) Prototype CZT linear baggage scanning system.

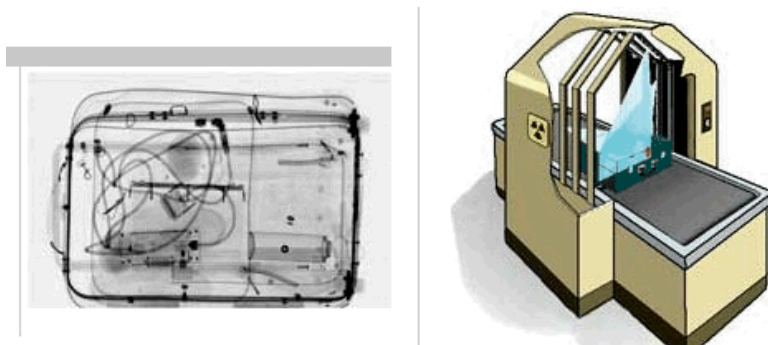
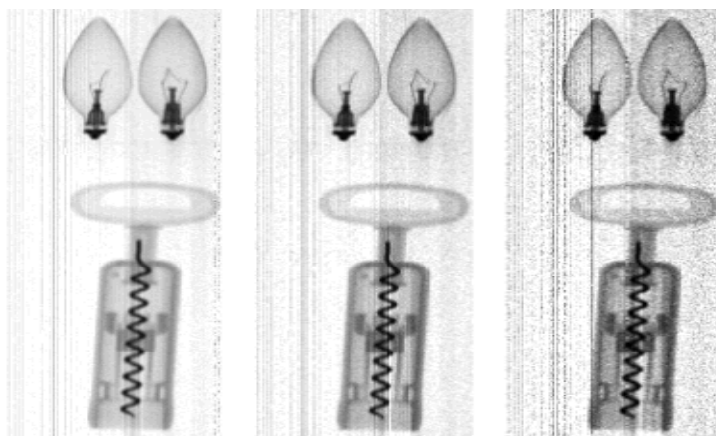


Figure 7: Raw, three-energy-bin radiograph of light bulbs and a corkscrew. From left image to right the energy thresholds were set approximately at 20, 35 and 60 keV, respectively.



¹⁹ Digirad 13950 Stowe Dr. Poway, CA 92064 **Phone:** 858-726-1600**Fax:** 858-726-1700; **Toll Free:** 800-947-6134 <http://www.digirad.com>

²⁰ Endicott Interconnect Technologies Inc. Corporate Headquarters Building 258 1093 Clark Street , Endicott, N.Y. 13760; **Phone:** 866 820-4820 **Fax:** 607 755-7000

²¹ Redlen Technologies, 1763 Sean Heights Central Saanich, BC V8M 1X6, Canada (250) 656-5411

The enabling technology for the ABIS (Automated Baggage Inspection System) is provided by a modular detector system²². This is built around custom linear CZT-detector pixel arrays which are read out by a proprietary signal processing integrated circuit (IC) embodying fast, multiple energy-band output functions. The design of the CZT arrays was modified during subsequent efforts to achieve improved photon-counting performance under high-flux conditions.

More recently²³, a redesign of the readout integrated circuit was undertaken to enhance energy-binning and rate capabilities and address the more practical issue of process longevity. To bring together the benefits of the optimized CZT detector and a new “XENA™” IC (X-ray ENergy-binning Applications), the NEXIS™ (N-Energy X-ray Image Scanning) detector system was developed. NEXIS supersedes the original ABIS design (Figure 7

shows an image taken with the new system) and incorporates features that favor product manufacturability and commercial viability.

In Appendix i and ii, we describe other activities focused on the development of CZT detector arrays for a variety of applications.

Linear x-ray Scanning Devices

An alternate approach to conventional digital cone-beam radiography is to synchronize the scan of a linear x-ray sensor with a narrow fan-beam x-ray source along the imaging field. The advantage of this technique is that allows the scan of large fields while minimizing the sensor area and also minimizing the amount of scattered radiation reaching the detector. The main disadvantages are the need for precise motion control of the source and sensor and

Figure 7: Depiction of a collimated stationary x-ray beam preparing to image a moving object with a stationary sensor.

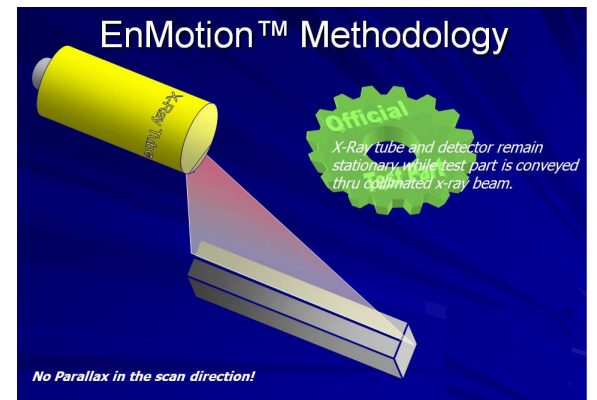


Figure 8: Sens-Tech supplies a range of linear X-ray sensors which use the XDAS detector head and signal processing boards to provide an array of any required length.



²² Developed by NOVA R & D NOVA R&D, Inc., 833 Marlborough Avenue, Suite 200, Riverside, CA 92507-2133, USA

²³ http://s3.amazonaws.com/zanran_storage/www.novarad.com/ContentPages/16825031.pdf

the need to maintain stable x-ray output over the duration of the scan. However, fixing the detector source²⁴ and sensor (Figure 7) can eliminate the potential synchronization problems.

Hamamatsu Photonics has introduced the **C10800** series of “Dual Energy” X-ray Line Scan Cameras specifically designed for imaging materials and objects requiring improved detection and composition classification. The technology allows for combining two radiographs acquired at two distinct energies (high energy and low energy) which allows density as well as other material characteristics to be determined. The vendor offers a variety of combinations of scintillator, filters and gain factor in order to optimize object and X-ray conditions for a users applications. The vendor further suggests contacting the company for information regarding interest in specific or unique applications.



Sens-Tech Ltd (STL) is a UK company which describes itself as “specializing in the supply of X-ray detection and data acquisition systems which are designed for industrial and security applications.” It claims the development of a flexible detection system architecture that enables systems to be customized for specific linescan and CT imaging applications. Descriptions provided by the company show examples of the use of this imaging technology in wood mills, particle board manufacture and steel thickness measurement. The company describes an “XDAS solution” which is alleged to provide a flexible approach for building customized detector configurations. The company supplies a range of linear X-ray sensors which uses an XDAS detector head and signal processing boards to provide an array of any required length. Detector pitch can be 2.5mm, 1.6mm, 0.8mm or 0.4mm. X-rays are detected using silicon photodiodes, with a range of scintillation materials. Gadox (Gd_2S_2O), CsI (Tl) and $CdWO_4$ are used to cover the X-ray energy range of 20keV to 300keV.

²⁴ “EnMotion” is a trademark of the Envision CmosXray LLC, 7800 King Street Anchorage, Alaska 99518. The company also provides an array of imaging devices for service to petroleum interests.

The **X-Scan Imaging Corporation XD8800** and **XDR8800** Series Line-Scan Camera offers dual energy imaging capability to differentiate materials in a variety of inspection applications by simultaneously capturing high-energy and low-energy images. The **XDR8800** Series is a more compact version of the earlier **XD8800 Series**. Specific features include; X-ray energy range options for low (25-100 keV) and high (45-160 KeV) energy imaging, 16-bit A/D conversion, low noise, high sensitivity, variable scan speed with position synchronization.

Appendices

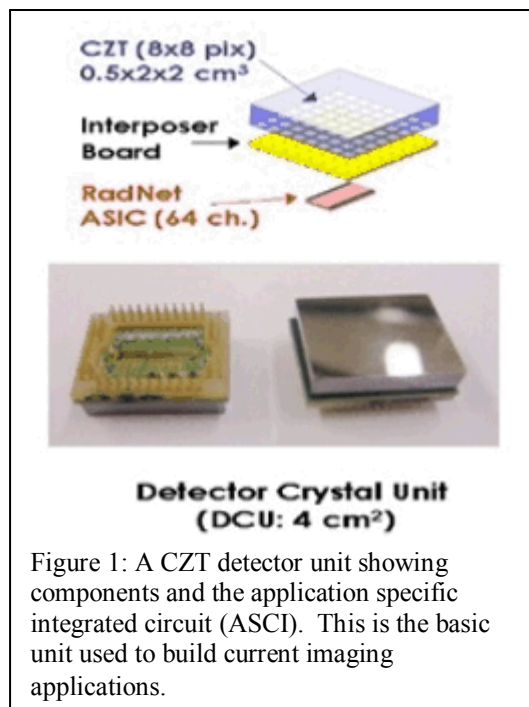
- i. Cadmium Zinc Telluride (CZT) Detectors: Imaging Applications
- ii. The HEXITEC Project
- iii. Scintillators
- iv. Comparison of CMOS Detectors for Mammography
- v. A Collection of Recent Imaging Technology Developments
- vi. Data Sheets for Commercial Medical Imaging Devices (2002 – 2008)
- vii. Detectors and Scintillator Materials; A Survey of Market Availability (Parts 1 and 2)
- viii. Titles

Appendix i: Cadmium Zinc Telluride (CZT) Detectors: Imaging Applications

Robert G. Lanier
December 12, 2011

Executive Summary

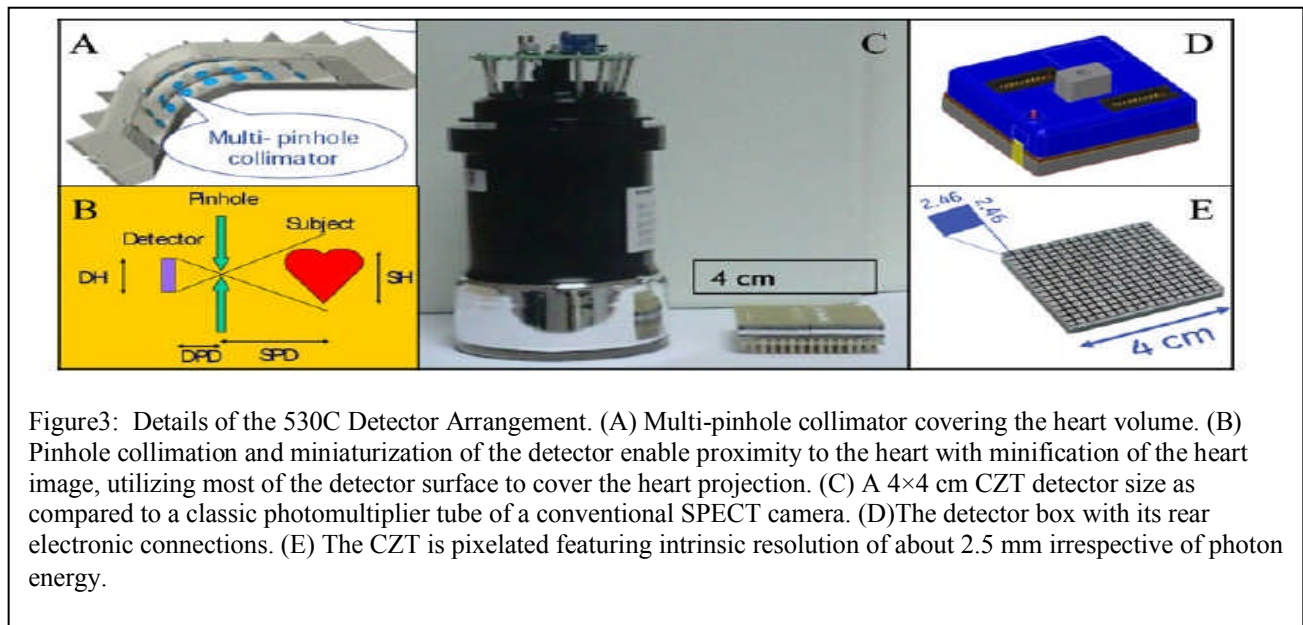
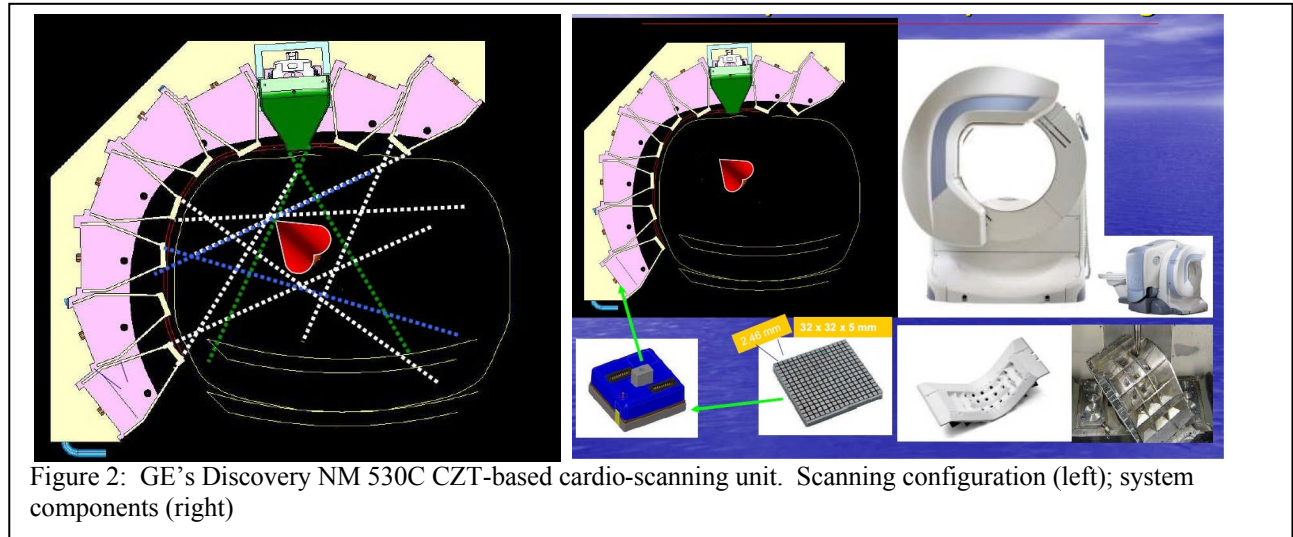
Over the last two decades, the semiconductor CdZnTe (CZT) has emerged as the material of choice for room temperature detection of hard X-rays and soft γ -rays²⁵. The techniques for growing the crystals, the design of the detectors, and the electronics used for reading data from the detectors have been considerably improved over the last few years²⁶. Moreover, the development of direct deposition methods for polycrystalline materials offers a promising route to large area imaging devices in the future. In what follows, a snapshot of the current state of the technology is presented. The discussion includes selected examples of both practical applications and results of forward-looking research.



While a variety of devices have been made for commercial imaging applications and tagged with a variety of brand names, their basic CZT detector element is similar to the one shown in Figure 1. That is, non-pixelated crystals larger than $\sim 4\text{cm}^2$ and thicker than about 7.5 – 10 mm have generally not been reported. The applications encountered use arrays of these crystal elements in various collimated and non-collimated configurations.

²⁵ The items described in this report are from approximately 2009 or later.

²⁶ See for example H. Krawczynski, I. Jung, J. Perkins, A. Burger, M. Groza, Proc. SPIE 5540 (2004) 1. astro-ph/0410077; H. Chen, S.A. Awadalla, F. Harris, et al., IEEE Trans. Nucl. Sci. 55 (2008) 1567 and Q. Li, A. Garson, P. Dowkontt, J. Martin, et al., in: Proc. NSS/MIC conference, 484, 2008. Available from: arXiv:0811.3201.



In the field of medical applications, CZT detectors present viable options for Positron Emission Tomography (PET) and Single Photon Emission Computed Tomography (SPECT). Space borne applications and those anticipated to be useful for US Homeland Security purposes include the development of coded mask and Compton imaging detectors for detection, localization, and identification of radiation sources²⁷.

²⁷ A. Zoglauer, M. Galloway, M. Amman, S.E. Boggs, J.S. Lee, P.N. Luke, L. Mihailescu, K. Vetter, C.B. Wunderer, 2009, IEEE Nuclear Science Symposium Conf. Rec. (NSS/MIC), 887 Available from: doi:10.1109/NSSMIC.2009.5402475 and J.M. Mitchell, C.E. Seifert, IEEE Trans. Nucl. Sci. 55 (2008) 769

Other compound semiconductor materials, notably GaAs, InP, TIB and HgI₂ continue to develop as material quality improves. However, for these materials the best spectroscopic results are limited to a very small number of limited applications and research devices²⁸.

As anecdotal evidence of present and future commercial interest in CZT materials, in February 2011, GE completed the acquisition of the assets of Orbotech Medical Solutions Ltd. (OMS), a subsidiary of Orbotech Ltd²⁹. The company manufactures the CZT detectors used in its "Alcyone" technology applications.

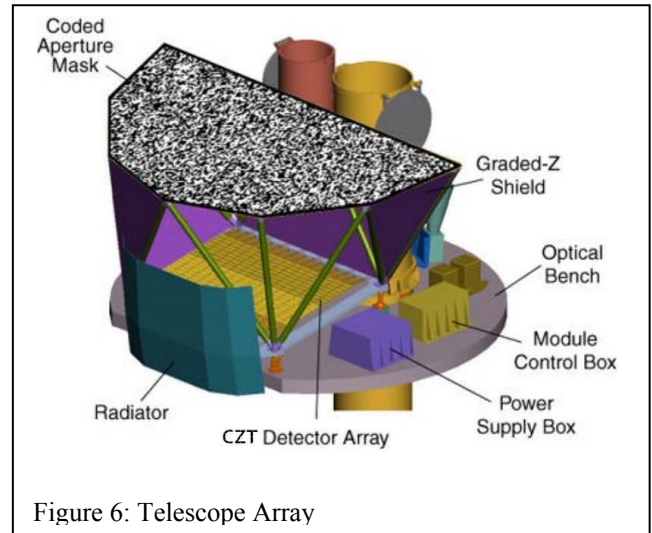


Figure 6: Telescope Array

Selected Applications, Research Reports and Fabrication Options

(1) The GE Discovery NM530C Imaging System

CZT technology³⁰ has been implemented in GE's nuclear cardiology platform, the Discovery NM 530C imaging system, where the radiation detectors are combined with a total of 19 detector heads appropriately arranged for cardiac scanning applications. The detector heads are directed towards the heart and the region around it. The target volume is a sphere of approximately 19 cm in diameter. Figure 2 shows more details of the components; Figure 3 expands on the details of the detector arrangement and compares it to standard PM technology units; and, finally, Figure 4 shows more detail of the collimator design. The D-SPECT imaging system from Spectrum Dynamics uses identical technology.

(2) Thick CZT Detectors

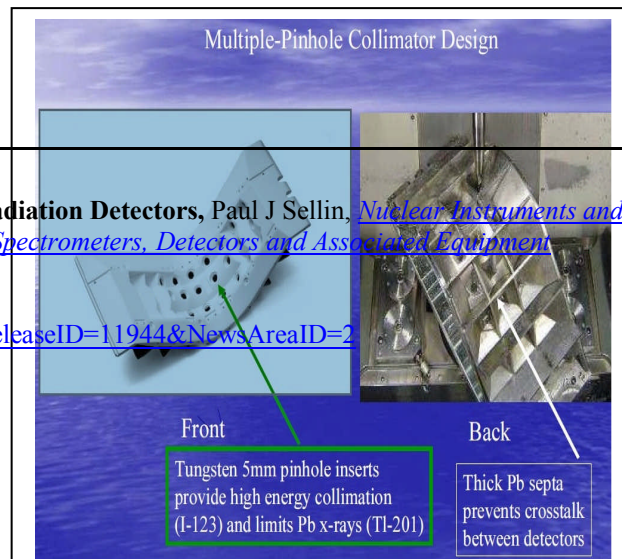


Figure 4: NM 530C Collimator Design

²⁸ **Recent Advances in Compound Semiconductor Radiation Detectors**, Paul J Sellin, *Nuclear Instruments and Methods in Physics Research Section A: Accelerators, Spectrometers, Detectors and Associated Equipment* Vol 513, Issues 1-2, 1 November 2003, Pages 332-339

²⁹ <http://www.genewscenter.com/content/detail.aspx?ReleaseID=11944&NewsAreaID=2>

³⁰ Referred to by GE as "Alcyone" technology.

Burst Telescope Parameters	
Property	Description
Aperture	Coded mask
Detecting Area	5200 cm ²
Detector	CdZnTe
Detector Operation	Photon Counting
Field of View	1.4 sr (partially coded)
Detection Elements	256 modules of 128 elements
Detector Size	4mm x 4mm x 2mm

Recent research reports³¹ on the systematic tests of thick (≥ 0.5 cm) CZT detectors with volumes between 2 cm³ and 4 cm³. The detectors studied achieved Full Width Half Maximum (FWHM) energy resolutions of 2.7 keV (4.5%) at 59 keV, 3 keV (2.5%) at 122 keV and 4 keV (0.6%) at 662 keV. The 59 keV and 122 keV energy resolutions are claimed to be among the world-best results for ≥ 0.5 cm thick CZT detectors. The data set is further used to study trends of how the energy resolution depends on the detector thickness and on the pixelpitch. The research reports no clear trends, indicating that achievable energy resolutions are largely determined by the properties of individual crystals. Finally, the researchers note that the results are achieved without applying corrections to the anode signals for the depth of the interaction. This implies that knowing and correcting for the interaction depth does not seem to be a pre-requisite for achieving sub-1% energy resolutions at 662 keV. Figure 5 shows some samples of thick, pixilated CZT detectors.

(3) The CZR Burst Alert Telescope

The Burst Alert Telescope (BAT) is a highly sensitive, large field of view instrument designed to provide critical data on gamma ray bursts (Figure 6). It is a coded aperture imaging instrument with a 1.4 steradian field-of-view with x-ray sensitivity in the energy range of 15-150 keV for coded imaging and a non-coded response up to 500 keV. The instrument uses a two-dimensional coded aperture mask (see Figure 6) and a large area solid state detector array (Figure 7) to detect weak bursts, and has a large field of view. The table shows the telescope parameters.

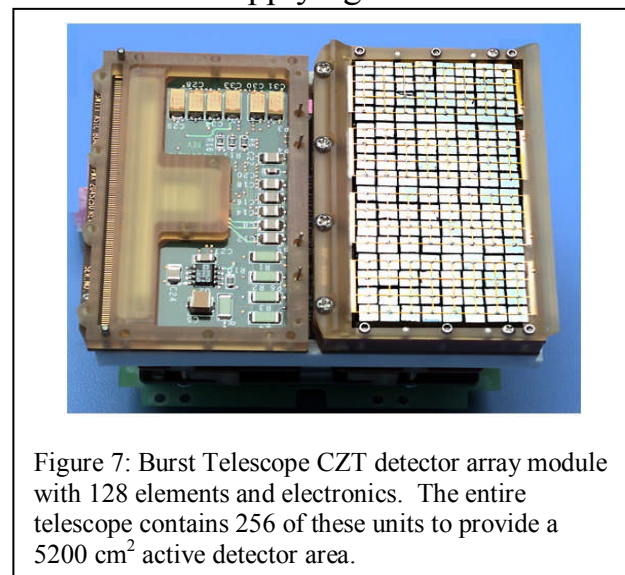


Figure 7: Burst Telescope CZT detector array module with 128 elements and electronics. The entire telescope contains 256 of these units to provide a 5200 cm² active detector area.

³¹Study of Thick CZT Detectors for X-ray and Gamma-Ray Astronomy; Qiang Lil., M. Beilicke, Kuen Lee, Alfred Garson III, Q. Guo, Jerrad Martin, Y. Yin, P.Dowkontt, G. De Geronimo, I. Jung, H. Krawczynski, *Astroparticle Physics*, **34**, 769 – 777 (2011)

(4) A modular high-resolution photon-counting x-ray detector

Researchers³² at Radiation Monitoring Devices Inc³³ claim to be developing a family of modular, highly configurable photon-counting, energy-discriminating, high-resolution imaging devices based on a novel combination of cadmium zinc telluride (CdZnTe) semiconductor radiation sensors and high-resolution custom application-specific integrated circuits. The concept, identified as an “Advanced Photon Counting Detector™ (APCD) module, is to combine these two high-performance components into small (e.g., 1x 1cm² and 2x 2cm²/ modules that tile seamlessly, forming detectors of arbitrary size and 2- or 3D shape (see Figure 8). It is expected that APCD components and APCD-based detectors will be designed for applications such as medical x-ray CT and munitions inspection, as well as for medical and nonmedical x-ray CT and radiography in general. APCD devices are also intended to be used to read out other solid-state sensors in addition to CdZnTe. Finally, the APCD design is also being upgraded to read out scintillators.

Each APCD module consists of a monolithic sensor (e.g., CdZnTe) of appropriate thickness to absorb X-rays, coupled to a CMOS APCD chip, incorporating at least 40 x 40 pixels of 250 x 250 μm per pixel or smaller (Figure 9). Each individual pixel will independently support a data rate high enough

³² See for example S. Kleinfelder, S. Lim, X. Liu, A. El Gama pixel sensor, *IEEE J. Solid-State Circuits* 36, pp. 2049, 2001. Kleinfelder, Fast high-resolution and multi-energy x-ray imag CZT arrays, SPIE Opt. Photon. Conf., 2010. Presentation 780 Solid-state photon-counting hybrid detector array for high-res *Symp. Radiat. Meas. Appl. (SORMA XII)*, 2010. Paper 0126

³³ Radiation Monitoring Devices, Inc; 44 Hunt Street; Watert LEAD-RMD (800-532-3763); Fax: 617-926-9980; Email: info@rmd.com

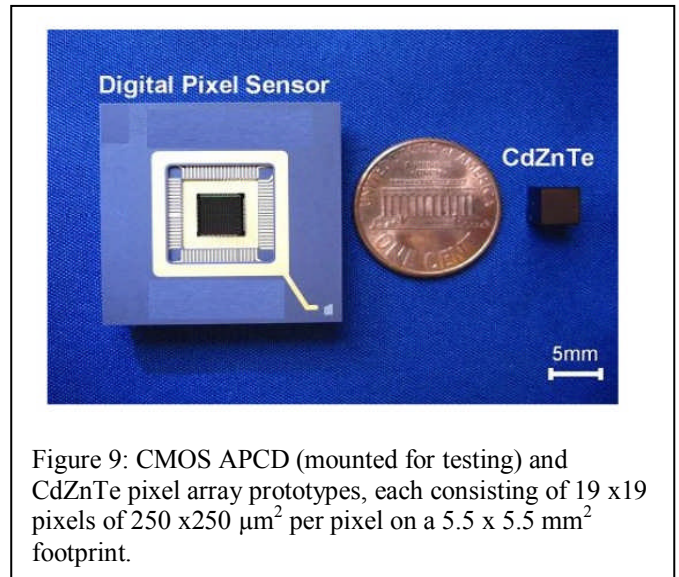


Figure 9: CMOS APCD (mounted for testing) and CdZnTe pixel array prototypes, each consisting of 19 x 19 pixels of 250 x 250 μm² per pixel on a 5.5 x 5.5 mm² footprint.

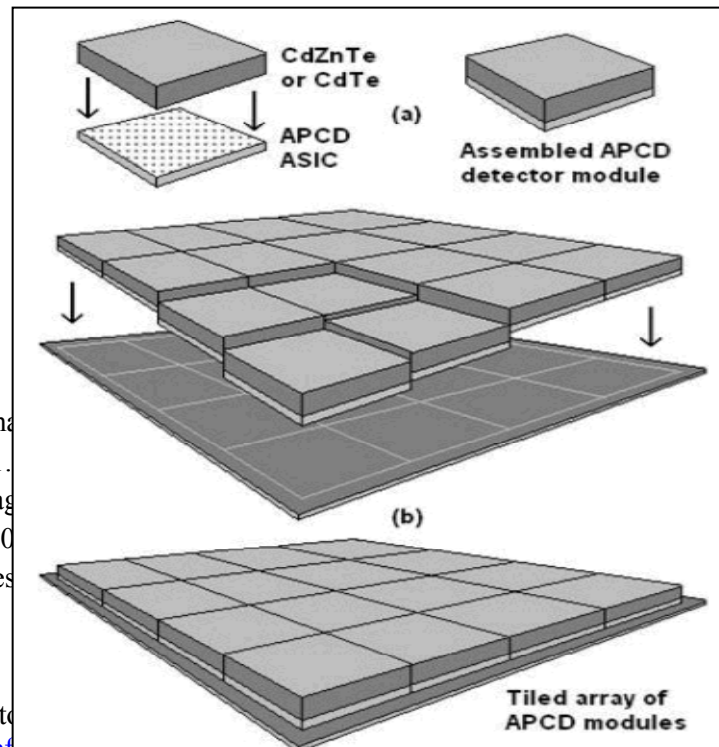


Figure 8: (a) CdZnTe or CdTe sensors will be bump-bonded to the APCD application-specific integrated circuit (ASIC) CMOS chips to form the APCD detector modules (e.g., a 2 x 2 cm² module of 80 x 80 pixels) (b) Modules may then be tiled to form APCD detectors, continuous pixel arrays of arbitrary size.

to effectively measure individual source X-rays, even at high flux. APCD modules will mount mechanically on a motherboard containing the necessary power, ground, control, and readout electronics, and can be individually removed and replaced for service.

Appendix ii: The HEXITEC Project

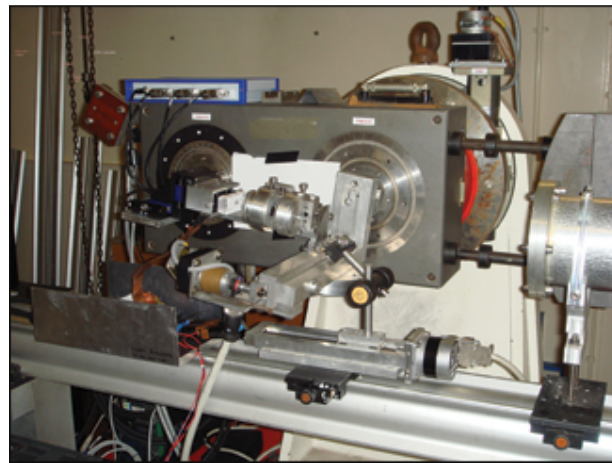
Robert G. Lanier
January 10, 2012

In 2006 English researchers began a collaborative program to develop CZT detector technology for various applications. The program was identified as the HEXITEC project (High Energy X-ray Imaging Technology) and involved five principle investigators at various English institutes with focused responsibility on the various elements of the research. The following view graphs describe the overall scope of the four-year, well-funded (£3 million) project.

Subsequent work in the intervening years has led to a color 3D X-ray system that allows material at each point of an image to be clearly identified. The technique is termed TEDDI (Tomographic Energy Dispersive Diffraction Imaging). The researchers claim that the technique has applications across a wide range of disciplines including medicine, security scanning and aerospace engineering.

The TEDDI method is claimed to be highly applicable to biomaterials, with the possibility of specific tissue identification in humans or identifying explosives, cocaine or heroin in freight. It could also be used in aerospace engineering, to establish whether the alloys in a weld have too much strain.

In the development of this technology two major challenges were overcome, which would be expected to have a positive impact on the overall future development of the technology:



University of Manchester researchers use this experimental setup as they work to develop a "color" X-ray scanner that uses additional wavelengths of light to detect the object's chemical structure. The technique is called tomographic energy dispersive diffraction imaging (TEDDI)

- The first was to produce pixellated spectroscopy grade energy-sensitive detectors. This was carried out in collaboration with Rutherford Appleton Laboratory, Oxford and Daresbury Laboratory, Cheshire.
- The second challenge was to build a device known as a 2D collimator, which filters and directs streams of scattered X-rays. The collimator device needed to have a high aspect ratio of 6000:1, meaning that its width to its length is more than that of the channel tunnel.

This collimator was built using a laser drilling method in collaboration with The University of Cambridge.

Further details on the HEXITEC project development have been reported. Three individual collections of related information on HEXITEC are appended to this report. These include:

- Viewgraphs outlining the original scope of the project
- A refereed publication document describing the development of the electronic interface (ASIC). The ASIC (application specific integrated circuit) provides charge preamp, shaping and peak detect on each pixel above a programmable threshold.
- Viewgraphs showing a general overview of related developments from the research



The HEXITEC Project

High Energy X-ray Imaging Technology

Focussed on large area pixellated CZT detectors

£3Million EPSRC funded project

4 year program involving 5 institutes

- also involves networks of application institutes and organisations

Started 2006

HEXITEC Project objectives

- fabricate large area CZT detector material for X-ray imaging
- characterise to improvement material performance
- develop cutting/polishing/contact-deposition and passivation techniques
- develop bump-bonding techniques for CZT
- develop pixellated spectroscopy ASIC for CZT
- insert this technology into a diverse network of scientific users
- create a sustainable base for continued CZT detector production

28.9.07 Barcelona

Hexitec

Paul Seller, RAL

HEXITEC Investigators (In order of functions)

Dr Andrew Brinkman, Durham University

- growth of 3 inch CZT by fast PVD (commercialised for CdTe PVD)

Dr Paul Sellin, Surrey University

- CZT characterisation (PL mapping, PICTS, IBIC, Alpha TOF, NCR mapping)
- development of contacts and passivation

Paul Seller, CCLRC

- detector fabrication from raw material
- detector characterisation (Spectroscopy, noise/temperature, small-pixel effect)
- large area ASIC development

Prof Bob Cemik, The University of Manchester Principle Investigator

- lead of Application Networks
 - Imaging + tomography for engineering
 - Space Science
 - Synchrotrons
 - Security
 - Medical and biological

Prof Paul Barnes, Birkbeck College London Materials Imaging Network

- TEDDI

28.9.07 Barcelona

Hexitec

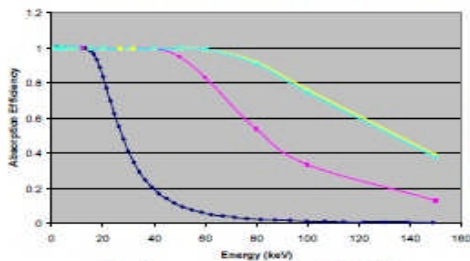
Paul Seller, RAL

CZT room-temp semiconductor detector

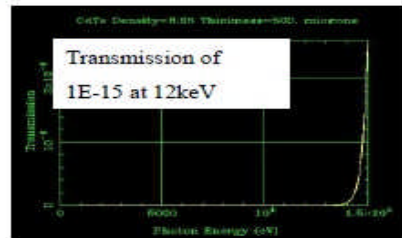
CZT has been proposed as good stopping power material and gives radiation-hard detectors in proton environments (HEP and space)

There is good reason believe it is good in low energy X-ray systems

- do not have oxide interfaces
- heavier atom than Si so low bulk damage



Usual reason to choose High-Z



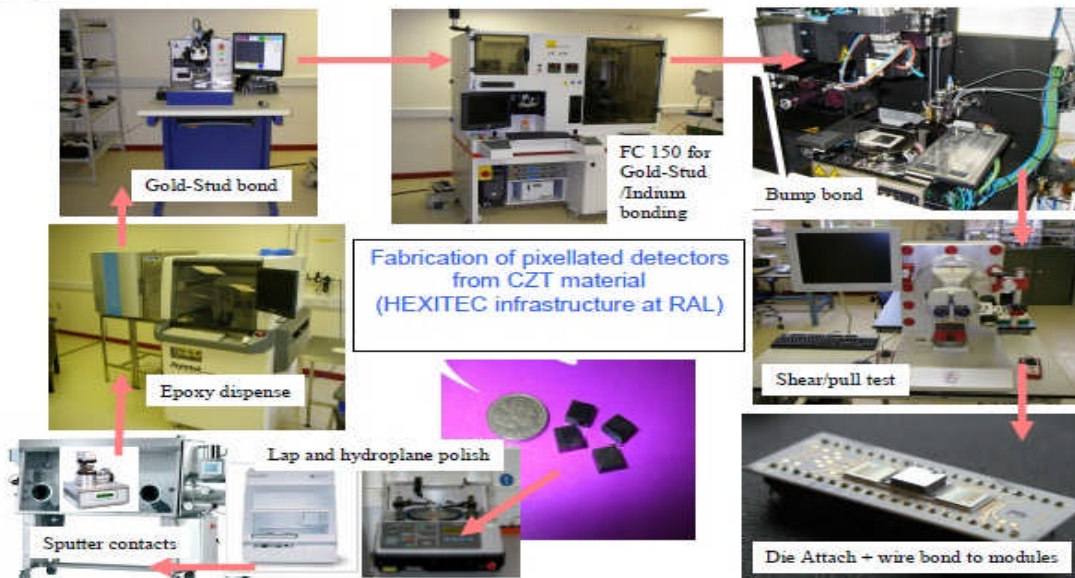
Another possible reason

- stop most of the X-rays so shield ASICs and bonding interface

28.9.07 Barcelona

Hexitec

Paul Seller, RAL



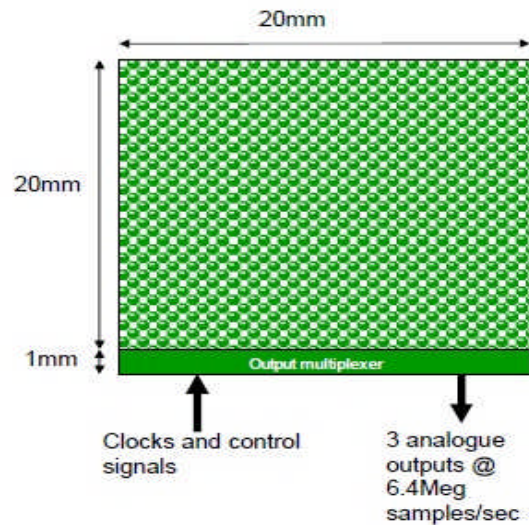
28.9.07 Barcelona

Hexitec

Paul Seller, RAL

HEXITEC ASIC OVERVIEW

- Bump bonded readout chip for CZT
- 80*80 pixels each 250um* 250um
- 1keV to 150keV dynamic range (x10 option)
- 200eV FWHM noise
- Sequential Rolling shutter readout (not data driven)
- Intended for 2mm thick CZT material
- 1000 frames a second (variable) readout rate



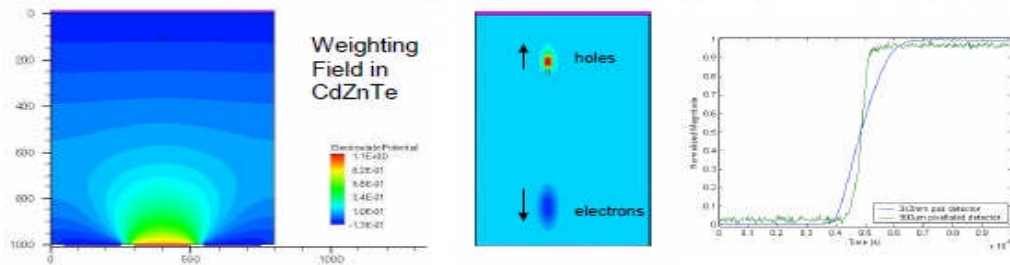
28.9.07 Barcelona

Hexitec

Paul Seller, RAL

HEXITEC ASIC: Simulations and measurements

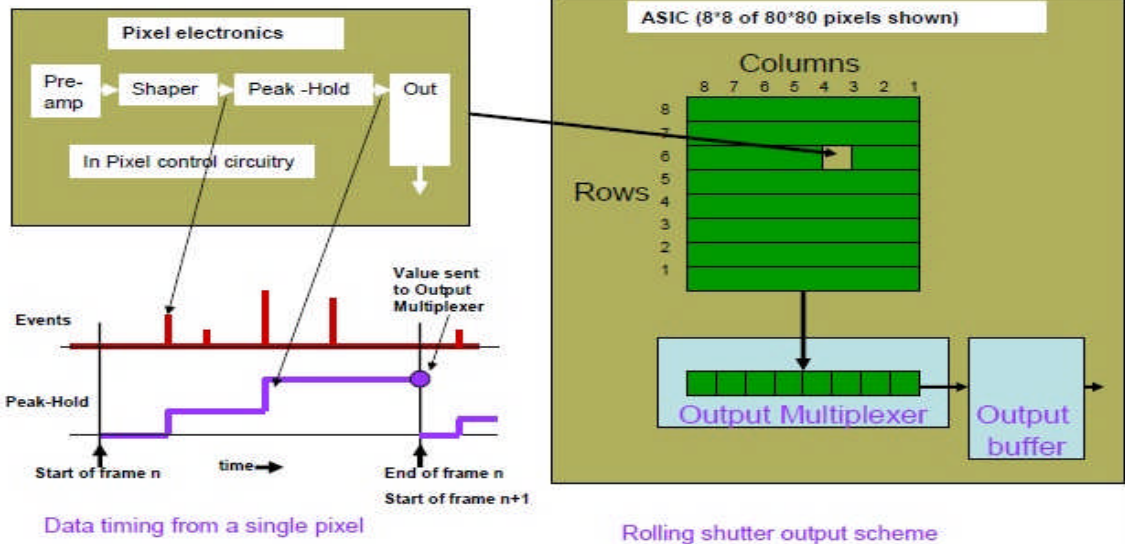
- With 250um pixels and 2mm thick detectors the small-pixel effect is quite strong
- See $\ll 1\mu\text{s}$ rise-time signals due to the electrons moving when close to the anode contact. Do not see the several microsecond electron and hole transit times through bulk
- Can chose a faster shaping time without significant ballistic deficit



28.9.07 Barcelona

Hexitec

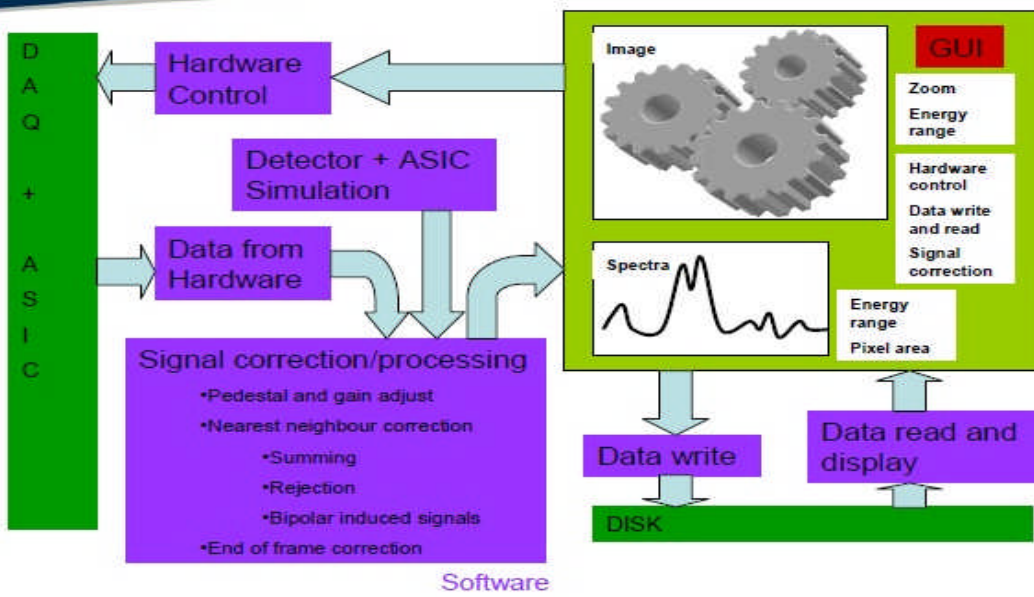
Paul Seller, RAL



28.9.07 Barcelona

Hexitec

Paul Seller, RAL



28.9.07 Barcelona

Hexitec

Paul Seller, RAL



Contents lists available at ScienceDirect

Nuclear Instruments and Methods in Physics Research A

journal homepage: www.elsevier.com/locate/nima

HEXITEC ASIC—a pixellated readout chip for CZT detectors

Lawrence Jones^{*}, Paul Seller, Matthew Wilson, Alec Hardie

STFC Rutherford Appleton Laboratory, Didcot OX11 0QX, UK

ARTICLE INFO

Available online 11 February 2009

Keywords:

X-ray
CdZnTe
Readout ASIC
Clock driven
Gold stud-bonded

ABSTRACT

HEXITEC is a collaborative project with the aim of developing a new range of detectors for high-energy X-ray imaging. High-energy X-ray imaging has major advantages over current lower energy imaging for the life and physical sciences, including improved phase-contrast images on larger, higher density samples and with lower accumulated doses. However, at these energies conventional silicon-based devices cannot be used, hence, the requirement for a new range of high Z-detector materials. Underpinning the HEXITEC programme are the development of a pixellated Cadmium Zinc Telluride (CZT) detectors and a pixellated readout ASIC which will be bump-bonded to the detector. The HEXITEC ASIC is required to have low noise (20 electrons rms) and tolerate detector leakage currents. A prototype 20×20 pixel ASIC has been developed and manufactured on a standard $0.35 \mu\text{m}$ CMOS process.

© 2009 Elsevier B.V. All rights reserved.

1. Overview

Cadmium Zinc Telluride (CZT) is a particularly attractive material for direct conversion semiconductor X-ray detectors. It has been demonstrated that pixellated devices down to $55 \mu\text{m}$ geometry can function with acceptable spectroscopic (colour X-ray) performance [1]. The HEXITEC ASIC has been designed specifically to provide very good spectroscopy for every incident photon at the expense of speed of acquisition. Our target applications (including synchrotron diffraction and tomography experiments as well as space science imaging) require very good energy resolution, and as a secondary requirement want speed. This later requirement is handled by the region of interest features, which allow fast readout in specified areas. Also this architecture which reads out all pixels, allows detector charge sharing and other correction algorithms to be investigated off-line.

The HEXITEC ASIC consists of 20×20 pixel on a pitch of $250 \mu\text{m}$. Each pixel contains a $52 \mu\text{m}$ bond pad which can be gold stud-bonded to a CZT detector. Fig. 1 shows a block diagram of the electronics contained in each HEXITEC ASIC pixel. Charge is read out from each of the CZT detector pixels using a charge amplifier, which has a selectable range and a feedback circuit which compensates for detector leakage currents up to 50 pA .

The output from the each charge amplifier is filtered by a $2 \mu\text{s}$ peaking circuit comprising a CR-RC shaper followed by a second-order low-pass filter. A peak hold circuit maintains the voltage at the peak of the shaped signal until it can be read out.

Three track-and-hold buffers are used to sample the shaper and peak hold voltages sequentially prior to the pixel being read

out. When readout occurs, the output from the pixel comprises the two samples from the shaper output and the one sample of the peak hold output. These three signals are used to veto-incorrect peak hold data due to partly developed signals or incorrect peak hold reset levels. Switches are enabled which connect 1 pixel in each column of the pixel array to shared column outputs. A calibration circuit is included for characterizing the pixel electronics.

Readout logic controls the sequencing of data from the HEXITEC ASIC pixel array. Fig. 2 shows a block diagram of the top level of the ASIC. For simplicity the chip uses a completely clock-driven architecture.

Three programmable registers can be used to define regions of interest within the pixel array. The first register defines the regions that will be read out, the second defines regions which will be powered down, and the third defines regions where the calibrate circuit is enabled.

The HEXITEC ASIC pixel array is read out using a rolling shutter technique. A row select register is used to select the row which is to be read out. The data from each pixel becomes available on all column outputs at the same time, and at this point the peak hold circuits in that row can be reset to accept new data. The data being held on the column output is read out through a column multiplexer. The column readout rate is up to 25 MHz and the total frame rate depends on the number of pixels being read out.

2. Functional description

2.1. Preamplifier

The preamplifier employs a single-ended folded-cascode architecture and has selectable input range of either 40 000 or

^{*} Corresponding author. Tel.: +441235446508; fax: +441235446508.
E-mail address: L.Jones@stfc.ac.uk (L. Jones).

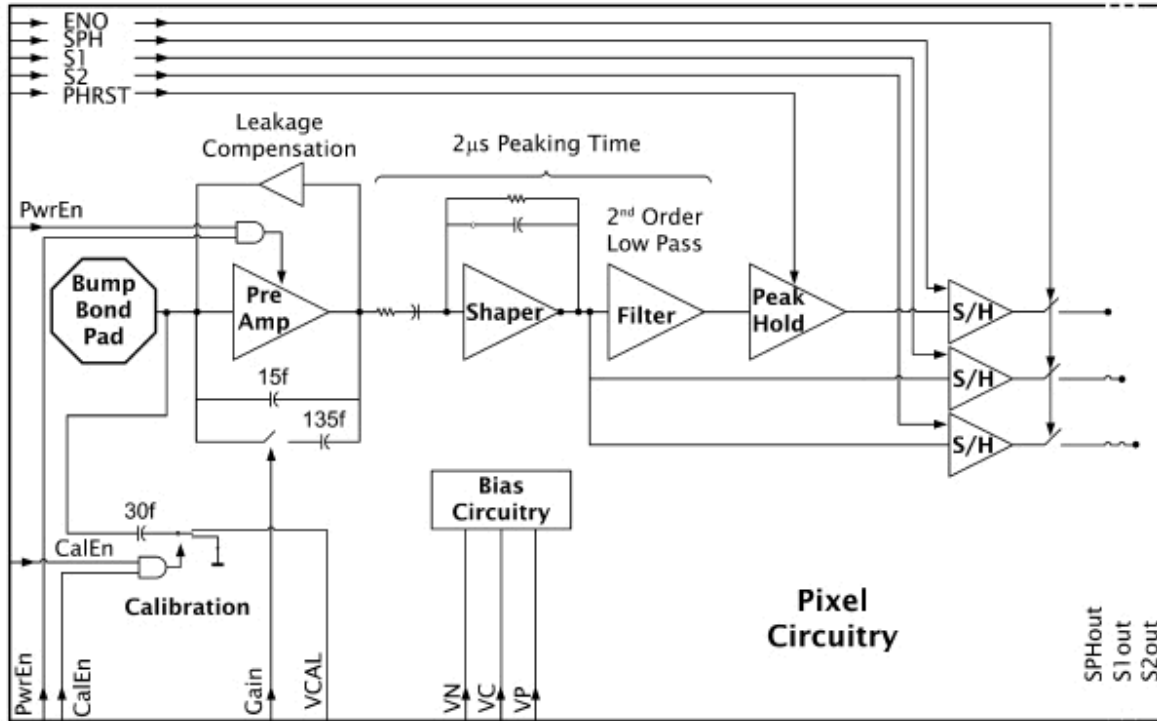


Fig. 1. Block diagram of pixel electronics.

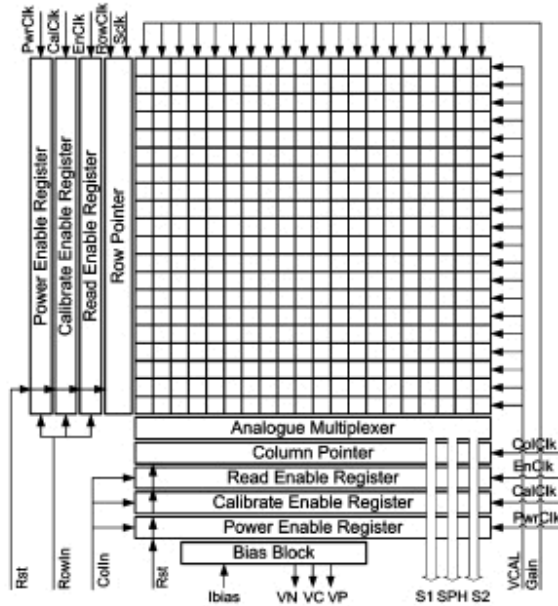


Fig. 2. Block diagram of the top level of the chip.

400000 electrons. A feedback circuit [2] provides DC stability and can source up to 250 pA of detector leakage current. The preamplifier input FET is biased at 1.65V to reduce power

consumption and can be powered down further by selecting a lower bias current through the FET. At this lower bias level the preamplifier remains operational but has higher electronic noise.

There are two main noise contributors within the preamplifier. The thermal noise of the input FET has been minimized by matching the size of this device to that of the detector capacitance and applying the maximum possible bias current within specification. The second major contribution is the current noise of the feedback circuit at the input to the preamplifier. In addition, there is an external noise contribution from the shot noise of the detector leakage current [4]. The noise specification for the ASIC has been defined at 5 pA detector leakage current.

2.2. Noise filtering

A band pass is used to filter noise and to improve double pulse resolution. A CR-RC type configuration is used employing a single-ended folded-cascode architecture as with the preamplifier.

Normally, shaping time is optimised to equalize the contributions of the major noise sources within a circuit. Longer shaping times reduce the thermal noise of the preamplifier input FET and shorter shaping times reduce the current noise of the preamplifier feedback circuit and the detector leakage. It was not possible to optimise the circuit in this way since the optimum shaping time was found to be too short for applications involving CZT detector signals, where charge collection times can be in the region of 1 µs. A compromise was reached, and the shaping time is set to 1.25 µs. However, the CR-RC circuit alone cannot filter out enough of the noise to meet the specification.

A second low-pass filter is used to attenuate the high-frequency noise at the output of the CR–RC shaper. The filter employs a second-order low-pass architecture and is required to filter excessive noise in the 1–10 MHz region. The effect on the pulse peaking time is to increase it to 2 μ s at the output of the low-pass filter (Figs. 3).

2.3. Data sampling

The peak amplitude of the filter output needs to be held long enough for it to be sampled prior to readout. This time will vary depending on when the signal occurs within a readout frame, and how many pixels have been selected for readout. This function is performed by the *peak hold* circuit [3]. A signal peak is held until its voltage can be sampled by a sample and hold circuit prior to readout, after which time the peak hold circuit is reset (Figs. 4).

However, there are two problems with the operation of the peak hold circuit which have to be addressed. Firstly, if peak hold

circuit reset occurs during the tail end of a filter signal, the circuit will not reset to the correct voltage level. If this happens, the peak hold circuit will not be able to see further signals whose magnitude is less than this voltage. Secondly, the peak hold circuit may be read out before a filter signal has fully formed. In this case the value read from the peak hold circuit will be incorrect.

It is necessary to determine when the peak hold signal has been sampled with respect to active signals on the filter output. This is to be done by sampling the filter output twice, one sample occurring before and the other occurring after the peak hold are sampled. A simple algorithm can then reject corrupt data.

2.4. Readout

A full-frame readout only requires three external control signals. *RowClk*, *ScIk*, and *ColClk* Fig. 5 shows a full-frame readout for a 5 rows and 5 column array of pixels. Prior to the readout cycle, the *Read Enable Register* should be programmed with the required rows and columns to be read out.

The *Row Pointer* is a shift register which controls the row which is being read out. It is clocked by the signal *RowClk* and shifts through only those rows which are programmed into the *Read Enable Register*, skipping over all those rows which are not. The signal *ScIk* is global to the chip but is used to generate the control signals internal to the row being read out. These control the peak hold circuit, sample and hold circuits, and the column output.

Like the *Row Pointer*, the *Column Pointer* controls which columns are to be read out through the analogue multiplexer. The *Column Pointer* reads only those columns programmed into the *Read Enable Register*. It is controlled using the signal *ColClk*, and the maximum clock period at which this can run is limited by the column-to-column readout speed which is about 40 ns. Data on each of the columns to be read out are multiplexed and buffered off the chip.

At the start of a frame readout, the *row pointer* and *column pointer* are both in a parked position. The first clock pulses on *RowClk* and *ColClk* move them to the first row and column to be read out. This means that at the end of a row readout cycle, an extra clock pulse is required on *ColClk* to return the *column pointer* to its parked position. Similarly, at the end of a full-frame readout, the *Row Pointer* must be returned to its parked position by *RowClk*.

Data appear on the outputs synchronized with *ColClk*. The dynamic output range is 1 V.

3. Status

The present status of the project is that a 20 \times 20 pixel prototype has been designed and manufactured but not yet tested. However, a smaller 1 pixel test structure has been tested to verify the design of the preamplifier, shaper, filter, and peak hold circuit.

Due to the low-bias currents in the preamplifier feedback circuit there was uncertainty in the accuracy of the transistor

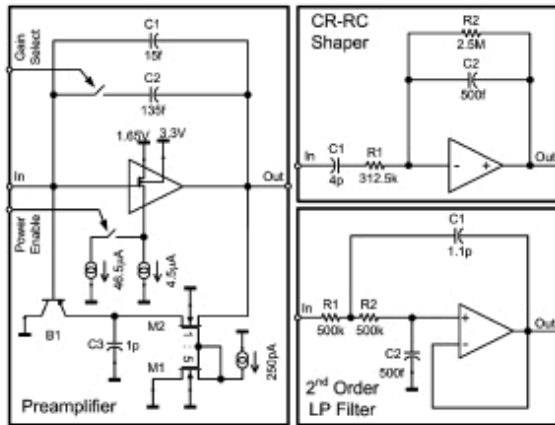


Fig. 3. Schematics of the preamplifier, shaper, and the second-order low-pass filter in the pixel electronics.

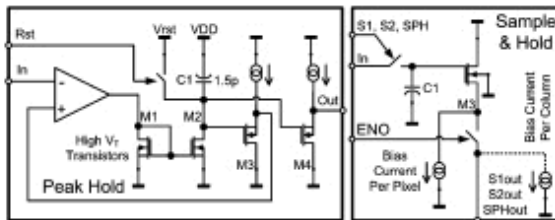


Fig. 4. Schematics of the peak hold circuit and the sample and hold circuit in the pixel electronics.

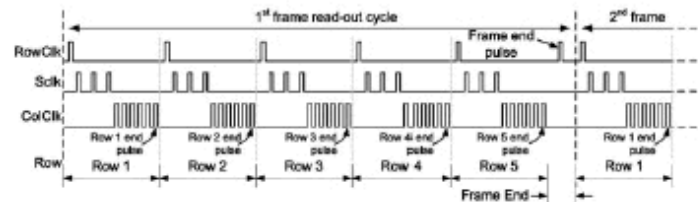


Fig. 5. External control signals for a 5 \times 5 array of pixels.

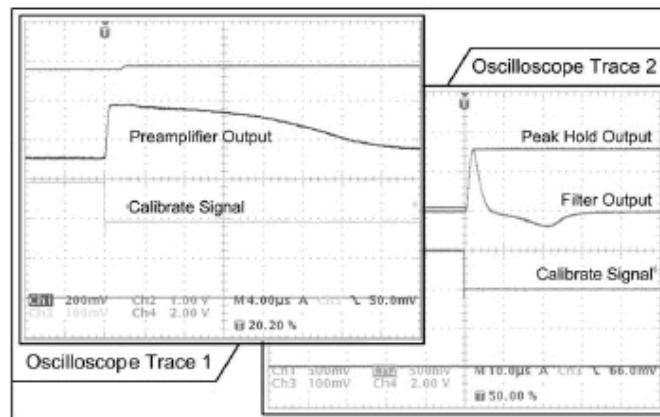


Fig. 6. Test results from a single-pixel test structure, showing output from the preamplifier, filter, and peak hold circuit.

simulation models. In addition, it was found during simulation that for certain process corners and temperatures the peak hold circuit suffered from droop due to sub-threshold currents in the transistors. It was decided to manufacture a test structure to verify the design of the pixel electronics. Fig. 6 shows some results which confirm this.

4. Conclusions

A prototype ASIC has been designed and manufactured for readout of pixellated CZT detectors. For simplicity, it has a completely clock-driven architecture. Following testing, an 80×80 pixel version of this will be manufactured.

Acknowledgements

HEXITEC is a collaboration between the universities of Manchester, Durham, Surrey, Birkbeck college and STFC. It is funded by EPSRC.

References

- [1] A. Shor, Y. Eisen, I. Mardor, Nuclear Instruments and Methods A 458 (2001) 42.
- [2] G. De Geronimo, P. O'Connor, V. Radeka, B. Yu, Nuclear Instruments and Methods in Physics Research A 471 (2001) 192.
- [3] G. De Geronimo, P. O'Connor, A. Kandasamy, Instruments and Methods in Physics Research A 484 (2002) 533.
- [4] P.N. Luke, M. Amman, J.S. Lee, P.F. Manfredi, IEEE Transactions on Nuclear Science NS-48 (3) (2001).



CdZnTe Energy Resolving Array Detectors

Paul Seller

Rutherford Appleton Lab

Acknowledgements:-

Many thanks to Matt Wilson, Matt Veale and Lawrence Jones and others at RAL.

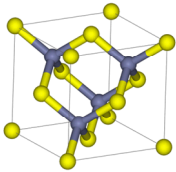
Also thanks for the work illustrated here from the Universities of Surrey, Manchester and Durham.

CZT Energy Resolving arrays

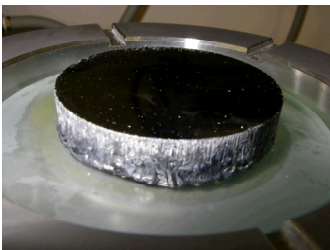
Paul Seller, RAL



Material



•CdTe Zinc-blend structure



3 inch Durham University CZT

- CdTe is a black looking crystal
- CZT has the Cd sites substituted for Zn. Mostly used as substrate for HgCdTe growth. (This substrate material is not detector grade.)
- Typically detectors are $\text{TeCd}_{1-x}\text{Zn}_x$ (x from 3% to 10%)
- Piezo-electric crystal so inherently micro-phonics in parallel plate configuration.
- Also Birefringent so can look at internal strains and fields with polarisers.
- Hard and very brittle (handle with care).
- Carcinogenic and accumulative.
- Produced at 1100C by HP Bridgeman, Travelling Heater and Multi Tube Physical Vapour Transport (PVD).
- Thin Layers by CSS or HWE 550C growth substrate but need to lattice match substrate.

Energy Resolving CZT arrays

Paul Seller, RAL

Properties

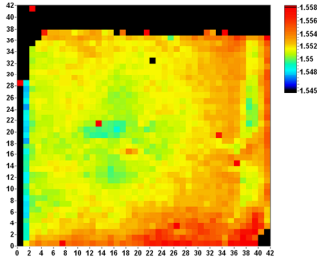


Photo luminescence map Band-gap and thus %Zn

•Band-gap CdTe= 1.5eV (Si =1.12eV) so room low leakage temperature semiconductor

•This is equivalent to 820nm so transparent to IR light above this wavelength (can see defects with IR)

•Zn added solely to increase Band-gap

$$E_g = 1.505 + (0.631x) + (0.128x^2)$$

•Radiation conversion (w) factor = 4.4eV per electron hole pair (40keV photon gives 10⁴ charge carriers)

•Fano Factor =0.1

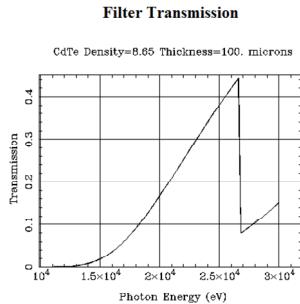
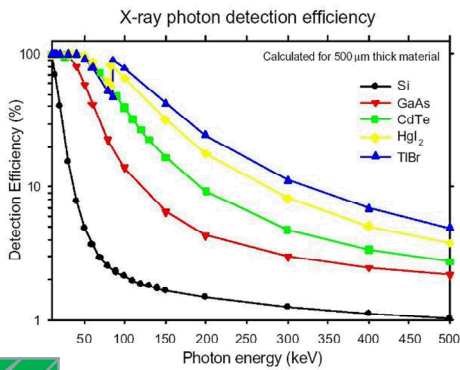
$$noise[\#] = \sqrt{n} \sqrt{F}$$

$$FWHM [eV] = 2.35 * w * \sqrt{n} \sqrt{F}$$

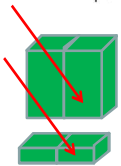
Energy Resolving CZT arrays

Paul Seller, RAL

Radiation Absorption



With thin layers watch the K-edge of Te and Cd at 22-27keV. Very high efficiency at 2mm thickness.

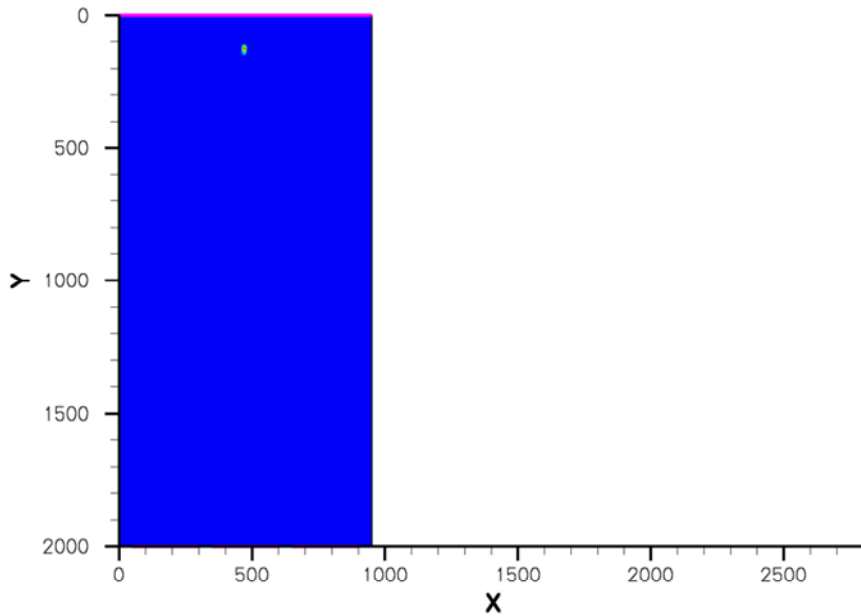


Parallax
With 500um of silicon stopping a 25keV beam a 250um voxel will have 2:1 parallax.

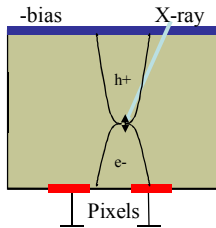
A 100um layer of CZT will have 0.4:1 parallax.

Energy Resolving CZT arrays

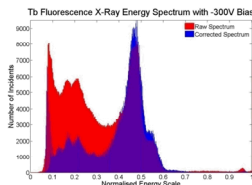
Paul Seller, RAL



Charge transport



- Electron mobility 1000 cm²/Vs (Si=1400)
- Hole mobility 50-80cm²/Vs (Si=480)
- Carrier lifetime ~2us
- $\mu\tau_e$ ~2x10⁻³ cm²/V
- $\mu\tau_h$ ~2x10⁻⁴ cm²/V
- (Holes take 2us to traverse 2mm)
- Charge diffusion ~100um typical for 2mm thick
- Bulk resistivity 3-9 x 10¹⁰ Ohm-cm (CdTe less)
- Leakage current 1nA/mm² (due to mid band states, reduced by Cl doping in CdTe, V or In in CZT)
- Small pixel effect important to give single carrier output signal. (Improves speed and spectrum)



Shockley-Ramo theorem

$$Q = q\phi_0(x)$$

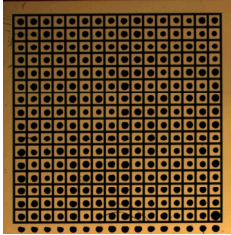
$$i = q\bar{v} \cdot \bar{E}_0(x)$$



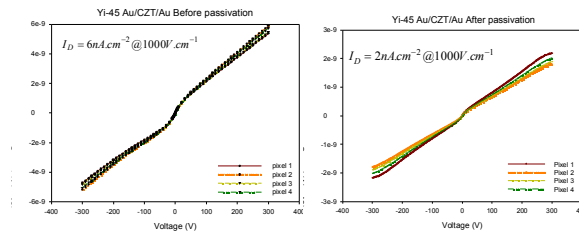
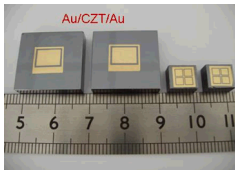
Energy Resolving CZT arrays

Paul Sellar, RAL

Contacts



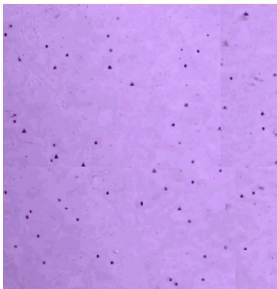
- CZT typically have Au or Pt contacts. Sputtered/evaporated pixels easy.
- CdTe:Cl detectors now can have Indium rectifying anode contacts to reduce leakage and inter-pixel isolation.
- Important to passivate sides to reduce leakage.
- Need to remove surface damage (100-200um) and TeO layers before contacting. Etch with Br:Methanol.
- Contacts increase resistance (less leakage than bulk)



Energy Resolving CZT arrays

Paul Seller, RAL

Manufacturers



Te precipitates

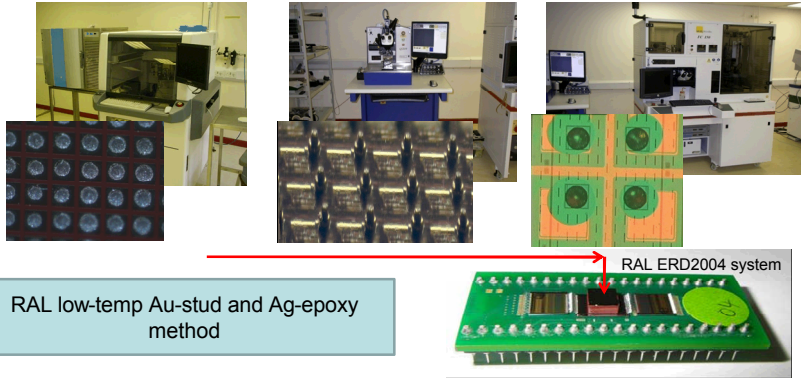
- Te precipitates and inclusions distributed in bulk, decorate twins and grain boundaries
- These cause charge trapping and leakage.
- At high fluxes the trapping (space charge) can distort the internal field and even stop operation (so-called polarisation). Need good hole transport to reduce this ($\mu\tau_h > 10^{-4} \text{ cm}^2/\text{V}$) to get to $>> 10^6 \text{ counts/s/mm}^2$
- Usually anneal the crystal in Cd vapour to reduce inclusions but it might still have trapping sites.
- Watch operating temperature as low temperature increases trapping.
- Can produce large CZT crystals with low trapping:
 - eV Products
 - Redlan
 - Bruker Baltic (only processing)
 - Orbotec
 - Durham University (CZT from Hexitec)
 - AcroRad (CdTe)
 - Kromek (CdTe)
 - Several Universities ????

Energy Resolving CZT arrays

Paul Seller, RAL

Interconnect

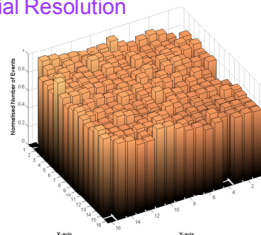
- Because CZT is very brittle and contacts are thin and fragile, difficult to use conventional ultrasonic wire bonding.
- Most CZT devices do not like going above 150C or 120C for a long time. Probably due to redistribution of doping and diffusion of contacts.
- So need a low temperature bonding process.
- Other institutes use Indium bonding but in both cases have to watch diffusion.



Energy Resolving CZT arrays

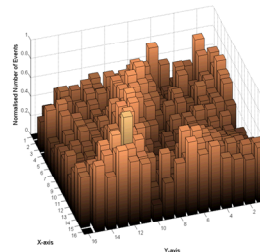
Paul Seller, RAL

Spatial Resolution

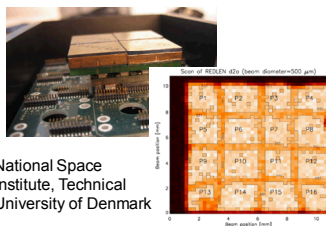


Silicon on ERD2004, uniformity almost at level of statistics.

We believe this is due to charge steering in the array due to space charge in the device. Others suggest it is actually the charge trapping which causes the non-uniformity.

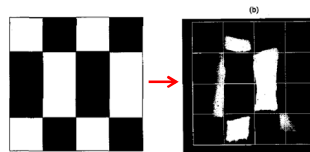


CZT on same ERD2004 device highly non-uniform



National Space
Institute, Technical
University of Denmark

Energy Resolving CZT arrays



BNL. Bolotnikov et al. showing distorted
internal fields in a thick detector.

Paul Seller, RAL

Examples of imaging systems

- Si detectors readout holes, as high-resistivity Si wafers are usually n-type with p+ implanted pixels.
- Holes are slow and get trapped in CZT so not good for pixellated readout.
-Need different pixellated readout electronics for CZT.....

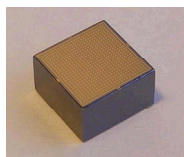
- Existing systems which synchrotron and HEP users are well aware of:
 - Medipix 1-2-3 CERN et. al.
 - Pilatus PSI/Detris
 - XPAD CPPM Marseille
 - MPEC Bonn University
 - CMS tracker, Atlas tracker, old LEP experiments
- Apart from CMS these are photon-counting with threshold not true energy resolving.

Energy Resolving CZT arrays

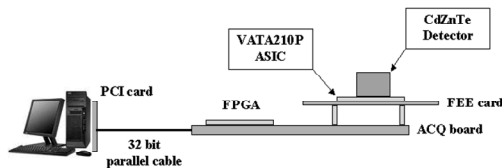
Paul Seller, RAL

Examples of imaging systems:- Ciemat , Acrorad (CdTe)

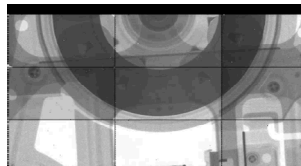
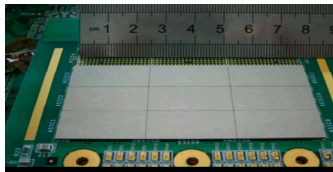
Ciemat CSTD 300um pixel Compton camera system for medical imaging



Bruker Baltic CZT



Acrorad CdTe 4-side buttable 100um pixels 50fps FPD. (Uses TSV technology on ASIC)

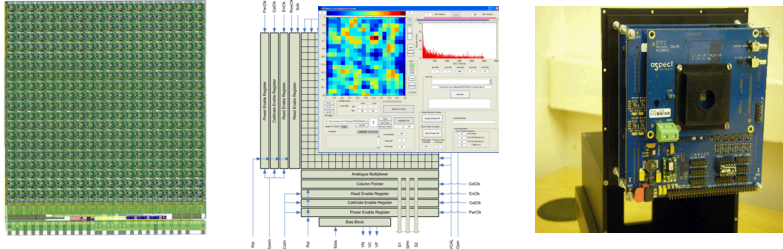


Energy Resolving CZT arrays

Paul Seller, RAL

Examples of imaging systems:- HEXITEC

- UK funded program to:
 - make CZT material by MTPVT technique.
 - make this into detectors.
 - bond to an energy resolving imaging ASIC
- ASIC is 80*80 pixels of 250um with 12 bit resolution spectroscopy up to 150keV (or 1.5MeV)
- Maximum readout rate is 80Meg pixels/sec
- Data acquisition system will sparcify data on fly and sends to PC by Camera-link
- Durham, Surrey, Manchester, Birkbeck and STFC.



20*20 rolling shutter ASIC and camera-link based readout system (80*80) by summer

Energy Resolving CZT arrays

Paul Seller, RAL

Example:- PORGRAMAYS Compton Gama camera for security applications

Portable Gamma Ray Spectrometer.
Compton Imaging and Spectroscopy

Partners:
STFC DL and RAL, Universities of Liverpool
and Manchester, John Caunt Scientific,
Centronic, Corus.

Funded by:
EPSRC and TSB



v Z. He et al, University of Michigan, IEEE NSS Conference Record, Hawaii 2007

CZT Energy Resolving Arrays

Paul Seller, RAL

Cobra



(Was Liverpool, Warwick, Sussex,
Birmingham Universities
+STFC)

1 meter cube of CZT crystals to look for
neutrino-less double β decay as a test
of the HEP Standard model.

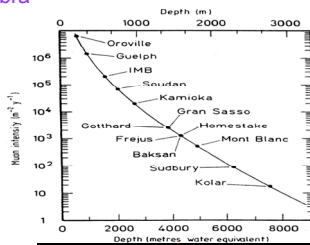
CZT is the source and the detector

10^{26} source atoms give one event per
year so need 100kg

Energy Resolving CZT arrays

Paul Seller, RAL

Cobra



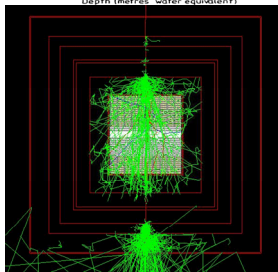
•Need to put the CZT in a mine to shield
background cosmic rays

•Need to make CZT from isotopically enriched
 ^{116}Cd

•Need to track interactions in the detector
volume to get 1-2% accuracy of 2.8MeV decay.
Need <200um voxel resolution.

•UK was proposing to use the PORGRAMRAYS
type technology.

•PPRP review in the UK decided not to follow
this. There is an international collaboration with
other physicists and CZT scientists

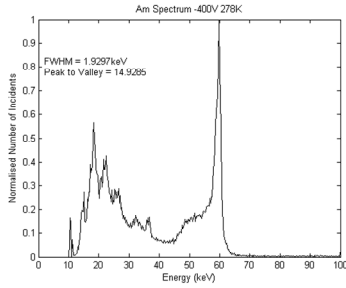


Energy Resolving CZT arrays

Paul Seller, RAL

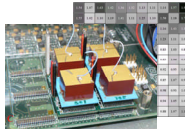


Energy Resolution

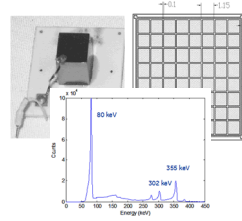


ERD2004 300um pixellated device. RAL. Am241 energy spectrum taken at 278K and -400V. Np peaks visible between 10 and 30keV. The escape peaks of Te and Cd at 33 and 37keV respectively.

Best resolutions on Bulk detectors being obtained are 0.8% FWHM dE/E with signal processing (Zhong He below)
Typically used for 100-700keV with either Coplanar-grid topology or double sided readout. To get this resolution one has to correct photopeaks for carrier trapping or use small pixel effect to reject hole signal.



Three-Dimensional Position Sensitive CdZnTe Detector Array for PNNL.
Zhong He, et. al. University of Michigan with Gamma Medica ASIC.



GE spectrometer with Rena-3 ASIC

Energy Resolving CZT arrays

Paul Seller, RAL

Appendix iii: Scintillators

Robert G. Lanier
January 4, 2012

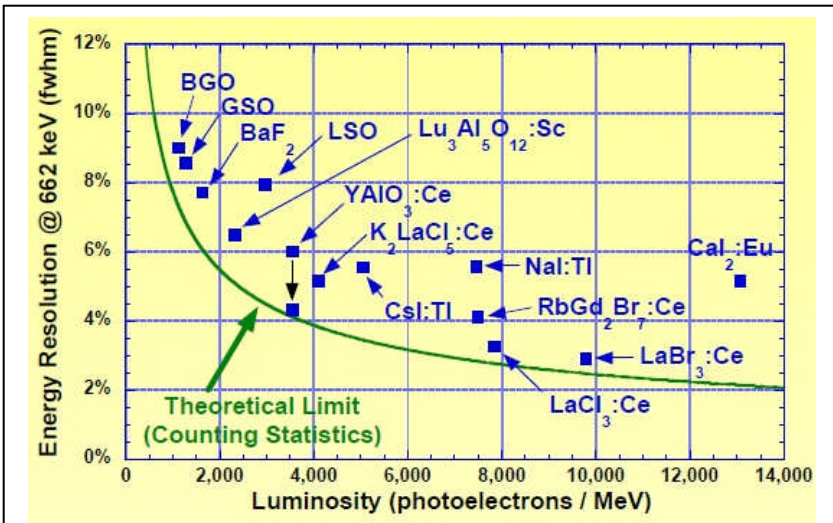
Executive Summary

	Nal:TI	Csl:TI	CaF2:Eu	BaF ₂	YAG:Ce	YAP:Ce	GSO:Ce	BGO	LaBr:Ce	CdWO ₄
Density [g/cm ³]	3.67	4.51	3.18	4.89	4.57	5.37	6.71	7.13	5.03	7.89
Max Emmision λ [nm]	415	550	435	325/220	550	370	440	480	430	470/540
Decay time [ns]	230	900	940	630	70	25	45	300	25	12
Resolution @ 662keV [%] ^(a)	8	5	6	12	5	7	10	14	3	10
Photon Yield [Photons/MeV]	38,000	52,000	23,000	10,000	8,000	10,000	9,000	2,500	60,500	13,000

(a) Resolution numbers are only indicative; energy resolution depends on crystal quality, thickness and other physical parameters.

The production of scintillator materials to service x-ray detection applications by indirect methods remains a very active development area. This remains true even as there are concurrent and aggressive ongoing research programs to develop and investigate new scintillators or to improve the performance of existing and more popularly used materials. The table above collects together a number of critical parameters associated with

scintillators either widely used for various applications or among those under more focused development. The figure compares the resolutions of each crystal and plots the value vs luminosity. The medical community relies heavily on scintillator



Resolution comparison of various scintillators; the disagreement between some of the luminosity values identified in the figure are severely at odds with those in the table above. The disagreement may be due to a geometric normalization inconsistency. In any case the relative ordering according to luminosity would be expected to be correct.

materials in their imaging applications and companies such as GE have their own in-house production facilities.

Three examples of the development of scintillator materials based on Lu and Y are described below. These include an example of research in the search for dopants that enhance certain desirable properties of these materials.

Property	Material				
	LSO	BGO	Lu(Y)AP	LaBr ₃	LYSO
Density (g/cm ³)	7.4	7.1	7.0 - 8.3	5.3	7.1
Energy Resolution	9%	15%	7% - 9%	3%	10%
Light Yield (relative to LSO)	1	< 0.2	0.5 - 0.7	2	1.2
Decay time (ns)	40	300	17	35	35
Physical robustness	Hard	Hard	Hard	Hygroscopic	Hard

Finally, the table in Appendix I catalogues the properties of a number of scintillator materials that have been developed for a variety of applications.

Lu(Y)AP, LuAP

LuYAP (lutetium yttrium aluminum perovskite) and LuAP (lutetium aluminum perovskite) crystals are a class of scintillators suitable for radiation detector modules for medical imaging and industrial applications, high energy physics, security scanning and research applications. These materials have very high density, fast decay times and provide competitive energy resolution.

Lu(Y)AP's good energy resolution, fast decay time and high stopping power makes it an alternative scintillation material for a number of advanced applications. Also, its robust high temperature performance is not typical of any other scintillating material.

In medical imaging Lu(Y)AP is essential in the phoswich design. It is an alternate choice for the next generation PET scanners and is expected to provide better image resolution, reduced scan time, reduced random noise and low scatter fraction.

Formula	Lu _{1-x} Y _x AlO ₃ : Ce
Z _{eff}	65
Stopping power	148
Attenuation length	1.05 cm at 511 KeV
λ _{peak}	365 nm
Refractive index	1.95
Molecular weight	224.13 g/mol
Crystal structure /phase	Orthorhombic / perovskite

In addition to medical imaging

diagnostics, the crystal's good linearity response makes it an alternate candidate for all applications where precise gamma ray spectroscopy is required, such as industrial, homeland security equipment and high energy physics.

	Physical Properties			Luminescence Properties	
	YAG	YAP		YAG	YAP
Density (g/cm ³)	4.57	5.37	Integrated light output (%NaI: Ti)	15	40
Hardness (Mho)	8.5	8.6	Wavelength of maximum emission (nm)	550	370
Index of refraction	1.82	1.95	Decay constant, ns	70	25
Crystal structure	Cubic	Rhombic	After glow (% at 6 ms)	<0.005	<0.005
Melting point, °C	1970	1875	Radiation length (cm)	3.5	2.7
Hygroscopic	No	No	Photon yield at 300 °K (103 Ph/MeV)	8	10
Linear coefficient of thermal expansion, 10 ⁻⁵ /K	0.8-0.9	0.4-1.1			
Cleavage	No	No			
Chemical formula	Y ₃ Al ₅ O ₁₂	YAlO ₃			

Opto Materials³⁴ is a company that provides Lu(Y)AP crystals and identifies itself as a unique supplier worldwide of high-quality crystals which are offered in large boule formats. These can be supplied as finished pixels or assembled into customer specified array or module configurations.

In particular, the crystal expresses a scintillation emission peak is at 365 nm, which matches well with the sensitivity spectrum of most PMTs with a light output that is twice that of BGO and a measured energy resolution at 662keV of 7% for 2x2x10 mm crystals. The 1/e decay time of LuAP is 17 ns, which is much shorter than the decay time of BGO. This allows high count rates and improved timing resolution.

³⁴ **Opto Materials S.r.l., Localita' Baccasara, Zona Industriale, 08048 Tortoli'(OG), Italy**
<http://www.optomaterials.com/Default.aspx>

YAG/YAP Single Crystal Scintillators³⁵

Made of yttrium aluminum garnet activated with trivalent cerium, the YAG exhibits ultrahigh light transmission (~97%) at 560nm. But the most important advantage is the high resistance of the single crystal scintillator to radiation damage. Other advantages include:

- Good signal-to-noise ratio.
- High temperature tolerance
- UHV "compatible"
- Refractive index: 1.84 at 550 nm
- Self-absorption: 20% for 5 mm light path

Made of yttrium aluminum perovskite, the YAP single crystal is a breakthrough in the light output efficiency. Its emitted spectrum peaks at 378nm. The decay time of the YAP crystal is faster than the YAG crystal (40ns vs. 80ns). A list of additional features is noted below:

- Good signal-to-noise ratio.

Properties of Rare-Earth (RE) Doped Ce:LSO Crystals				
Scintillator Crystal	Rare Earth Concentration	Crystal Dimensions [mm³]	Energy Resolution @ 511 keV [keV]	Photoelectron Yield [Photo-electrons/MeV]
ScLSO	1 at% Sc	10 x 10 x 2	15.9	4822
ScLSO	1 at% Sc	10 x 10 x 20	16.1	4344
LaLSO	1 at% La	10 x 10 x 2	10.8	5474
LaLSO	1 at% La	10 x 10 x 20	10.2	4696
GdLSO	1 at% Gd	10 x 10 x 2	16.6	5500
LYSO	4.47 at% Y	10 x 10 x 20	13.8	4840
LSO		10 x 10 x 2	13.1	4470

³⁵ Available from **SPI Supplies / Structure Probe, Inc.**, 569 East Gay Street, West Chester, PA 19380; spi3spi@2spi.com

- High temperature tolerance
- Refractive index: 1.82

Ce:LSO Scintillators

Cerium doped lutetium oxyorthosilicate crystal, i.e., Ce: (LSO), is an efficient scintillator: It exhibits a very high light output (above 27000 photons/MeV), has high density (7.4gm/cm^3), exhibits a short decay time (27ns) and has a suitable emission wavelength (420 nm).

Compared with LSO, both GSO and YSO have lower melting points and are easy to be doped into LSO crystals to essentially any percentage because of the similarity in crystal structure. Thus, the mixed scintillators LGSO and LYSO crystals are often presented as alternate choices. For example, LYSO presents similar scintillation properties and may be a good alternative to LSO. In addition, the addition of other rare earth (RE) ions may improve the distribution of Ce and the LSO photoelectron yield of LSO crystals. Recently, researchers³⁶ have used several rare earth elements, such as Y, La, Sc and Gd ions, as dopants in LSO crystals to investigate these doping effects on crystal growth and scintillation properties. The table above shows some of the results of these doping effects on the scintillation properties of the Ce:LSO.

³⁶ *Influence of Rare Earth (RE) Doping on the Scintillation Properties of LSO Crystals*, Laishun Qin, Guohao Ren, Sheng Lu, Dongzhou Ding, and Huanying Li, IEEE Transactions on Nucl. Sci., **55**, No 3, pp 1216-1220, June 2008

Appendix I: Compilation of Scintillator Materials and Their Properties

Scintillator Material	Emission Wavelength	Decay Time	Interference Index	Radiation Sensitivity
Gd ₂ O ₂ S:Tb (P43)	green (peak at 545 nm)	1.5 ms decay to 10%	low afterglow	high X-ray absorption, for X-ray, neutrons and gamma
Gd ₂ O ₂ S:Eu	red (627 nm)	850 μs decay	afterglow	high X-ray absorption, for X-ray, neutrons and gamma
Gd ₂ O ₂ S:Pr	green (513 nm)	7 μs decay	no afterglow	high X-ray absorption, for X-ray, neutrons and gamma
Gd ₂ O ₂ S:Pr,Ce,F	green (513 nm)	4 μs decay	no afterglow	high X-ray absorption, for X-ray, neutrons and gamma
Y ₂ O ₂ S:Tb (P45)	white (545 nm)	1.5 ms decay	low afterglow for low-energy X-ray	
Y ₂ O ₂ S:Eu (P22R)	red (627 nm)	850 μs decay	low afterglow for low-energy X-ray	
Y ₂ O ₂ S:Pr	white (513 nm)	7 μs decay	low afterglow for low-energy X-ray	
Zn(0.5)Cd(0.4)S:Ag (HS)	green (560 nm)	80 μs decay	afterglow	efficient but low-res X-ray
Zn(0.4)Cd(0.6)S:Ag (HSr)	red (630 nm)	80 μs decay	afterglow	efficient but low-res X-ray
CdWO ₄	blue (475 nm)	28 μs decay	no afterglow	intensifying phosphor for X-ray and gamma
CaWO ₄	blue (410 nm)	20 μs decay	no afterglow	intensifying phosphor for X-ray
MgWO ₄	white (500 nm)	80 μs decay	no afterglow	intensifying phosphor
Y ₂ SiO ₅ :Ce (P47)	blue (400 nm)	120 ns decay	no afterglow for electrons	suitable for photomultipliers
YAlO ₃ :Ce (YAP)	blue (370 nm)	25 ns decay	afterglow for electrons	suitable for photomultipliers
Y ₃ Al ₅ O ₁₂ :Ce (YAG)	green (550 nm)	70 ns decay	no afterglow for electrons	suitable for photomultipliers
Y ₃ (AlGa) ₅ O ₁₂ :Ce (YGG)	green (530 nm)	250 ns decay	low afterglow for electrons	suitable for photomultipliers
CdS:In	green (525 nm)	<1 ns decay	no afterglow	ultrafast for electrons
ZnO:Ga	blue (390 nm)	<5 ns decay	no afterglow	ultrafast for electrons
ZnO:Zn (P15)	blue (495 nm)	8 μs decay	no afterglow for low-energy electrons	
(ZnCd)S:CuAl (P22G)	green (565 nm)	35 μs decay	low afterglow for electrons	
ZnS:CuAlAu (P22G)	green (540 nm)	35 μs decay	low afterglow for electrons	
ZnCdS:AgCu (P20)	green (530 nm)	80 μs decay	low afterglow for electrons	
ZnS:Ag (P11)	blue (455 nm)	80 μs decay	low afterglow for alpha particles and electrons	
anthracene	blue (447 nm)	32 ns decay	no afterglow	
plastic (EJ-212)	blue (400 nm)	2.4 ns decay	low afterglow for alpha particles and electrons	
Zn ₂ SiO ₄ :Mn (P1)	green (530 nm)	11 ms decay	low afterglow for electrons	
ZnS:Cu (GS)	green (520 nm)	decay in minutes	long afterglow for X-rays	
NaI:Tl	for X-ray	alpha	and electrons	
CsI:Tl	green (545 nm)	5 μs decay	afterglow for X-ray, alpha and electrons	
6LiF/ZnS:Ag (ND)	blue (455 nm)	80 μs decay	for thermal neutrons	
6LiF/ZnS:CuAlAu (NDg)	green (565 nm)	35 μs decay	for neutrons	

Appendix iv: Comparison of CMOS Detectors for Mamography

Robert G. Lanier

April 4, 2012

A PhD thesis³⁷ submitted in 2011 to the University College London entitled *Evaluation of Digital X-ray Detectors for Medical Imaging Applications* contains a useful collection of data on the performance comparisons of several currently available digital x-ray systems. The primary focus of the thesis was to study the standard electro-optical performance evaluation of two novel CMOS (complementary metal oxide semiconductor) active pixel sensors against three commercial systems: (1) Remote RedEye HR, an active pixel sensor, (2) Hamamatsu C9732DK, a passive pixel sensor, and (3) an Anrad SMAM, an amorphous Se thin film transistor array. The novel systems were (1) a Large Area Sensor (LAS) built by a UK Consortium³⁸ and (2) a Dexela CMOS X-ray detector from Perkin Elmer. Figure 1 below displays the relative performance of these systems through the comparisons of their respective presampling Modulation Transfer Functions (PMTF) and quantum detection efficiency (QDE).

The thesis also contains a table (reproduced below) that compares the x-ray performance of 13 detectors used in mammography.

³⁷ *Evaluation of Digital X-ray Detectors for Medical Imaging Applications* by Anastasios C. Konstantinidis, a Thesis Submitted to the University College London for the Degree of Doctor of Philosophy, Department of Medical Physics and Bioengineering University College London, England (2011)

³⁸ The RC-UK Basic Technology Programme which involves 11 research centers throughout the United Kingdom. The aim of this consortium is to develop CMOS APS for a broad range of scientific applications.

Figure 2: Comparison of the x-ray Performance of Different Detectors Used in Mammography.

Detector	Detector technology	X-ray absorber material	Radiation quality	pMTF 50% (x;y – lp/mm)	DQE peak (x;y) at specific DAK level
FUJIFILM AMULET	a-Se TFT	200 µm a-Se	W/Rh (28 kV)	4.4	0.75 at 103 µGy
Sectra MicroDose	Direct photon counting	Crystalline Si wafer	W/Al (28 kV)	6.2; 3.3	0.63; 0.61 at 113 µGy
Fischer Senoscan	CCD	180 µm CsI:Tl	W/Al (28 kV)	5.5	0.24 at 131 µGy
GE Senographe 2000D	a-Si:H TFT	100 µm CsI:Tl	Mo/Mo (28 kV) (RQA-M 2)	4	0.53 at 131 µGy
Hologic Lorad Selenia	a-Se TFT	200 µm a-Se	Mo/Mo (28 kV) (RQA-M 2)	5.8	0.59 at 92.5 µGy
LAS	CMOS APS	150 µm CsI:Tl	W/Al (28 kV)	1.5	0.73 at 60.3 µGy
Hamamatsu C9732DK	CMOS PPS	160 µm CsI:Tl	W/Al (28 kV)	3.3	0.48 at 120.5 µGy
Dexela 2932	CMOS APS	150 µm CsI:Tl	W/Rh (25 kV)	2.7	0.59 at 105.7 µGy (HFW mode)
Dexela 2932	CMOS APS	150 µm CsI:Tl	W/Rh (25 kV)	2.7	0.61 at 57.8 µGy (LFW mode)
Dexela 2932	CMOS APS	150 µm CsI:Tl	W/Al (28 kV)	3.3	0.55 at 121.6 µGy (HFW mode)
Dexela 2932	CMOS APS	150 µm CsI:Tl	W/Al (28 kV)	3.3	0.55 at 59.7 µGy (LFW mode)
Anrad SMAM	a-Se TFT	200 µm a-Se	W/Al (28 kV)	6.1; 5.3	0.67; 0.66 at 108.6 µGy
Remote RadEye HR	CMOS APS	85 µm Gd ₂ O ₂ S:Tb	W/Al (28 kV)	4.3	0.33 at 120.5 µGy

Appendix v: A Collection of Recent Imaging Technology Developments

Robert G. Lanier
January 3, 2012
May 15, 2012 (updated)

Executive Summary

A collection of encapsulated summaries of recent technology developments in the area of x-ray imaging is presented. The list presented is not exhaustive but it is representative of most of the major advances in this technological area.

Specifically, the excerpts highlight advances in scintillator development and high-resolution detectors along with their associated electronic components. Generally, the examples presented focus on capturing x-ray information in the energy range associated with medical imaging applications (i.e. ~ 30 keV – 160- keV).

However, a few items are mentioned from astronomical and space-borne research sources that cover energy ranges outside this domain. These have been included to cover the possibility that the electronics developed for these applications would overlap with general US Homeland Security interests.

The presentation format first presents a brief list of the technologies identified. This is followed by an expanded list where the technology is identified followed by the name of the institution, company or consortium responsible for its development. This is followed by a website references where more information may be found and a short descriptive text. Finally, a figure is included to provide a visual reference to the technology.

In one or two cases, the company offering to sell the technology also offers professional engineering services to provide an interested patron with the option of partnering with the company to develop a unique or “one of” application of the technology. These examples are noted as part of the exposition excerpts as well.

1. **Flash Pad** - GE
2. **PHOTON 100** - Bruker AXS
3. **XinRay Systems** - Siemens.
4. **Digital Silicon Photomultipliers** – Phillips
5. **CdZnTe (CZT) Detectors**– Redlen
6. **Lensfree Optical Tomography** – UCLA Research
7. **D-SPECT System** - Spectrum Dynamics
8. **XDAS detector boards V3** – Sens Tech
9. **Ultrafast Ceramic Scintillator (UFC)** - Siemens.
10. **Advanced X-Ray Detectors**– DxRay Inc
11. **CCD Detector Development**– MPI Halbleiterlabor,
12. **DEPFET Detectors** - MPI Halbleiterlabor
13. **HICAM Gamma Camera** – HICAM Collaboration
14. **LuAG Scintillator Array** – Japan Research
15. **Strip Detectors** – Baltic Scientific Instruments
16. **The Solid-State X-Ray Image Intensifier (SSXII)** – SUNY Researchers
17. **RadEye™ X-ray Sensor Modules** - Teledyne Rad-ikon Imaging
18. **The INTEGRAL Soft Gamma-Ray Imager (ISGRI)** – ACORAD
19. **CCD 485 with Fiber Optic Faceplate** – Fairchild Imaging
20. **CMOS Linear Arrays**– Fairchild Imaging
21. **Selenium-based Flat panel X-ray Detector** – Toshiba
22. **SAPHIRE (scintillator avalanche photoconductor with high-resolution emitter readout) Detector** - .University-Industry Collaboration
23. **(DEXI) diffraction-enhanced x-ray imaging instrument** – Nesch, LLC
24. **Linear scanning sensors with gas-based detector modules for X-ray imaging**– Korean Collaboration
25. **Security Detectors; High-energy X-ray Platforms** - Varian

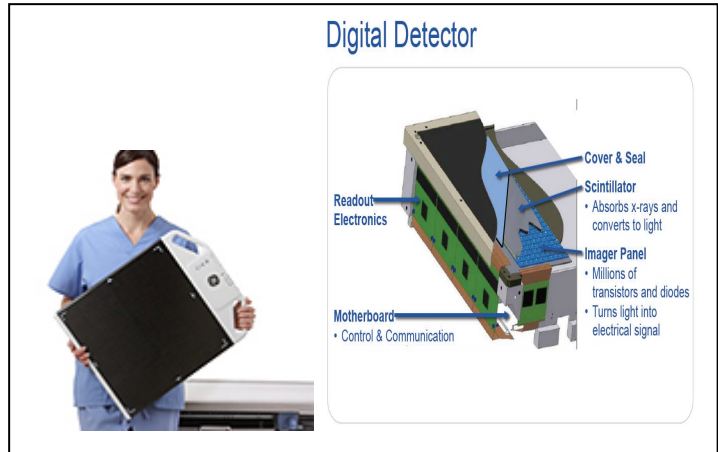
Flash Pad - GE

<http://www.gehealthcare.com/euen/radiography/radiography-flashpad.html>

<http://www.newdesignworld.com/press/story/236923>

http://www.wcet.us/wpcontent/uploads/2010/08/5_GE_Healthcare_tour.pdf

FlashPad is the first wireless detector to operate with Ultra- Wideband (UWB) connectivity. Rather than compete with other information on WI-FI networks, it communicates independently on a dedicated, high-priority channel—so data is transferred with speed and reliability. FlashPad can acquire multiple images in less than a second—so it can deliver advanced applications such as VolumeRAD* and Dual Energy Subtraction— helping enhance clinical confidence. As a digital detector, FlashPad enables you to image patients at less dose than CR and do it more quickly. The unit uses a CsI scintillators.



PHOTON 100 - Bruker AXS

http://www.bruker-axs.com/photon100_cmos_sensor_single_crystal_crystallography.html

Diffracted X-ray photons are converted into visible light using high resolution phosphor screens and introduce charges on the sensor. These charges are readout from each pixel through a readout bus, similar to a random access memory. This inherently makes [CMOS detectors](#) resistant to overexposure and charge overflows causing blooming and streaking.



Active area 100-cm² CMOS Sensor
Cooling Air cooled
Sensor format 1024 * 1024
Sensor Full well 4,000,000 (electrons, 10242)
Pixel size 96 μm
Demagnification 1:1 (no taper)

XinRay Systems - Siemens.

<http://nanopatentsandinnovations.blogspot.com/2010/01/siemens-unveils-fast-computer-tomograph.html>

A fast computer tomograph (CT) system enabled by carbon nanotubes for airport x-ray scans of people and baggage is being developed by Siemens and Xintek in a joint venture. [Siemens](#) Researchers are investigating the use of small, fast X-ray sources based on nanotubes. In combination with a computer tomograph (CT) scanner, these could serve to generate high-quality images of rapid processes within the human body, such as the dispersion of a contrast medium. It will take several years before such X-ray sources can be used in practical applications.



Digital Silicon Photomultipliers – Phillips

<http://www.dicardiology.com/article/major-progress-made-fully-digital-light-detection-technology>

<http://www.research.philips.com/initiatives/digitalphotoncounting/news/backgrounders/091008-photon-counting.html>

<http://indico.cern.ch/getFile.py/access?contribId=11&sessionId=7&resId=0&materialId=slides&confId=117424>

A new digital silicon photomultiplier (SiPM) technology has been developed with applications in both X-ray and nuclear imaging. The technology scales a single-pixel sensor to a fully integrated 64-pixel sensor with a sensing surface of more than 10 square centimeters.

The unit is capable of counting single photons and detecting their arrival time with an accuracy of around 60 picoseconds and are scalable to large-area applications. Like photomultiplier tubes, SiPM's are capable of measuring extremely low light levels, to the point of being able to detect single photons.

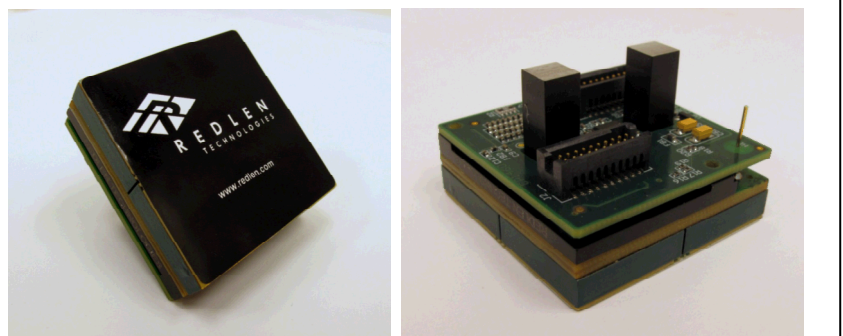


The company claims that the technology's scalability could have a major impact on the medical imaging field, particularly positron emission tomography. The technology offers a rugged, light weight, solid-state alternative to large-area sensors using photomultiplier tubes. Additionally, it consumes very little power. A prototype 8 by 8 pixel array consumes less than one W, and it is insensitive to magnetic fields.

CdZnTe (CZT) Detectors– Redlen

<http://www.redlen.com/wp-content/uploads/2011/06/Redlen-Nuclear-Imaging-Module-Shortform-Datasheet.pdf>

Redlen Technologies claims to be “...leading the revolution in high-performance, CZT-based radiation detection and imaging technology” and is developing “...a new generation of high-performance equipment in ... “Nuclear Cardiology, CT Scanning, Airport Baggage Scanning and Dirty Bomb Detection”. The company further claims that it is accomplishing this by “... proprietary CZT semiconductor production technology....” which provides low-cost CZT radiation with “superior” resolution.



CZT detector module (left) mounted with electronic interface (right)

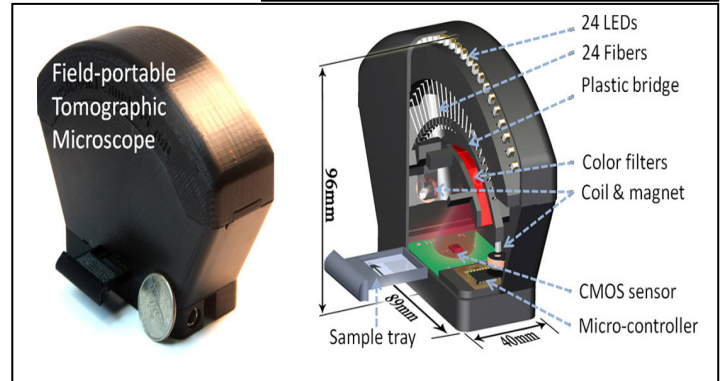
Lensfree Optical Tomography – UCLA Research

<http://spie.org/x84293.xml?highlight=x2416&ArticleID=x84293>

A device capable of achieving tomographic microscopy of micro-objects over large imaging volumes has been developed. Lensfree Optical Tomography (LOT) can provide a useful tool for lab-on-a-chip platforms and high-throughput imaging applications in low-resource settings. Using emerging sensor-array architectures,

researchers hope to extend the angular range of illumination to, for example, $\pm 80^\circ$. These may offer improved pixel-response at even higher incident angles and should allow the achievement of neanisotropic 3D resolution at the sub-micrometer scale.

A photograph (left) and schematic diagram (right) is shown of the field-portable lensfree tomographic microscope. Individual LEDs butt-coupled to multimode optical fibers provide multiple angles of illumination. Optical fibers are electromagnetically actuated to implement source-shifting based pixel super-resolution at each illumination angle.



D-SPECT System - Spectrum Dynamics

<http://www.itnonline.com/tech/spect-cardiac-imaging-system-incorporates-czt-modules>
<http://www.spectrum-dynamics.com/>

Spectrum Dynamics' D-SPECT (single photon emission computed tomography) system uses a cadmium zinc telluride (CZT) nuclear imaging detector, which enable high resolution, low-dose nuclear imaging. The design incorporates nine rotating columns of CZT detectors that are able to focus on specific anatomical points in the body, thereby improving the signal-to-noise-ratio. This also eliminates the need to rotate the gantry or the patient to sample the organ of interest.



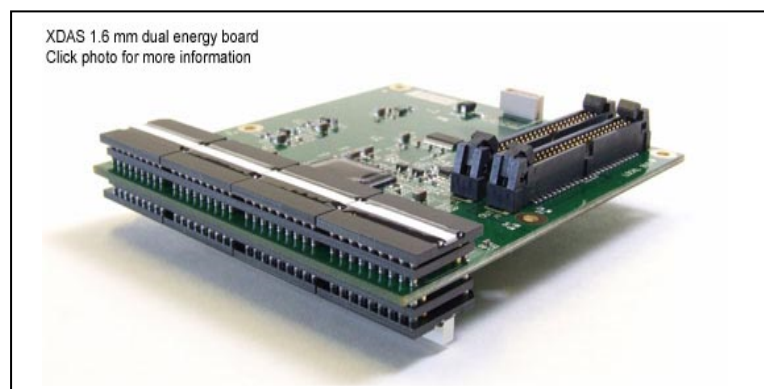
Solid-state CZT based detectors, combined with advanced reconstruction algorithms, provide the foundation for rapid imaging and clinical applications not possible with conventional sodium iodide based detectors. They also enable dramatic reductions in radiation dose to the patient and significant improvements in image quality.

The Redlen M1762 nuclear imaging module provides a 40 x 40 mm CZT imaging array with 256 pixels. The module provides direct digital readout and averages less than 6 percent energy resolution for Tc-99 based imaging. The module is a key building block to enable a new generation of direct conversion low-dose, high-resolution nuclear imaging cameras.

XDAS detector boards V3 – Sens Tech

<http://www.sens-tech.com/Products/XDAS/>

The XDAS X-Ray Data Acquisition System provides a highly flexible means of creating an array of linear X-rays sensors, read out in digital format. The XDAS-V3 version has recently been launched to replace XDAS-V2 and provides many new features. The XDAS-V2 version remains available.

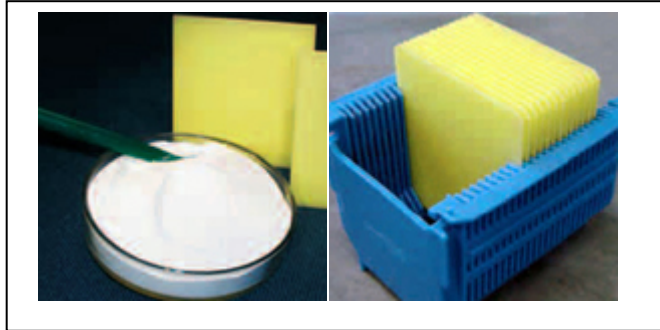


The system has a modular architecture, enabling system designers to build their own detectors with detector boards arranged as required. These may be in a linear or 'L' shaped format or with multiple rows for CT detector applications, where the detectors are arranged around a ring. Detectors can be supplied with 2.5mm, 1.6mm, 0.8mm or 0.4mm pitch.

Ultrafast Ceramic Scintillator (UFC) - Siemens.

http://www.medical.siemens.com/webapp/wcs/stores/servlet/CategoryDisplay~q_catalogId~e_-11~a_categoryId~e_1033570~a_catTree~e_100010,1007660,12752,1033569,1033570~a_langId~e_-11~a_storeId~e_10001.htm

UFC or Ultra Fast Ceramic is a scintillator material which quickly and efficiently transforms radiation from the X-ray tube into light signals. These signals in the visible spectrum are in turn picked up by photodiodes, transforming them into electric signals, which are computed to become visual 2D or 3D images.

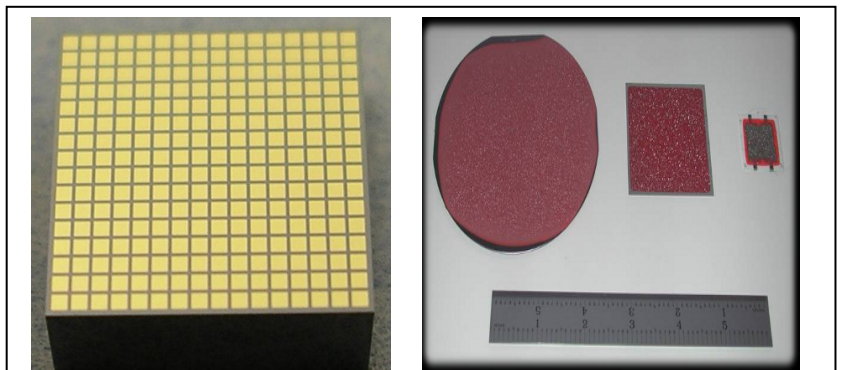


Conventionally, other single crystalline substances are used in X-ray detectors such as cadmium tungstate (CdWO_4), or cesium iodide (CsI). The Siemens Ultra Fast Ceramic uses instead a crystal lattice of the rare earth compound gadolinium oxysulfide (GOS) along with other dopants. The exact concentrations are proprietary. UFC has a large X-ray absorption coefficient and due to its fast decay, reacts very rapidly to changes in X-ray intensity. The vendor claims that UFC is superior to conventional detector materials in ways which include light output, decay time and drift. Competing products are also marketed by GE-Healthcare under the trade names GemstoneTM and HiLightTM.

Advanced X-Ray Detectors– DxRay Inc

<http://www.dxray.com/>

DxRay, Inc. claims that it researches, develops, markets and manufactures the next generation of detector technology for digital x-ray imaging. It further claims expertise in semiconductor detector materials such as silicon, mercuric iodide, cadmium zinc telluride, and cadmium telluride and in the most advanced high density ASICs (Application Specific Integrated Circuits) for solid state radiation sensor applications. The company's business model combines expertise and intellectual property, including patents and know-how related to semiconductor sensor technologies with ASIC multichannel amplification and processing electronics. As such, the company claims to be able to carry out the most advanced x-ray imaging sensor developments. Examples of the company's products are shown in the figure.

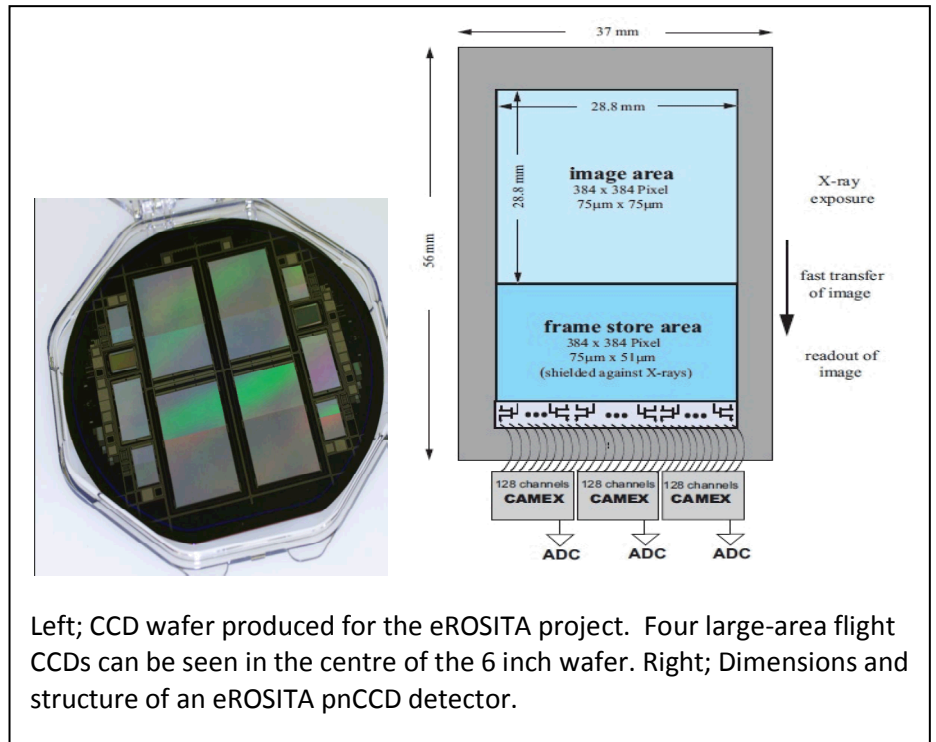


Left; CdTe Pixel Detector with Pitch of 0.5mm; Right; Examples of polycrystalline mercuric iodide x-ray detector films grown on various substrates.

CCD Detector Development– MPI Halbleiterlabor,

<http://ieeexplore.ieee.org/stamp/stamp.jsp?tp=&arnumber=5873711>

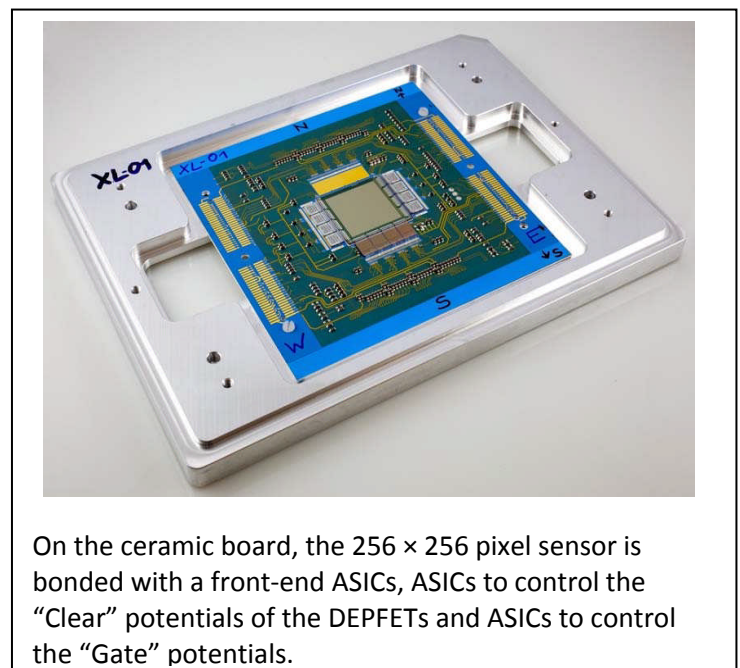
The German X-ray telescope eROSITA is the core instrument on the Russian satellite Spectrum-Roentgen-Gamma (SRG). Its scientific goal is the exploration of the X-ray Universe in the energy band from about 0.3 keV up to 10 keV with excellent energy, time and spatial resolution and large effective telescope area. For high-resolution detection of X-ray photons, frame transfer pnCCDs and their associated front-end electronics have been developed. The back-illuminated, 450 μm thick and fully depleted pnCCDs with a 3 cm x 3 cm large image area have been produced. By means of the concept of back-illumination and full depletion of the chip thickness, high quantum efficiency is obtained over the entire energy band of interest. An analog signal processor with 128 parallel channels was also developed for readout of the pnCCD signals. This ASIC permits fast and low noise signal filtering. For a detailed characterization of the CCD detectors an appropriate control, supply and data acquisition electronics system was developed.



DEPFET Detectors - MPI Halbleiterlabor

<http://ieeexplore.ieee.org/stamp/stamp.jsp?tp=&arnumber=5873713>

DEPFET detectors are silicon active pixel sensors for X-ray imaging spectroscopy. They will be used for the MIXS instrument of BepiColombo planetary mission and they are expected to be used for the Wide Field Imager of the International X-ray Observatory currently under study by ESA,



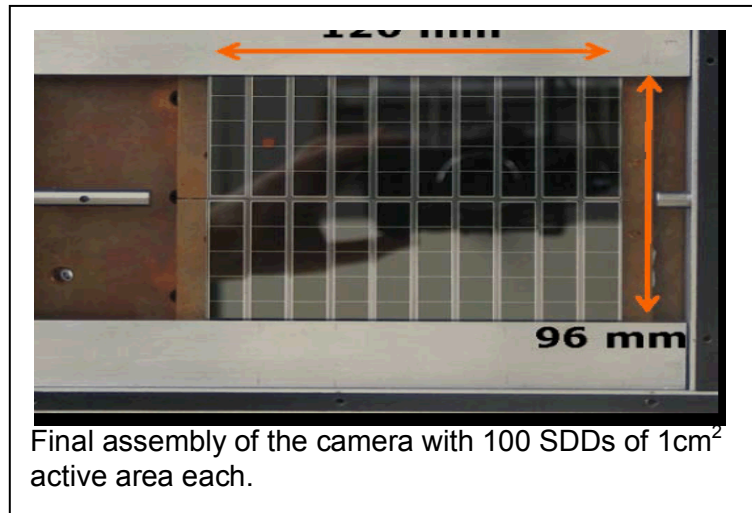
NASA and JAXA. New DEPFET matrixes with 256×256 pixels of $75 \mu\text{m}$ pitch have been produced, mounted on ceramic boards with dedicated frontend electronics and integrated in a new set-up able to acquire large-format images and spectra.. Energy resolution as low as 129 eV FWHM at 5.9 keV has been obtained including all single events of the matrix back illuminated at -40°C and read out at a 300 frames per second rate.

HICAM Gamma Camera – HICAM Collaboration

<http://ieeexplore.ieee.org/stamp/stamp.jsp?tp=&arnumber=5874116>

A new compact and high-resolution ($<1\text{mm}$) Anger camera to be used in clinical and research environments where high overall spatial resolution and system compactness are required. The use of Silicon Drift Detectors (SDDs) as scintillator photodetectors, characterized by high quantum efficiency and low electronic noise, is the particular aspect of this camera.

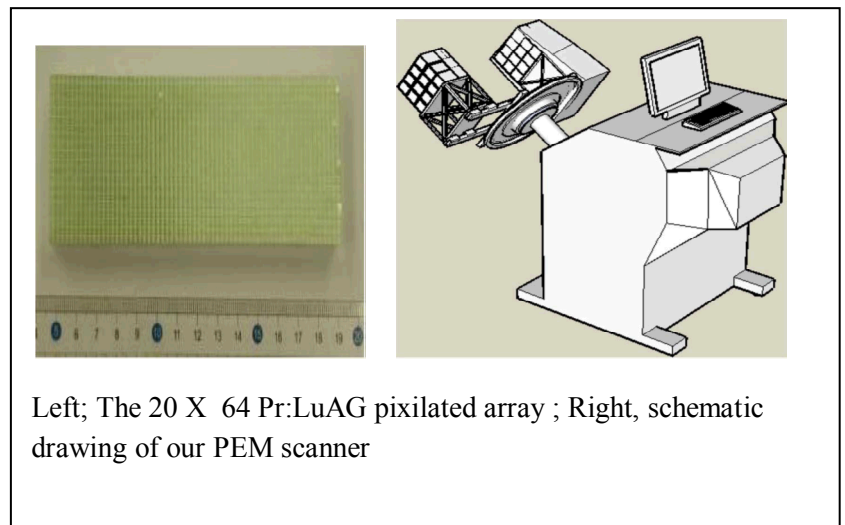
Two prototypes were produced during the project. The smaller one, composed of 25 SDDs with a $5 \times 5\text{cm}^2$ active area, has been used for a first assessment of the performances and first trials in small animal imaging. The larger prototype, developed following the same architecture, is composed of 100 SDDs of 1cm^2 active area each, in a $10 \times 10\text{cm}^2$ array. We report on the results of imaging measurements carried out with the prototypes and on the analysis of the performances achieved.



LuAG Scintillator Array – Japan Research

<http://ieeexplore.ieee.org/stamp/stamp.jsp?tp=&arnumber=5485089>

A Pr:LuAG scintillator pixilated with 0.1 mm Ba SO₄ was developed to be used for high-efficiency positron emission mammography (PEM). A one camera unit consisted of 20×64 pixels optically coupled with three H8500-03 multi anode PMTs. The PEM required four cameras on each side. Using eight cameras, a PEM was successfully fabricated. Spatial resolutions for a point source, a line-like source, and a



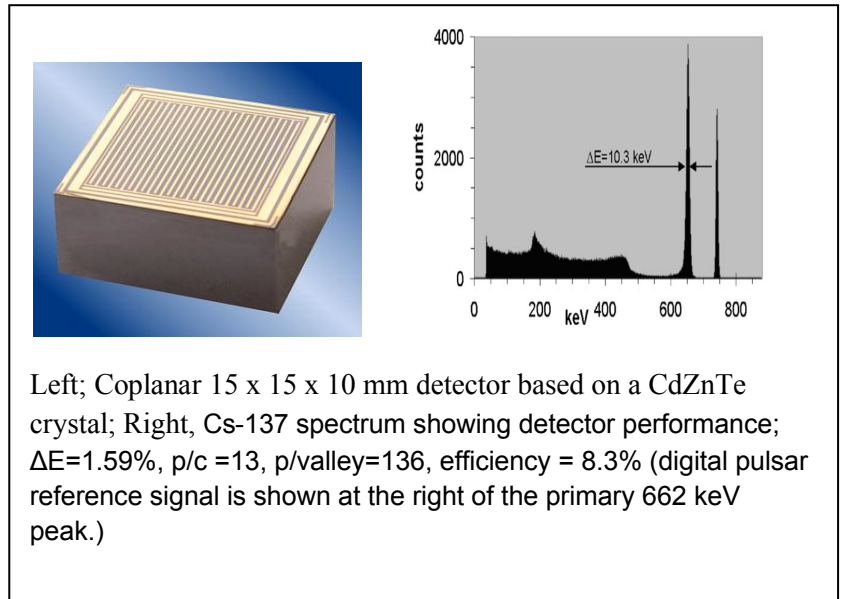
Left; The 20×64 Pr:LuAG pixilated array ; Right, schematic drawing of our PEM scanner

breast phantom were investigated. When the breast phantom was observed, 4 mm spatial resolution was achieved.

Strip Detectors – Baltic Scientific Instruments

http://www.bsi.lv/strip_detectors_eng.html

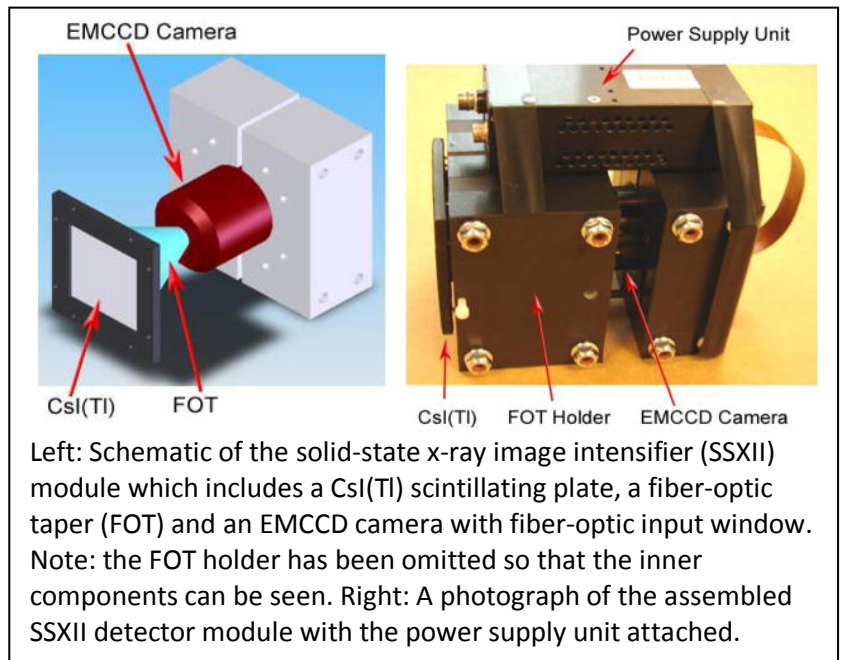
The company offers that it develops and fabricates CdZnTe/CdTe type detectors along with the accompanying electronics based on general electronic components and ASICs. They claim that they manufactures detectors by request and further claim flexibility in their technological processes, engineering design services and custom fabrication of small and medium volumes of devices.



The Solid-State X-Ray Image Intensifier (SSXII) – SUNY Researchers

<http://www.ncbi.nlm.nih.gov/pmc/articles/PMC2557100/figure/F1/>

The solid-state x-ray image intensifier (SSXII) is an EMCCD-based x-ray detector designed to satisfy an increasing need for high-resolution real-time images, while offering significant improvements over current flat panel detectors (FPDs) and x-ray image intensifiers (XII). FPDs are replacing XIIs because they reduce/ eliminate veiling glare, pincushion or s-shaped distortions and are physically flat. However, FPDs suffer from excessive lag and ghosting and their performance has been disappointing for low-exposure-per-frame procedures due to excessive instrumentation-noise. XIIs and FPDs both have limited resolution capabilities of ~ 3 cycles/mm. To overcome these limitations a prototype

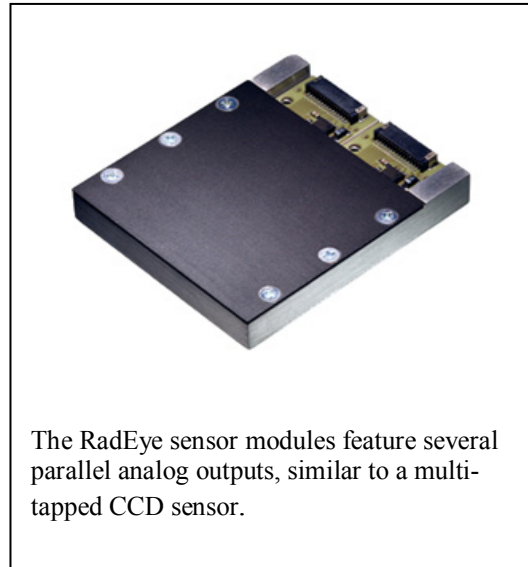


SSXII module has been developed, consisting of a $1k \times 1k$, $8 \mu\text{m}$ pixel EMCCD with a fiber-optic input window, which views a $350 \mu\text{m}$ thick CsI(Tl) phosphor via a 4:1 magnifying fiber-optic-taper (FOT). Arrays of such modules will provide a larger field-of-view. Detector MTF, DQE, and instrumentation-noise equivalent exposure (INEE) were measured to evaluate the SSXII's performance using a standard x-ray spectrum (IEC RQA5), allowing for comparison with current state-of-the-art detectors. The highest-resolution mode has a $32 \mu\text{m}$ effective pixel size. Comparison images between detector technologies qualitatively demonstrate these improved imaging capabilities provided by the SSXII.

RadEye™ X-ray Sensor Modules - Teledyne Rad-icon Imaging

<http://www.rad-icon.com/products-radeye.php>

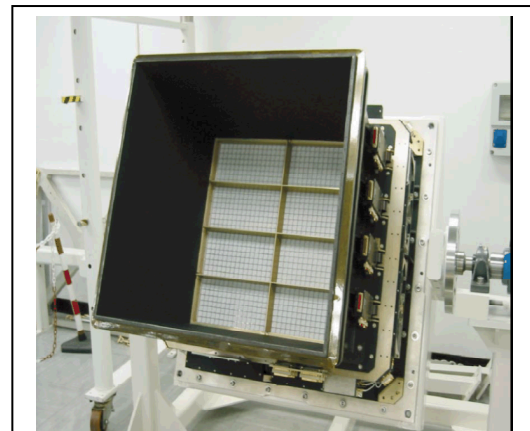
The RadEye series large-area x-ray sensor modules are packaged x-ray image sensors that consist of several tiled RadEye sensors in a robust aluminum housing with scintillator and graphite entrance window. The standard product line features sensor modules with active areas ranging from $50 \times 50 \text{mm}$ (2" square) up to $100 \times 100 \text{mm}$ (4" square), although larger custom configurations are also possible. All modules are available either with direct-coupled GdOS (Gadox) scintillator for low-energy (<50kV) and low-dose applications, or with an integrated fiber-optic faceplate (FOP) for applications requiring higher x-ray energies (up to 160kV) and dose rates.



The INTEGRAL Soft Gamma-Ray Imager (ISGRI) – ACRO RAD

http://www.aanda.org/index.php?option=com_article&access=standard&Itemid=129&url=/articles/aa/full/2003/43/aaINTEGRAL62/aaINTEGRAL62.right.html

The figure shows a view of the detection plane of the ISGRI camera formed with 8 independent detector modules. Each pixel of the camera is a CdTe detector read out by a dedicated integrated electronic channel. Altogether, there are 16,384 detectors (128×128) and an equal number of electronic channels. Each detector is a 2 mm thick CdTe:Cl crystal of $2 \text{ mm} \times 4 \text{ mm} \times 4 \text{ mm}$ with platinum electrodes deposited with an electroless (chemical) process. The ACRO RAD company provided 35 000 detectors in total for the various models of ISGRI. All detectors have been screened for their spectroscopic performance and

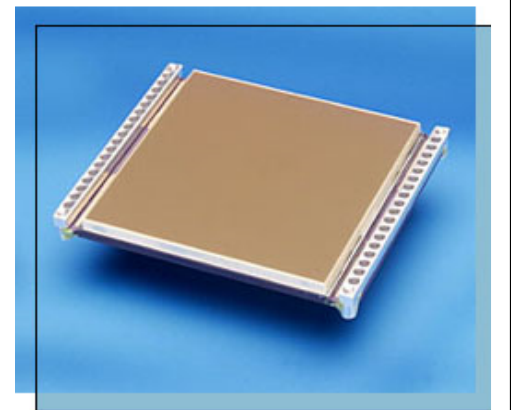


stability under a 100 V bias at 20deg C. The imager has demonstrated robust performance and shows absolutely no signs of degradation after 9 months in orbit.

CCD 485 with Fiber Optic Faceplate – Fairchild Imaging

http://www.fairchildimaging.com/products/fpa/custom/ccd_485fiberoptic.htm

The CCD 485 is a sensor which consists of a charge coupled device (CCD), ceramic substrate, fiber optic faceplate and scintillator. The CCD chip was designed for high resolution scientific, medical and industrial applications. The unit is organized as a matrix array of 4096 horizontal by 4097 vertical imaging elements. The pixel pitch is 15 μ m and has 100% fill factor. The imaging area may be operated in either buried channel mode for high dynamic range or Multi-Pinned Phase (MPP) mode for low dark current. Three-phase clocking is employed in the imaging area. The imaging area is divided into four quadrants. Each quadrant may be clocked independently.. The CCD 485 may be clocked such that the full array is read out from any one of the four output amplifiers. The fiber optic faceplate and scintillator is attached to the top of the CCD for high resolution X-ray imaging. The CCD 485 is one of 6 CCD arrays offered by the vendor and described as “high performance charge coupled devices intended for use in advanced aerospace, industrial, medical and scientific imaging applications”. The company further identifies these products as available in front illuminated as well as back illuminated configurations.

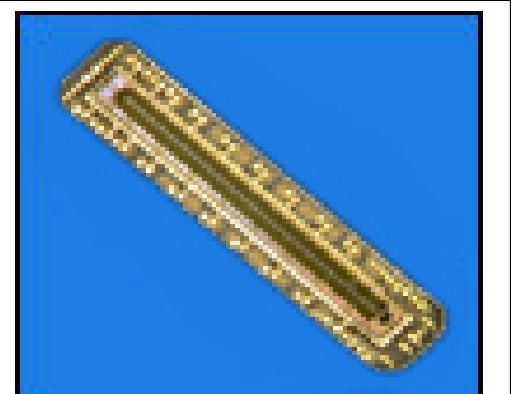


4096 x 4097 Photosite CCD
15- μ m x 15m pixel
61.2 x 61.2 mm Image Area
4080 x 4080 Optically Active Pixels
Full Frame Architecture
Multi-Pinned Phase (MPP) Option

CMOS Linear Arrays– Fairchild Imaging

http://www.fairchildimaging.com/CMOS_linear_arrays.asp

The [Active Reset™](#) CMOS imager is designed for high-sensitivity, high-conversion gain and low read noise applications. This device provides a data rate up to 80MHz and operates in three modes providing tailored choices for specific applications.



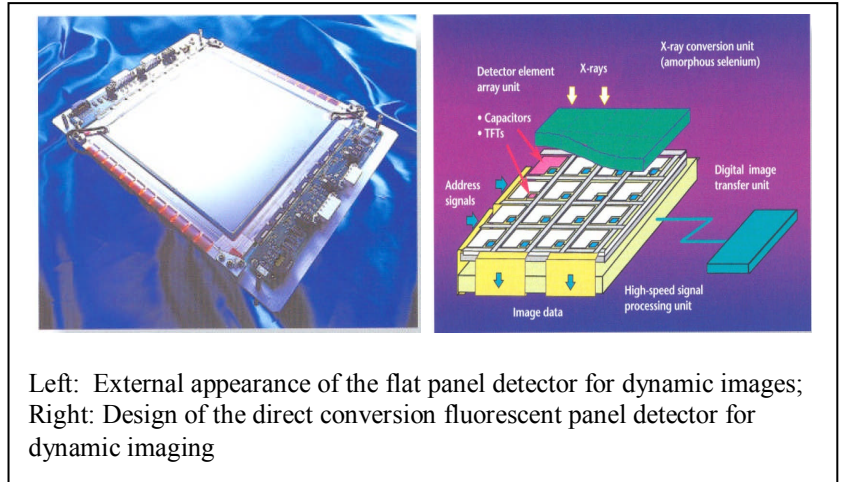
2048 x 1, 7 μ m pixel pitch

Selenium-based Flat panel X-ray Detector - Toshiba

http://european-hospital.com/media/article/2338/Selenium_Based_Flat_Panel_X_ray_1_2001.pdf

A selenium-based flat panel X-ray detector for digital fluoroscopy and radiography has been developed. This detector captures X-rays and converts them directly to digital dynamic and static images with high spatial resolution and contrast. The detector permits fluoroscopy at a rate of up to 30 images per second, making it possible to visualize medical conditions otherwise not easily observed. It is anticipated that a variety of detectors for a full range of digital X-ray applications from

general radiography to angiography will be developed. The detector specifications include an effective field of view: of 23 x 23 cm, 150 μm pixel pitch, and a selenium thickness: 1000 μm .



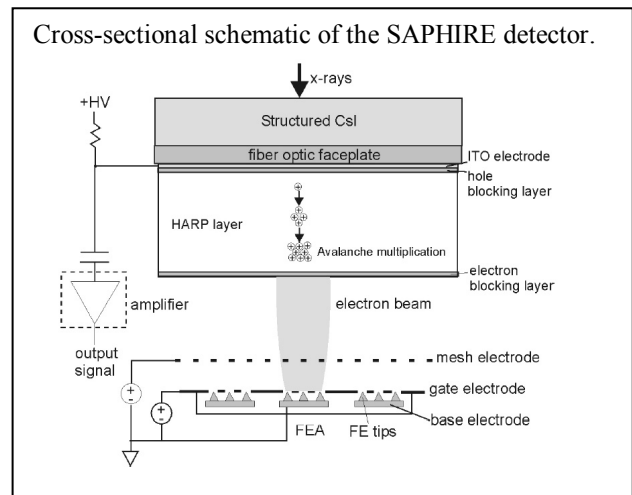
Left: External appearance of the flat panel detector for dynamic images; Right: Design of the direct conversion fluorescent panel detector for dynamic imaging

SAPHIRE (scintillator avalanche photoconductor with high-resolution emitter readout) Detector - .University-Industry Collaboration

<http://spie.org/x23956.xml>

Existing active-matrix flat-panel imagers (AMFPIs) use a two-dimensional array of thin-film transistors to read out a charge image generated by an x-ray image sensor. In ‘direct conversion’ this sensor is an x-ray photoconductor, while in ‘indirect conversion’ the sensor is a scintillator coupled with discrete photodiodes. These methods have two main limitations. First, in low-dose applications such as fluoroscopy (real-time x-ray medical imaging), electronic noise degrades the performance behind dense tissues. Second, the smallest pixel size currently used for digital mammography, 70μm, may not be adequate in some cases.

The SAPHIRE concept (shown in Fig XX) is expected to overcome these limitations. The design consists of a needle-structured cesium iodide (CsI) scintillator, optically coupled (for example, through fiber optics) to a uniform thin layer of amorphous selenium (a-Se) photoconductor, with a Se thickness of 4 – 25μm. The selenium layer is operated in avalanche multiplication mode, and is called HARP (high avalanche rushing amorphous photoconductor)³⁹. The visible photons emitted from the scintillator pass through a transparent indium tin oxide



³⁹ K. Tanioka, J. Yamazaki, K. Shidara, *et al.*, *Avalanche-mode amorphous selenium photoconductive target for camera tube*, **Adv. Electron. Electron Phys.** **74**, pp. 379–387, 1988.

(ITO) bias electrode to generate electron-hole pairs near the top of the HARP layer. Applying a positive voltage to the ITO causes holes to move toward the bottom (free) surface of the HARP. On the way, they experience avalanche multiplication under an electric field strength $E_{Se} > 90\text{V}/\mu\text{m}$ which is an order of magnitude higher than is typically used in direct-conversion a-Se x-ray detectors. The holes form an amplified charge image at the bottom surface of the HARP layer, which is read out with electron beams generated by a two-dimensional field-emitter array (FEA), which is placed at a short distance ($\sim 1\text{--}2\text{mm}$) below the scintillator-HARP structure. The FEA pixels are addressed by orthogonal gate and base lines.

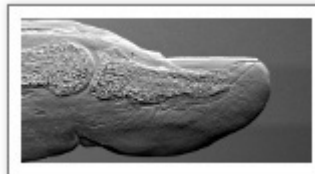
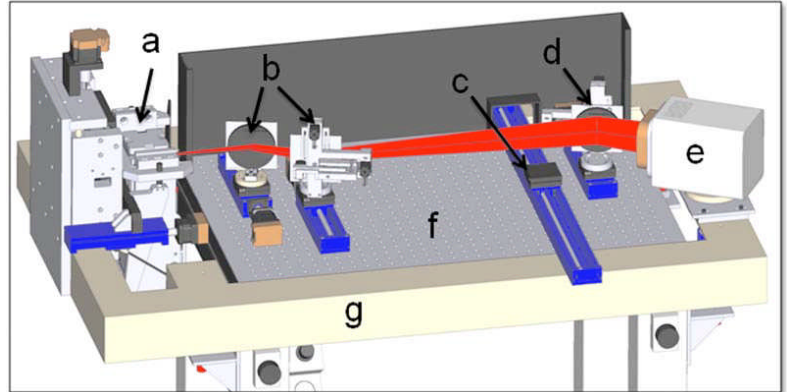
(DEXI) diffraction-enhanced x-ray imaging instrument – Nesch, LLC

http://www.neschllc.com/products/additional_info.html

The diffraction-enhanced x-ray imaging (DEXI) instrument uses a conventional x-ray source to image the internal structure of an object.

In laboratory tests, a human cadaveric thumb (see figure inset) was used as a test-sample to demonstrate the imaging capability of the instrument. A 22 keV monochromatic x-ray beam is prepared using a mismatched, two-crystal monochromator; a silicon analyzer crystal is placed in a parallel crystal geometry with the monochromator allowing both diffraction-enhanced imaging and multiple-imaging radiography to be performed. The DEXI instrument was found to have an experimentally determined spatial resolution of $160 \pm 7 \mu\text{m}$ in the horizontal direction and $153 \pm 7 \mu\text{m}$ in the vertical direction. As applied to biomedical imaging, the DEXI instrument can detect soft tissues, such as tendons and other connective tissues, that are normally difficult or impossible to image via conventional x-ray techniques.

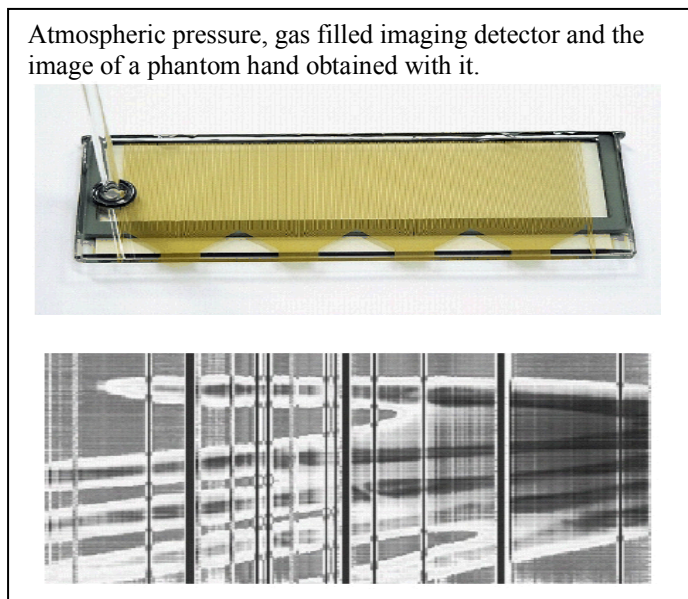
A perspective schematic of the DEXI instrument: (a) 2.2 kW Ag x-ray tube and multiaxis positioning cradle; (b) mismatched, two-crystal monochromator; (c) sample compartment; (d) analyzer crystal; (e) high-resolution, digital x-ray detector; (f) inner-vibration-isolation platform; and (g) outer-vibration-isolation platform.



Linear scanning sensors with gas-based detector modules for X-ray imaging— Korean Collaboration

http://iopscience.iop.org/1748-0221/6/03/C03004/pdf/1748_0221_6_03_C03004.pdf

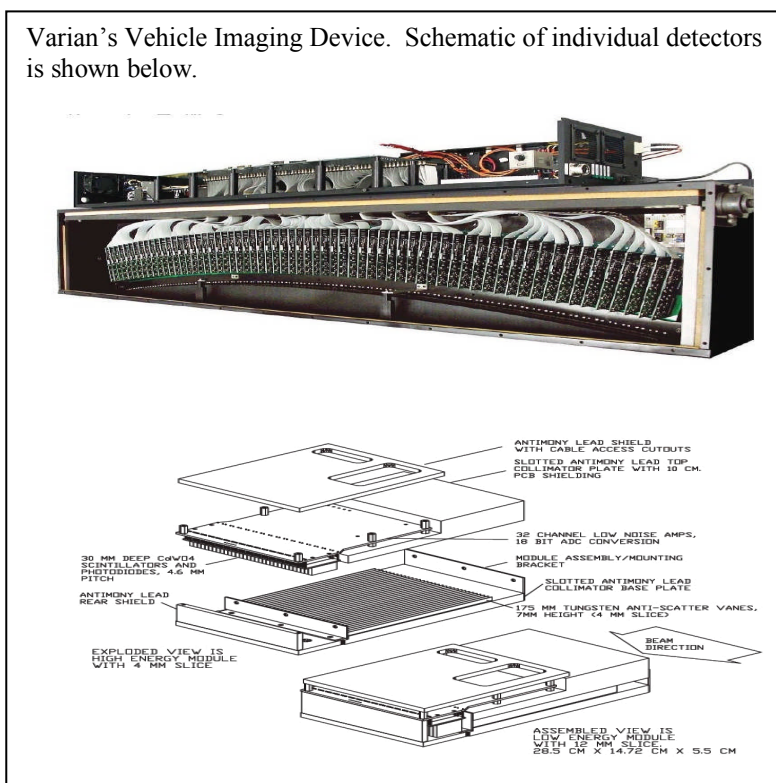
Korean researchers have manufactured an x-ray image sensor by using a plasma display panel (PDP) fabrication process that can be used to obtain scanning images. The schematic of the linear scanning sensor is shown in the figure. The sensors are parallel-plate-type scanning detectors which consist of a sealed chamber with an electrode plane and data strip line. The electric signal generated by the ionization of electrons and positive ions in the sensor was evaluated for various gas mixtures — Xe (100), Xe/CO₂ (90/10), and Xe/CO₂ (80/20) — at atmospheric pressure. Normally gas typed sensors have used high pressure (above 3 atm.) gas fills. A hand-phantom image acquired with the detection system is shown in the bottom portion of the figure.



Security detectors; High-energy X-ray Platforms – Varian

http://www.varian.com/us/security_and_inspection/products/detectors/

Varian claims that it is the premier supplier of high-energy X-ray platforms for cargo security systems. The vendor claims offering a modular design that allows the construction of units scalable to virtually any size application with modules that are easily field replaceable. The system uses the company's ACTIS software which is designed to integrate the X-ray source and detectors for seamless and optimized image processing. Detector arrays are constructed as individual modules that can be configured in arrays that meet custom size requirements. Shown in the figure is a schematic of a 32-channel module.



Appendix vi: Data Sheets for Commercial Medical Imaging Devices (2002 – 2008)

Robert G. Lanier
March 22, 2012

The data described here summarize various operating and cost parameters for all the medical imaging devices placed into service between 2002 and 2008. A magazine, *Advance for Imaging & Radiation Oncology*, assembled and published these charts for a wide range of technologies used in medical imaging but ceased in 2009. Contact with the publisher suggests that it is unlikely that the magazine will

Table I: Summary of PDF images of vendor product fcomparisons.

Digital Radiography	Computed Radiography	PET/CT/SPECT	Gamma Camera
CR-DR January 2008.pdf	CR-DR January 2008.pdf	PET-CT May 2007.pdf	Gamma Cameras January 2007.pdf
CR-DR July 2006.pdf	CR-DR July 2006.pdf	CT January 2006.pdf	Gamma Cameras April 2005.pdf
DR June 2005.pdf	CR June 2005.pdf	PET-CT February 2005.pdf	Gamma Cameras July 2003.pdf
DR June 2004.pdf	CR June 2003.pdf	CT July 2004.pdf	
DR July 2002.pdf		PET May 2003.pdf	
		CT March 2003.pdf	
		SPECT-CT May 2006.pdf	

begin these compilations in the foreseeable future.

In discussions with author of several of these charts, I was told that the process is quite labor intensive and each chart literally represents a man month or two of effort.

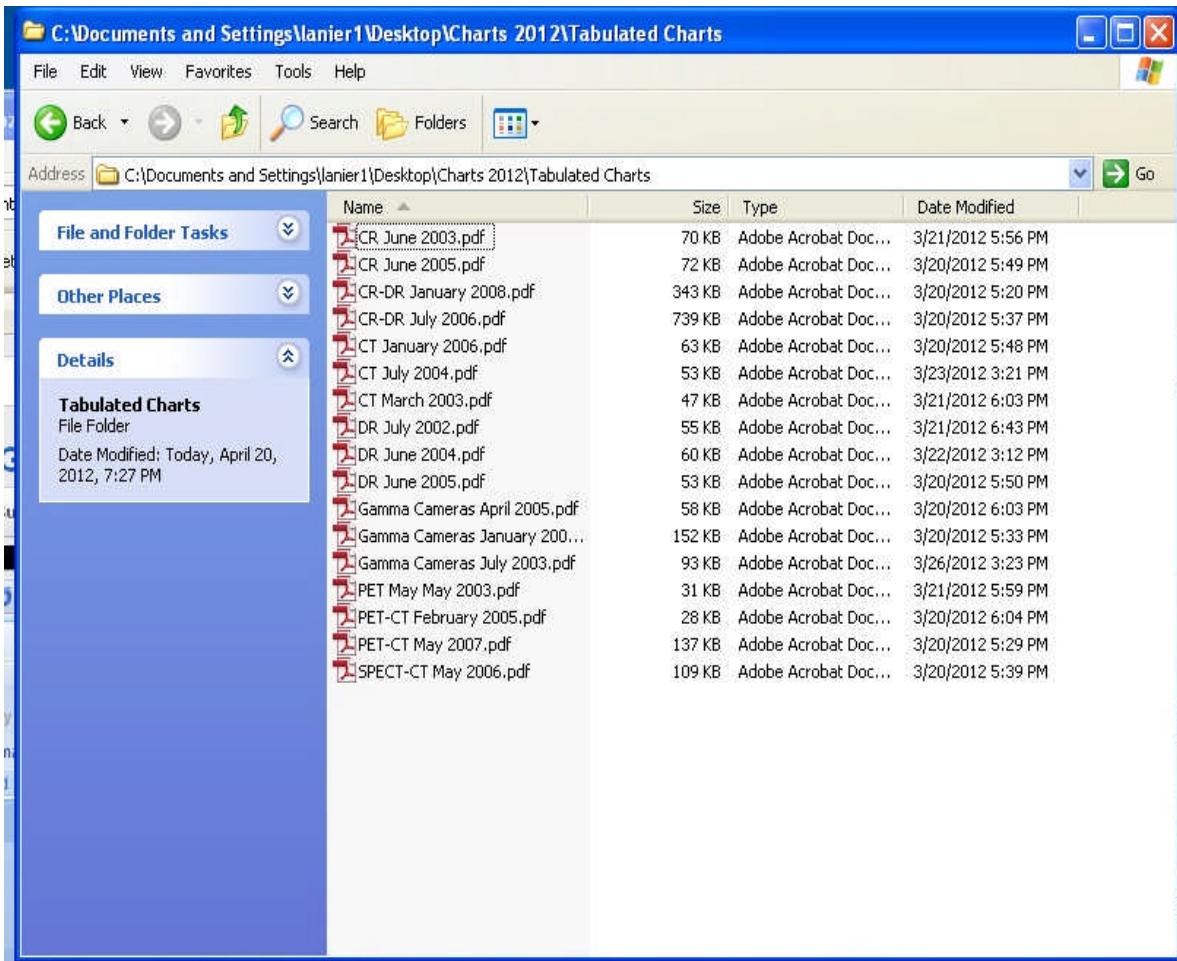
The charts are available electronically and are identified in Table 1 above:

A spread sheet has been prepared that identifies the units for which charts are available. An example of this summary spread sheet, Table II, is shown on the following page. The table lists the following information: (1) the class of systems represented, (2) the “pdf” image of the chart, and then in successive order (3) instrument vendor and (4) the various models for which more complete data are presented in the chart. Figure 1 shows the collection of pdf files representing vendor charts and Figures 2 & 3 is an example chart.

Table II: Example table showing compilation structure of each tabulated data sheet

	Vendor	Product Name				
	Digital Radiographic System January 2008					
	CR-DR January 2008.pdf					
1	Canon USA Inc. Lake Success, NY www.usa.canon.com/dr	CRDI-40EG	CRDI-40EC	CRDI-50G	CRDI-50C	CRDI-31
2	Carostream Health Inc. Rochester, NY www.carostreamhealth.ca	Kodak DirectView DR 9500	Kodak DirectView DR 7500	Kodak DirectView DR 3500		
3	Fujifilm Medical Systems USA Inc. Stamford, CT www.fujimed.com	Velocity-U	Velocity-T	Velocity-UPP	Velocity-TFP	ClearView-ES
4	iCRca Inc. Torrance, CA www.icrcompany.com	iDR				
5	IDC (Imaging Dynamic Company) Calgary, AB, CAN	X-Series 2200	X-Series 1600 Plus	X-Series 11600	X-Series 1590	
		(X3C or X4C technology platform)				
6	Konica Minolta Medical Imaging USA Inc www.medical.konicaminolta .us	REGIUS 370				
7	Philips Medical Systems North America Bathell, WA www.medical.philips.com	DigitalDiagnost Compact	DigitalDiagnost VR chest room	DigitalDiagnost VM multipurpose single	DigitalDiagnost TH tube-detector	Errenta DR
8	Quantum Medical Imaging Rensselaer, NY www.quantummedical.net	Q-Red DR Ceiling Mounted Single or Dual Panel DR System	Q-Red Floor Mounted Tube Stand Single or Dual Panel DR System	Q-Red QV 800 or QV 9000 Single Receptor DR System		
9	RF SYSTEM lab. Nagano, Japan www.rfsystemlab.com	NAOMI				
10	Siemens Medical Solutions Inc. Malvern, PA www.siemens.com	AXIOM MULTIX M	Aristar FX Plus	AXIOM Aristar VX	AXIOM Aristar MX	

Figure 1: Collected pdf files containing information on vendor comparisons



Appendix vii: Detectors and Scintillator Materials; A Survey of Market Availability

Part I: Detectors (6 pages)

The tables below present the results of a survey of x-ray imaging devices used in medicine and industry. The survey is not exhaustive but reasonably presents a cross section of what vendors currently offer. Each vendor provides a data sheet that contains information that it regards as useful to the consumer and may not publish other information because of proprietary concerns. As such, the technical specifications which are publicly available vary considerably. The table's intent was to highlight important operating parameters of each device. Unfortunately, because of the large variability in data sheet content, many entries are listed as "not available" (NA).

#	Manufacturer	Model Number	Detector Type	Scintillator Type	Detector Size (Total Pixels)	Detector Size (Active Pixels)	Pixel Pitch (µm)	Physical Detector Size (Total Area cm ²)	MTF	DOE	Dynamic Range	non-Linearity	Wavelength Response/Energy Range [keV]	Integration time	Readout Noise (electrons)
1	Opoelectronics Perkin Elmer	XRD 1620 AJ	Amorphous Si	Kodak Lanex Fine, Lanex Fast, or CsI	2048 x 2048	2024 x 2024	200	1678	80% @ 0.5 lp/mm 30% @ 2.0 lp/mm For CsI Option: 75 kVp, 20mm Al filtration, 7mm Al HVL	56% @ 0.5 lp/mm 28% @ 2.0 lp/mm	> 80 dB	<1%	40 - 15, 000 keV	333 ms (minimum)	NA
2	Opoelectronics Perkin Elmer	XRD 1620 AN	Amorphous Si	Kodak Lanex Fine, Lanex Fast, or CsI	2048 x 2048	2024 x 2024	200	1678	80% @ 0.5 lp/mm 30% @ 2.0 lp/mm For CsI Option: 75 kVp, 20mm Al filtration, 7mm Al HVL	56% @ 0.5 lp/mm 28% @ 2.0 lp/mm	> 75 dB	<1% (10% to 90% of FSR)	40 - 15, 000 keV	285.6 ms (minimum)	NA
3	Perkin Elmer	XRD 1622 AO, AP	Amorphous Si	CsI, Ti or various Ge2025: Tb (GOS) fluorescent screens	2048 x 2048	NA	200	1678	67% (1 cy/mm) 33% (2 cy/mm) with CsI	75% (0 cy/mm) 56% (1 cy/mm) 37% (2 cy/mm) for RO45 with CsI	> 74 db (40) > 87 db (4P)	NA	20 - 15,000 keV	NA	NA
4	Opoelectronics Perkin Elmer	XRD 1640 AN/ES	Amorphous Si	Kodak Lanex Fine, Lanex Fast, or CsI	1024 x 1024	1012 x 1012	400	1678	80% @ 0.25 lp/mm 33% @ 1.0 lp/mm For CsI Option: 75 kVp, 20mm Al filtration, 7mm Al HVL	56% @ 0.25 lp/mm 28% @ 1.0 lp/mm	> 75 dB	<1% (10% to 90% of FSR)	20 - 15,000 keV	66.45 variable	NA
5	Opoelectronics Perkin Elmer	XRD 0640 ML/MG IND	Amorphous Si	Kodak Lanex Fine, Lanex Fast, or CsI	512 x 512	500 x 500	400	419	80% @ 0.25 lp/mm 30% @ 1.0 lp/mm	56% @ 0.25 lp/mm 28% @ 1.0 lp/mm	> 80 dB	<1% (10% to 90% of FSR)	40 - 350 keV	135 ms - 5s in 1 ms intervals or 135 ms - 12.8 s in 8 fixed steps	NA
6	Opoelectronics Perkin Elmer	XRD 0640 AL/AG IND	Amorphous Si	Kodak Lanex Fine, Lanex Fast, or CsI	512 x 512	500 x 500	400	419	80% @ 0.25 lp/mm 30% @ 1.0 lp/mm	56% @ 0.25 lp/mm 28% @ 1.0 lp/mm	> 80 dB	<1% (10% to 90% of FSR)	40 - 200 keV	135 ms - 5s in 1 ms intervals or 135 ms - 12.8 s in 8 fixed steps	NA
7	Opoelectronics Perkin Elmer	XRD 512 - 400 CL	Amorphous Si	Kodak Lanex Fine, Lanex Fast, or CsI	512 x 512	500 x 500	400	419	80% @ 0.25 lp/mm 30% @ 1.0 lp/mm	56% @ 0.25 lp/mm 28% @ 1.0 lp/mm	> 80 dB	<1% (10% to 90% of FSR)	30 - 200 keV	variable	NA
8	Opoelectronics Perkin Elmer	XRD 512 - 400 EL/EG	Amorphous Si	Kodak Lanex Fine, Lanex Fast, or CsI	512 x 512	500 x 500	400	419	80% @ 0.5 lp/mm 30% @ 2.0 lp/mm For CsI Option: 75 kVp, 20mm Al filtration, 7mm Al HVL	56% @ 0.5 lp/mm 28% @ 2.0 lp/mm	> 80 dB	<1% (10% to 90% of FSR)	20 - 15,000 keV	135 ms - 5s in 1 ms intervals or 135 ms - 12.8 s in 8 fixed steps	NA
9	Teledyne DALSA	Helios 10 MD	CMOS	Min-R 2190 DR2-Std	2000 x 2560	na	96	472	82% @ 1lp/mm for Min-R 2190 for DR2-STD	NA	78 dB	NA	NA	RMS @ 1fps = 2 ADU	
10	Teledyne DALSA	SkaGraph8	CMOS	Min-R 2190 DR2-Std	2048 x 2048	2000x2048	96	388	82% @ 1lp/mm for Min-R 2190 for DR2-STD	NA	72	NA	NA	RMS @ 1fps = 1 ADU	
11	Teledyne DALSA	SkaGraph8 EV	CMOS	Min-R 2190 DR2-Std	2048 x 2048	2000x2048	96	388	82% @ 1lp/mm for Min-R 2190 for DR2-STD	NA	72	NA	NA	RMS @ 1fps = 1 ADU	

#	Manufacturer	Model Number	Detector Type	Scintillator Type	Detector Size (Total Pixels)	Detector Size (Active Pixels)	Pixel Pitch (µm)	Physical Detector Size (Total Area, cm ²)	MTF	DOE	Dynamic Range	non-Linearity	Wavelength Response/Energy Range (keVp)	Integration time	Readout Noise (electrons)
12	Teledyne DALSA	SixGraph-8 PT	CMOS	Min-R 2190 DR2-Std	2048 x 3048	2000x2048	96	388	82% @ 2.0 lp/mm for Min-R 2190 70% @ 1lp/mm for DR2-STD	NA	72	NA	NA	NA	RMS @ 1fps > 1 ADU
13	Teledyne DALSA	SixGraph-10 EV	CMOS	Min-R 2190 DR2-Std	2048 x 3048	2000x2048	96	388	82% @ 1lp/mm for Min-R 2190 70% @ 1lp/mm for DR2-STD	NA	72	NA	NA	NA	RMS @ 1fps > 1 ADU
14	Teledyne DALSA	SixGraph-10 MID/TBD	CMOS	Min-R 2190 DR2-Std	2048 x 3048	2000x2048	96	388	82% @ 1lp/mm for Min-R 2190 70% @ 1lp/mm for DR2-STD	NA	72	NA	NA	NA	RMS @ 1fps > 1 ADU
15	Radicon Imaging Corp	RadEye8	CMOS	Kodak Min-R 2190 or Lanex Fine or Lanex Fast F or Lanex Fast B	2048 x 2048	NA	48	172	80% @ 2.0 lp/mm Lanex Fine; 72% @ 2.0 lp/mm Min-R 2190; 45% @ 2.0 lp/mm Lanex Fast F; 15% @ 2.0 lp/mm Lanex Fast B	NA	85dB	NA	NA	quoted as = (start pulse frequency)-1	150
16	Radicon Imaging Corp	RadEye4	CMOS	Kodak Min-R 2190 or Lanex Fine	1024 x 2048	NA	48	48	80% @ 2.0 lp/mm Lanex Fine; 72% @ 2.0 lp/mm Min-R 2190; 45% @ 2.0 lp/mm Lanex Fast F; 15% @ 2.0 lp/mm Lanex Fast B	NA	85dB	NA	10 - 160 keV (EV model)	quoted as = (start pulse frequency)-1	150
17	DALSA Radicon Imaging Corp	RadEye3	CMOS	Kodak Min-R 2190 or Lanex Fine	1024 x 1536	NA	48	36	80% @ 2.0 lp/mm Lanex Fine; 72% @ 2.0 lp/mm Min-R 2190; 45% @ 2.0 lp/mm Lanex Fast F; 15% @ 2.0 lp/mm Lanex Fast B	NA	85dB	NA	10 - 160 keV (EV model)	549	150
18	DALSA Radicon Imaging Corp	RadEye2	CMOS	Kodak Min-R 2190 or Lanex Fine	1024 x 1024	NA	48	24	80% @ 2.0 lp/mm Lanex Fine; 72% @ 2.0 lp/mm Min-R 2190; 45% @ 2.0 lp/mm Lanex Fast F; 15% @ 2.0 lp/mm Lanex Fast B	NA	85dB	NA	10 - 160 keV (EV model)	549	150
19	Teledyne DALSA	RadEye 1	CMOS	unspecified	na	512 x 1024	48	17	NA	>30%	85	NA	NA	(start pulse frequency)-1	150
20	Teledyne DALSA	RadEye 100	CMOS	unspecified	na	512 x 1024	96	48	NA	>50%	86	NA	NA	550913* (clock frequency)-1	250
21	DALSA Radicon Imaging Corp	Shad-o-Box 1024	CMOS	Kodak Min-R 2190 or Lanex Fine	1024 x 1024	NA	48	24	80% @ 2.0 lp/mm Lanex Fine; 72% @ 2.0 lp/mm Min-R 2190;	NA	85dB	NA	10 - 160 keV (EV model)	NA	not specified in "electron" units
22	Hamamatsu	C9352DK-14	CCD	Direct Deposit Csi	1228 x 624	1216 x 616	200	6	NA	NA	3100 (no units)	20 - 90kVp	NA	NA	2600 1000
23	Hamamatsu	C7921CA-29 Flat Panel Sensor	CMOS	Coli Flipped scintillator plate	1056 x 1056	1032 x 1012	50	27	2-85% @ 1lp/mm (in units of CTF = contrast transfer function)	NA	2900 (saturation charge/noise ratio)	spec sheet displays linear-log trace	20 - 100	NA	(quoted as "rms noise swing width")

#	Manufacturer	Model Number	Detector Type	Scintillator Type	Detector Size (Total Pixels)	Detector Size (Active Pixels)	Pixel Pitch (µm)	Physical Detector Size (Total Area, cm ²)	MTF	DOE	Dynamic Range	non-Linearity	Wavelength Response/Energy Range [keVp]	Integration time	Readout Noise (electrons)
24	Hamamatsu	C89123K-06 Flat Panel Sensor	CMOS	GOS	2496 x 2304	2472 x 2184	50	144	2.90% @ 1 lp/mm (in units of CTF = contrast transfer function)	NA	3200 (no units given)	NA	20 - 110	NA	700 [quoted as "rms noise"]
25	Hamamatsu	C7942 Flat Panel Sensor	CMOS	CsI	2400 x 2400	2240 x 2368	50	144	NA	NA	2000 (no units given)	NA	NA	NA	1100 [quoted as "rms noise"]
26	Hamamatsu	C7943 Flat Panel Sensor	CMOS	CsI	1248 x 1248	1216 x 1248	100	156	NA	NA	4300 (no units given)	NA	NA	NA	2300 [quoted as "rms noise"]
27	Hamamatsu	C7942CA-02 Flat Panel Sensor	CMOS	CsI	2400 x 2400	2240 x 2344	50	144	NA	NA	2000 (no units given)	NA	NA	NA	1100 [quoted as "rms noise"]
28	Hamamatsu	C7943CA-02 Flat Panel Sensor	CMOS	CsI	1248 x 1248	1216 x 1220	100	156	NA	NA	4300 (no units given)	NA	NA	NA	2300 [quoted as "rms noise"]
29	Hamamatsu	C7942CA-22 Flat Panel Sensor	CMOS	CsI Flipped scintillator plate	2400 x 2400	2240 x 2344	50	144	2.85% @ 1 lp/mm (in units of CTF = contrast transfer function)	NA	2000 (saturation charge/noise ratio)	spec sheet displays linear log-log trace	20 - 100	NA	2300 [quoted as "rms noise swing width"]
30	Hamamatsu	C7943CA-22 Flat Panel Sensor	CMOS	CsI Flipped scintillator plate	1248 x 1248	1216 x 1220	100	156	2.83% @ 1 lp/mm (in units of CTF = contrast transfer function)	NA	4300 (no units given)	NA	20 - 100	NA	1300 [quoted as "rms noise swing width"]
31	Hamamatsu	C79423K-25 Flat Panel Sensor	CMOS	GOS deposited POP	2400 x 2400	2316 x 2316	50	144	NA	NA	850 (saturation charge/noise ratio)	spec sheet displays linear log-log trace	20 - 150	NA	1000 [quoted as "rms noise swing width"]
32	Hamamatsu	C7930-01 Flat Panel Sensor	MOS	CsI	4416 x 3520	NA	50	387	NA	NA	NA	NA	NA	NA	NA
33	Hamamatsu	C7921CA-09 Flat Panel Sensor	CMOS	CsI	1056 x 1056	1032 x 1012	50	28	NA	NA	2900 (no units given)	NA	20 - 100	NA	1000 [quoted as "rms noise"]
34	Hamamatsu	C79321CA-02 Flat Panel Sensor	CMOS	CsI	1056 x 1056	1032 x 1012	50	148	NA	NA	2900 (no units given)	NA	Apply 1 mm thick Fe filter in case 100 - 150 keVp	NA	1000 [quoted as "rms noise"]
35	Hamamatsu	C7942CK-12 Flat Panel Sensor	CMOS	CsI	2400 x 2400	2240 x 2344	50	144	NA	NA	2000 (no units given)	NA	20 - 80	NA	1100 (no units given)
36	Hamamatsu	S7361	FFT-CCD	Fiber Optic Plate with unspecified scintillator	NA	600 x 400	48	6	NA	NA	15 000 (no units)	NA	NA	NA	80 [quoted as "rms noise"]
37	Hamamatsu	C100135X Flat Panel Sensor	CMOS	CsI	1056 x 1056	1032 x 1000	50	28	NA	NA	3800 (no units given)	NA	20 - 150	NA	2600 [quoted as "rms noise"]
38	Hamamatsu	C10322D Flat Panel Sensor	CMOS	CsI	624 x 624	600 x 616	200	156	NA	NA	3200 (no units given)	NA	20 - 90	NA	2600 [quoted as "rms noise"]

#	Manufacturer	Model Number	Detector Type	Scintillator Type	Detector Size (Total Pixels)	Detector Size (Active Pixels)	Pixel Pitch (µm)	Physical Detector Size (Total Area cm ²)	MTF	DOE	Dynamic Range	non-Linearity	Wavelength Response/Energy Range [kVp]	Integration time	Readout Noise (electrons)
39	Hamamatsu	C19000 Flat Panel Sensor	CMOS	Direct Deposited CsI	624 x 624	608 x 616	200	156	NA	NA	3600 (no units given)	NA	20 - 90	NA	2900 (quoted as "rms noise")
40	Hamamatsu	C9311DX Flat Panel Sensor	CMOS	Direct Deposited CsI	1248 x 1152	1232 x 1120	100	144	NA	NA	2600 (no units given)	NA	20 - 80	NA	1500 (quoted as "rms noise")
41	Hamamatsu	C9290DP Flat Panel Sensor	CMOS	CsI	624 x 624	608 x 616	200	156	NA	NA	NA	NA	<80	NA	NA
42	Varian Medical Systems	PaScan 1313	Amorphous Si	Detached CsI, DRZ Plus, or Gd2O2S:Tb (Kodak Lanex Screen)	1024 x 1024	NA	127	169	≥55% @ 1 lp/mm	NA	NA	NA	40 - 160	NA	NA
43	Varian Medical Systems	PaScan 2020+	Amorphous Si	Integral columnar CsI:TI	1024 x 1024	NA	194	396	≥55% @ 1 lp/mm	70% ± 5%	72	Non-uniformity - 1% of max full scale	40 - 150	NA	NA
44	Varian Medical Systems	PaScan 2520E+	Amorphous Si	Detached CsI, DRZ Plus, or Gd2O2S:Tb (Kodak Lanex Screen)	1536 x 1920	1516 x 1900	127	475	> 48% @ 1 lp/mm CsI screen (80 kVp)	NA	NA	NA	20 - 90	NA	NA
45	Varian Medical Systems	PaScan 2520D/VCL	Amorphous Si	Detached CsI, DRZ Plus, or Gd2O2S:Tb (Kodak Lanex Screen)	1536 x 1920	1496 x 1874 (CsI, direct deposit)	127	475	> 48% @ 1 lp/mm CsI screen (80 kVp)	Direct Deposit CsI: 70% ± 5% Other Scintillator options: ≥ 60%	NA	NA	40 - 150	NA	NA
46	Varian Medical Systems	PaScan 3030+	Amorphous Si	Integral columnar CsI:TI	NA	1526 x 1526	194	888	≥55% @ 1 lp/mm	70% ± 5%	80 dB standard modes; 98 dB DGS modes	NA	40 - 150	NA	NA
47	Varian Medical Systems	PaScan 4030E	Amorphous Si	DRZ Plus	2304 x 3200	2304 x 3200	127	1189	≥45% @ 1 lp/mm	> 30% (with DRZ Plus)	NA	NA	40 - 150	NA	NA
48	Varian Medical Systems	PaScan 4030CB	Amorphous Si	Integral columnar CsI:TI	2048 x 1536	2048 x 1536	194	1183	> 45% @ 1 lp/mm CsI screen (80 kVp)	70% ± 5%	(saturation/line): Dual/Dynamic Gain modes 18000:1; Full Resolution Mode 3000:1; Fluro Modes 1500:1	Non-uniformity - 1% of maximum	40 - 150	NA	NA
49	Varian Medical Systems	PaScan 4343R	Amorphous Si	Direct Deposit CsI, Detached CsI, DRZ Plus	3072 x 3072	3052 x 3052	139	1823	NA	70% ± 5%	NA	NA	40 - 150 kVp	NA	NA
50	Varian Medical Systems	PaScan 4336R	Amorphous Si	Direct Deposit CsI, Detached CsI, DRZ Plus	3072 x 2560	3052 x 2540	139	1520	NA	N	NA	NA	40 - 150	NA	NA
51	DIRA	Dira 5A	CCD	Gadod	indirect	N	156	1248	NA	14% @ 70kV	≥ 72 dB	NA	NA	NA	NA
52	DIRA	Dira 9	CCD	Gadod	indirect	N	130	1600	NA	35% @ 70kV	≥ 80 dB	NA	NA	NA	NA
53	DIRA	Dira 9C	CCD	CsI	indirect	N	130	1600	NA	45% @ 70kV	≥ 80 dB	NA	NA	NA	NA
54	DIRA	Dira 16	CCD	Gadod	indirect	N	96	1600	NA	35% @ 70kV	≥ 78 dB	NA	NA	NA	NA
55	DIRA	Dira 16C	CCD	CsI	indirect	N	96	1600	NA	40% @ 70kV	≥ 78 dB	NA	NA	NA	NA
56	DIRA	Dira 9N	CCD	Gadod	indirect	N	140	1849	NA	50% @ 70kV	≥ 80 dB	NA	NA	NA	NA
57	DIRA	Dira 9NC	CCD	CsI	indirect	N	140	1849	NA	56% @ 70kV	≥ 80 dB	NA	NA	NA	NA
58	DIRA	Dira 16N	CCD	Gadod	indirect	N	105	1849	NA	50% @ 70kV	≥ 78 dB	NA	NA	NA	NA
59	DIRA	Dira 16NC	CCD	CsI	indirect	N	105	1849	NA	56% @ 70kV	≥ 78 dB	NA	NA	NA	NA

#	Manufacturer	Model/Number	Detector Type	Scintillator Type	Detector Size (Total Pixels)	Detector Size (Active Pixels)	Pixel Pitch (µm)	Physical Detector Size (Total Area cm ²)	MTF	DQE	Dynamic Range	non-Linearity	Wavelength Response/Energy Range [keV]	Integration time	Readout Noise (electrons)	
60	DIRA	DFP4343 G5	CMOS	Gadox	indirect	N	NA	NA	NA	NA	NA	NA	NA	NA	NA	
61	DIRA	DFP4343 G7	CMOS	CsI	indirect	N	NA	NA	NA	NA	NA	NA	NA	NA	NA	
62	DIRA	DFP4343 C5	CMOS	Gadox	indirect	N	NA	NA	NA	NA	NA	NA	NA	NA	NA	
63	DIRA	DFP4343 C7	CMOS	CsI	indirect	N	NA	NA	NA	NA	NA	NA	NA	NA	NA	
64	Allied Vision Technologies	CCD-11000XR/ COOL-11000XR	CCD	CsI	4024 x 2680 or 2012 x 1340 (2 x 2 binning) 1024 x 896 or 512 x 448 (2 x 2 binning)	NA	9	8.64	NA	NA	≥ 60 dB	NA	20 - 150	NA	< 60	
65	Allied Vision Technologies	XRC 1100	CCD	Gd2O2S	512 x 448 (2 x 2 binning)	NA	170	255	NA	NA	≥ 60 dB	NA	30 - 250	NA	NA	
66	Allied Vision Technologies	XRC 1200	CCD	Gd2O2S	512 x 448 (2 x 2 binning)	NA	100	87	NA	NA	≥ 60 dB	NA	30 - 250	NA	NA	
67	Phononic Science	HR CCD Camera	CCD	GdO3 or CsI	NA	NA	.26 Available 3.22, 6.45, 10.37,14.39, 23.03	NA	NA	NA	NA	NA	NA	NA	> 7	NA
68	Phononic Science	megapixel HR CCD Camera	CCD	Gd2O2S:Tb	1382 x 1040	NA	NA	NA	NA	NA	NA	NA	NA	NA	4 - 5	NA
69	Phononic Science	4 megapixel HR CCD Camera	CCD	Gd2O2S:Tb	2048 x 2048	NA	NA	NA	NA	NA	NA	NA	NA	NA	47 - 9	NA
70	Phononic Science	11 megapixel VHR CCD Camera	CCD	Gd2O2S:Tb	4008 x 2672	NA	NA	NA	NA	NA	NA	NA	NA	NA	14 - 18	NA
71	Phononic Science	16 megapixel VHR CCD Camera	CCD	Gd2O2S:Tb	4096 x 4096	NA	15	NA	NA	NA	NA	NA	NA	NA	10 - 12	NA
72	IGE	DXR250V	a-Si	GOS	2048 x 2048	NA	200	NA	NA	NA	10000:1	NA	NA	NA	NA	NA
73	IGE	DXR500L	a-Si	CsI	3072 x 2400	NA	100	NA	NA	NA	10000:1	NA	NA	NA	NA	NA
74	Detection Technology	X-Scan L-Shape	Dual Energy Modular Scintillator-photodiode linear array	NA	NA	NA	1.5 mm, 1.6 mm or 2.5 mm	NA	NA	NA	NA	NA	NA	NA	NA	NA
75	Detection Technology	X-Scan LCS 2.3	Modular Scintillator-photodiode linear array	CeWO4 or CsI(Tl)	NA	NA	2.3 mm	NA	270	NA	>.15 bits	NA	450Kcp = 9MeV	NA	NA	NA
76	Detection Technology	X-Scan LCS 4.6	Modular Scintillator-photodiode linear array	CeWO4 or CsI(Tl)	NA	NA	4.6 mm	NA	270	NA	>.15 bits	NA	450Kcp = 9MeV	NA	NA	NA
77	Detection Technology	X-Scan LCS 9.2	Modular Scintillator-photodiode linear array	CeWO4 or CsI(Tl)	NA	NA	9.2 mm	NA	565	NA	>.15 bits	NA	450Kcp = 9MeV	NA	NA	NA
78	Detection Technology	X-Scan 0.2 HE	Si photo diodes	CeWO4	NA	NA	0.2 mm	NA	NA	NA	> 8000 (no units given)	< 1%	50 = 600 kVp	2 - 4 ms	NA	NA
79	Detection Technology	X-Scan 0.2 HE	Si photo diodes	CeWO4	NA	NA	0.4 mm	NA	NA	NA	> 8000 (no units given)	< 1%	50 = 600 kVp	1.4 - 4 ms	NA	NA
80	Detection Technology	X-Scan 0.2 HE	Si photo diodes	CeWO4	NA	NA	0.8 mm	NA	NA	NA	> 8000 (no units given)	< 1%	50 = 600 kVp	1.5 - 2.0 ms	NA	NA
81	Detection Technology	X-Scan 0.4U-1434	NA	GOS	NA	NA	0.4 mm	NA	NA	NA	> 8000 (no units given)	< 1%	20 - 160kVp	1.5 ms	NA	NA
82	Detection Technology	X-Scan 0.4U-13B2	NA	GOS	NA	NA	0.4 mm	NA	NA	NA	> 8000 (no units given)	< 1%	20 - 160kVp	1.5 ms	NA	NA
83	Detection Technology	X-Scan 0.4U-14B5	NA	GOS	NA	NA	0.4 mm	NA	NA	NA	> 8000 (no units given)	< 1%	20 - 160kVp	1.5 ms	NA	NA
84	Detection Technology	X-Scan 0.4U-1331	NA	GOS	NA	NA	0.4 mm	NA	NA	NA	> 8000 (no units given)	< 1%	20 - 160kVp	1.5 ms	NA	NA
85	Detection Technology	X-Scan 0.8U-1434	NA	GOS	NA	NA	0.8 mm	NA	NA	NA	> 8000 (no units given)	< 1%	20 - 160kVp	0.67 ms	NA	NA

#	Manufacturer	Model Number	Detector Type	Scintillator Type	Detector Size (Total Pixels)	Detector Size (Active Pixels)	Pixel Pitch (µm)	Physical Detector Size (Total Area cm ²)	MTF	DOE	Dynamic Range	non-Linearity	Wavelength Response/Energy Range [kVp]	Integration time	Readout Noise (electrons)
86	Detection Technology	X-Scan 0.8U-3174	NA	GOS	NA	NA	0.8 mm	NA	NA	NA	> 8000 (no units given)	< 1%	20 - 160kVp	1.5 ms	NA
87	Detection Technology	XD-Scan cd (L8-1)	NA	NA	NA	NA	0.8 mm	NA	NA	NA	> 100 (no units given)	< 1%	20 - 160kVp	NA	NA
88	Detection Technology	XD-Scan cd (M4-2)	NA	NA	NA	NA	0.4 mm, 0.6 mm	NA	NA	NA	> 500 (no units given)	< 1%	20 - 160kVp	NA	NA
89	Detection Technology	XD-Scan cd (HE-3)	NA	NA	NA	NA	0.2 mm, 0.4 mm, 0.8 mm, 1.5 mm	NA	NA	NA	> 2000 (no units given)	< 1%	20 - 160kVp	NA	NA
90	Detection Technology	XD-Scan 0.2F3	linear array	GOS	NA	NA	0.2 mm	NA	NA	NA	> 2000 (no units given)	< 1%	20 - 160kVp	NA	NA
91	Detection Technology	XD-Scan 0.4F3	linear array	GOS	NA	NA	0.4 mm	NA	NA	NA	> 2000 (no units given)	< 1%	20 - 160kVp	NA	NA
92	Detection Technology	XD-Scan 0.8F3	linear array	GOS	NA	NA	0.8 mm	NA	NA	NA	> 2000 (no units given)	< 1%	20 - 160kVp	NA	NA
93	Detection Technology	XD-Scan 1.5F3	linear array	GOS	NA	NA	1.5 mm	NA	NA	NA	> 2000 (no units given)	< 1%	20 - 160kVp	NA	NA
94	Toshiba	FDX4343	amorphous Si	Cd	NA	3008 x 3072	143	1888	± 3.6% @ 2 lp/mm	> 70%	NA	NA	40 - 150kVp	NA	NA
95	Perkin Elmer Devela	1207	CMOS; active pixel	Cd; 150 µm; or Cd; 600 µm; Gadox	NA	1536 x 864	74.8	75	> 20% @ 6 lp/mm	> 70% @ 0.5 lp/mm	66 - 70 db	NA	NA	NA	NA
96	Perkin Elmer Devela	1512	CMOS; active pixel	Cd; 150 µm; or Cd; 600 µm; Gadox	NA	1944 x 1536	74.8	167	> 20% @ 6 lp/mm	> 70% @ 0.5 lp/mm	66 - 70 db	NA	NA	NA	NA
97	Perkin Elmer Devela	2315	CMOS; active pixel	Cd; 150 µm; or Cd; 600 µm; Gadox	NA	3072 x 1944	74.8	334	> 20% @ 6 lp/mm	> 70% @ 0.5 lp/mm	66 - 70 db	NA	NA	NA	NA
98	Perkin Elmer Devela	2923	CMOS; active pixel	Cd; 150 µm; or Cd; 600 µm; Gadox	NA	388 x 3072	74.8	667	> 20% @ 6 lp/mm	> 70% @ 0.5 lp/mm	66 - 70 db	NA	NA	NA	NA
99	Konica Minolta AeroDR		NA	Cd	NA	2428 x 2428	175	1865	NA	NA	NA	NA	NA	NA	NA

Part II: Scintillators (2 pages)

The tables below present the results of a survey of scintillators used in x-ray imaging devices. The survey is not exhaustive but reasonably presents a collection of the more common items used. Each vendor provides a data sheet that contains information that it regards as useful to the consumer and may not publish other information because of proprietary concerns. As such, the technical specifications which are publicly available vary considerably. The table's intent was to highlight important operating parameters of each device. Unfortunately, because of the large variability in data sheet content, many entries are listed as "not available" (NA).

#	Manufacturer	Title/ID Number	Chemical Formula	Density (g/cm ³)	Dimensions	Thickness (µm)	Wavelength of Max Emission (nm)	Decay Time (ns)	Relative Light output [%]	Afterglow (% at 6 ms)	Energy Resolution (FWHM at 662 keV)	Hygroscopic (Y/N)	Comment
1	Kodak	Lanex Fine	Gd ₂ O ₂ S:Tb	4.5		200	550	150		2.5	N/A	No	
2	Kodak	Mira-R Medium	Gd ₂ O ₂ S:Tb										
3	Kodak	Lanex Fast	Gd ₂ O ₂ S:Tb										
4	Kodak	Lanex Fast B	Gd ₂ O ₂ S:Tb										
5	Siemens	NA	CSI	4.51	up to 45 cm x 45 cm	600 - 800	NA	980	130	after 30 ms (ppm) 100	NA	NA	Thallium doped CSI in a cluninar structure deposited on a substrate
6	Siemens	NA	UPC	7.34	up to 45 cm x 45 cm	600 - 800	NA	2500	100	after 30 ms (ppm) 32	NA	NA	Doped gadolinium oxysulfide in a polycrystalline structure
7	Siemens	NA	CdWO ₄	7.9	up to 45 cm x 45 cm	600 - 800	NA	8900	40	after 30 ms (ppm) 160	NA	NA	
8	Hamamatsu	J6671	CsI(Tl)	NA	30.5mm x 21mm	150	NA	NA	70	NA	High light Output	NA	Fiber Optic Plate with CsI scintillator Contact Transfer function @ 10µp/mm = 18% Effective area = 27 x 17 mm
9	Hamamatsu	J6671-01	CsI(Tl)	NA	30.5mm x 21mm	150	NA	NA	40	NA	High Resolution	NA	Fiber Optic Plate with CsI scintillator Contact Transfer function @ 10µp/mm = 33% Effective area = 27 x 17 mm
10	Hamamatsu	J6673	CsI(Tl)	NA	50mm x 10mm	150	NA	NA	70	NA	High light Output	NA	Fiber Optic Plate with CsI scintillator Contact Transfer function @ 10µp/mm = 18% Effective area = 47 x 7 mm
11	Hamamatsu	J6673-01	CsI(Tl)	NA	50mm x 10mm	150	NA	NA	40	NA	High Resolution	NA	Fiber Optic Plate with CsI scintillator Contact Transfer function @ 10µp/mm = 33% Effective area = 47 x 7 mm
12	Hamamatsu	J6675	CsI(Tl)	NA	18 mm x 18 mm	150	NA	NA	70	NA	High light Output	NA	Fiber Optic Plate with CsI scintillator Contact Transfer function @ 10µp/mm = 18% Effective area = 15 x 15 mm
13	Hamamatsu	J6675-01	CsI(Tl)	NA	18 mm x 18 mm	150	NA	NA	40	NA	High Resolution	NA	Fiber Optic Plate with CsI scintillator Contact Transfer function @ 10µp/mm = 33% Effective area = 15 x 15 mm
14	Hamamatsu	J6677	CsI(Tl)	NA	50 mm x 50 mm	150	NA	NA	70	NA	High light Output	NA	Fiber Optic Plate with CsI scintillator Contact Transfer function @ 10µp/mm = 18% Effective area = 47 x 47 mm
15	Hamamatsu	J6677-01	CsI(Tl)	NA	50 mm x 50 mm	150	NA	NA	40	NA	High Resolution	NA	Fiber Optic Plate with CsI scintillator Contact Transfer function @ 10µp/mm = 33% Effective area = 47 x 47 mm
16	Hamamatsu	J6679	CsI(Tl)	NA	circular area 26.5 mm ²	150	NA	NA	70	NA	High light Output	NA	Fiber Optic Plate with CsI scintillator Contact Transfer function @ 10µp/mm = 18% Effective area = 23.5 dia. mm
17	Hamamatsu	J6679-01	CsI(Tl)	NA	circular area 26.5 mm ²	150	NA	NA	40	NA	High Resolution	NA	Fiber Optic Plate with CsI scintillator Contact Transfer function @ 10µp/mm = 33% Effective area = 23.5 dia. mm
18	Hamamatsu	J6734	CsI(Tl)	NA	50 mm x 50 mm	150	NA	NA	125	NA	High light Output	NA	Amorphous carbon plate with CsI scintillator Contact Transfer function @ 10µp/mm = 12% Effective area = 48 x 48 mm
19	Hamamatsu	J8734-01	CsI(Tl)	NA	50 mm x 50 mm	150	NA	NA	50	NA	High Resolution	NA	Amorphous carbon plate with CsI scintillator Contact Transfer function @ 10µp/mm = 25% Effective area = 440 x 440 mm
20	Hamamatsu	J8977	CsI(Tl)	NA	468 mm x 468 mm	600	NA	NA	250	NA	High light Output	NA	Amorphous carbon plate with CsI scintillator Contact Transfer function @ 10µp/mm = NA Effective area = 48 x 48 mm

#	Manufacturer	Title/ID Number	Chemical Formula	Density (g/cm ³)	Dimensions	Thickness (µm)	Wavelength of Max Emission (nm)	Decay Time (ns)	Relative Light output [%]	Afterglow (% at 6 ms)	Energy Resolution (FWHM at 662 keV)	Hygroscopic (Y/N)	Comment
21	Hamamatsu	J897B	CsI(Tl)	NA	50 mm x 50 mm	150	NA	NA	70	NA	NA	NA	Aluminum plate with CsI scintillator Contact Transfer function @ 10lp/mm = 20% Effective area = 48 x 48 mm
22	Hamamatsu	J9657	CsI(Tl)	NA	468 mm x 468 mm	600	NA	NA	150	NA	NA	NA	Aluminum plate with CsI scintillator Contact Transfer function @ 10lp/mm = NA Effective area = 48 x 48 mm
23	Mitsubishi	Green Medium 300	Gd ₂ O ₂ S:Tb	NA	NA	NA	NA	NA	NA	NA	High sharpness	NA	intensifying screen phosphor (green)
24	Mitsubishi	Green Regular 400	Gd ₂ O ₂ S:Tb	NA	NA	NA	NA	NA	NA	NA	Standard speed	NA	intensifying screen phosphor (green)
25	Mitsubishi	Green Fast 600	Gd ₂ O ₂ S:Tb	NA	NA	NA	NA	NA	NA	NA	Super high speed	NA	intensifying screen phosphor (green)
26	Mitsubishi	M5/Blue medium speed 100	CaWO ₄	NA	NA	NA	NA	NA	NA	NA	Medium speed	NA	intensifying screen phosphor (blue)
27	Mitsubishi	H5/Blue High Plus 160	CaWO ₄	NA	NA	NA	NA	NA	NA	NA	High speed	NA	intensifying screen phosphor (blue)
28	Mitsubishi	High Plus/Blue 210	CaWO ₄	NA	NA	NA	NA	NA	NA	NA	Very high speed	NA	intensifying screen phosphor (blue)
29	Mitsubishi	Super Special/Blue 500	Rare Earth Type	NA	NA	NA	NA	NA	NA	NA	Maximum speed	NA	intensifying screen phosphor (blue)
30	Mitsubishi	DRZ-STD	Gd ₂ O ₂ S:Tb	x-ray attenuation = 42%	Protect Layer 6; phosphor 140; support layer 250 = total 396	NA	NA	Relative Brightness = 145%	NA	NA	NA	NA	Suggested use = DR applications; MTF @ 2lp/mm= 0.49
31	Mitsubishi	DRZ-PLUS	Gd ₂ O ₂ S:Tb	x-ray attenuation = 53%	Protect Layer 6; phosphor 208; support layer 250 = total 464	NA	NA	Relative Brightness = 173%	NA	NA	NA	NA	Suggested use = DR applications; MTF @ 2lp/mm= 0.36
32	Mitsubishi	DRZ-HIGH	Gd ₂ O ₂ S:Tb	x-ray attenuation = 66%	Protect Layer 9; phosphor 310; support layer 188 = total 507	NA	NA	Relative Brightness = 229%	NA	NA	NA	NA	Suggested use = DR applications; MTF @ 2lp/mm= 0.16
33	Mitsubishi	PI-200	Gd ₂ O ₂ S:Tb	NA	Protect Layer 6; phosphor 436; support layer 188 = total 630	NA	NA	Relative Brightness = 122%	NA	NA	NA	NA	Suggested use = portal radiography; MTF @ 2lp/mm= 0.11
34	Mitsubishi	DRZ-HIGH	Gd ₂ O ₂ S:Tb	NA	Protect Layer 9; phosphor 310; support layer 188 = total 507	NA	NA	Relative Brightness = 100%	NA	NA	NA	NA	Suggested use = portal radiography; MTF @ 2lp/mm= 0.16

Appendix viii: Titles

Robert G. Lanier
January 13, 2012

In researching imaging technologies, a number of articles were uncovered that might be appropriate for individuals interested in pursuing additional information on technologies that are either in the process of maturing or undergoing investigation because of their future promise to imaging applications. The list represents only a handful of articles encountered during this literature search and no particular criteria were applied in their selection except that they appeared to speak to aspects of imaging technology.

The list identifies the title of the article, the author list and the web address where the text of the article may be found.

Development of an LYSO based gamma camera for positron and scinti-mammography

H-C Liang^{a,b}, M-L Jan^a, W-C Lin^a, S-F Yu^a, J-L Su^b and L-H Shen^a

http://iopscience.iop.org/1748-0221/4/08/P08009/pdf/1748-0221_4_08_P08009.pdf

Comparative evaluation of single crystal scintillators under x-ray imaging conditions

OPEN ACCESS [4th International Conference on Imaging Technologies in Biomedical Sciences](#)

I G Valais^{a,b}, S David^a, C Michail^a, C D Nomicos^c, G S Panayiotakis^b and I S Kandarakis^b

http://iopscience.iop.org/1748-0221/4/06/P06013/pdf/1748-0221_4_06_P06013.pdf

A new x-ray imaging technique for radiography mode of flat-panel imager

Proc. SPIE 6510, 651047 (2007); doi:10.1117/12.709079

Jiang Hsieh, Michael J. Flynn K. Suzuki, S. Ikeda, and K. Ueda ; Hitachi Medical Corp. (Japan)
R. Baba Hitachi Ltd. (Japan)

<http://scitation.aip.org/getpdf/servlet/GetPDFServlet?filetype=pdf&id=PSISDG006510000001651047000001&idtype=cvips&doi=10.1117/12.709079&prog=normal>

On the Development of Digital Radiography Detectors : A Review

Ho Kyung Kim, Ian Alexander Cunningham, Zhye Yin and Gyuseong Cho

<http://www.imaging.robarts.ca/~icunning/SiteResources/publications/2008%20ijpem%2009-86%20Kim%20Review.pdf>

Inorganic Scintillators in Positron Emission Tomography

Carel W.E. van Eijk*

<http://www.springerlink.com/content/4227881124t1x170/fulltext.pdf>

Development of High-image Quality and High Durability Direct Conversion Digital Radiography System “FDR AcSelerate”

Hirotaka Watano, Fumito Nariyuki, Shiniji Imai, Toshiyuki Nabeta, Uyichi Hosoi, Tetsuya Tsuji, Keita Watanabe, Jun Enomoto and Masaru Sato.

http://www.fujifilm.com/about/research/report/055/pdf/index/ff_rd055_002_en.pdf

Proposal of New Organic CMOS Image Sensor for Reduction in Piel Size

Mikio Ihama, Tetsurou Mitsui, Kamiatsu Nomura, Yoshiki Maehara, Hiroshi Inimata, Takashi Gotou and Yutaka Takeuchi

http://www.fujifilm.com/about/research/report/055/pdf/index/ff_rd055_004_en.pdf

Advantages and Use of CdZnTe Detectors in Safeguards Measurements

Rolf Arlt, Victor Ivanov and Kevin Parnham

<http://www.evmicroelectronics.com/pdf/Applications/Advantages%20and%20use%20of%20CdZnTe.pdf>

Performance evaluation of D-SPECT: a novel SPECT system for nuclear cardiology

Kjell Erlandsson¹, Krzysztof Kacperski, Dean van Gramberg and Brian F Hutton

http://iopscience.iop.org/0031-9155/54/9/003/pdf/0031-9155_54_9_003.pdf

Quantum Dot Composite Radiation Detectors

Mario Urdaneta, Pavel Stepanov, Irving Weinberg, Irina Pala and Stephanie Brock²

http://www.intechopen.com/source/pdfs/17231/InTechQuantum_dot_composite_radiation_detectors.pdf

CZT detector in multienergy x-ray imaging with different pixel sizes and pitches: Monte Carlo simulation studies

Yu-Na Choi, Hee-Joung Kim*, Hyo-Min Cho, Chang-Lae Lee, Hye-Suk Park, Dae-Hong Kim, Seung-Wan Lee, Hyun-Ju Ryu

<http://scitation.aip.org/getpdf/servlet/GetPDFServlet?filetype=pdf&id=PSISDG00796100000179614H000001&idtype=cvips&doi=10.1117/12.878357&prog=normal>

Large-area mercuric iodide x-ray imager

G. Zentai, L. Partain, R. Pavlyuchkova, G. Virshup, A. Zuck, L. Melekhov, O. Dahren, A. Vilensky and H. Gilboa

http://independent.academia.edu/GeorgeZentai/Papers/665079/Large_area_mercuric_iodide_X-ray_imager

Comparison of Mercuric Iodide and Lead Iodide X-Ray Detectors for X-Ray Imaging Applications

G. Zentai, *Member*, L. Partain, R. Pavlyuchkova, C. Proano, M. Schieber, K. Shah, P. Bennett, L. Melekhov, and H. Gilboa

<http://ieeexplore.ieee.org/stamp/stamp.jsp?arnumber=01710230>

X-ray detection using bulk GaAs

A.D. Holland, A.D.T. Short, and T. Cross

http://pdn.sciencedirect.com/science?_ob=MiamiImageURL&_cid=271580&_user=8139564&_pii=0168900294907242&_check=y&_origin=article&_zone=relatedPdfPopup&_coverDate=1994-07-15&_piiSuggestedFrom=S0168900296003464&_wchp=dGLzVIV-zSkzS&_md5=39cd119877d6a983fa11423020acde28/1-s2.0-0168900294907242-main.pdf

Review of X-ray Detectors for Medical Imaging

Martin Hoheisel

http://www.esrf.eu/events/conferences/IWORID7/FinalProgramme/hoheisel_1.pdf

Comparison of HgI₂, CdTe and Si (p-i-n) X-ray detectors

J.S. Iwanczyk, B.E. Patt, Y.J. Wang, A. Kh. Khusainov

http://pdn.sciencedirect.com/science?_ob=MiamiImageURL&_cid=271580&_user=8139564&_pii=S0168900296004949&_check=y&_origin=article&_zone=toolbar&_coverDate=01-Oct-1996&_view=c&_originContentFamily=serial&_wchp=dGLbVIV-zSkWb&_md5=1ea23beb72501f529ea5395acad969fa/1-s2.0-S0168900296004949-main.pdf

Amorphous and Polycrystalline Photoconductors for Direct Conversion Flat Panel X-Ray Image Sensors

Safa Kasap, Joel B. Frey, George Belev, Olivier Tousignant, Habib Mani, Jonathan Greenspan, Luc Laperriere, Oleksandr Bubon, Alla Reznik, Giovanni DeCrescenzo, Karim S. Karim and John A. Rowlands

<http://www.mdpi.com/1424-8220/11/5/5112/>